**Beuth Hochschule für Technik Berlin**
University of Applied Sciences

Fernstudieninstitut
Studiengang Medizinische Informatik

# Combined EEG and MEG for improving source analysis in patients with focal epilepsy

Masterarbeit
zur Erlangung des Grades eines Master of Science (M.Sc.)

**eingereicht von: Dr. med. Philipp Küpper**
**(Matrikel-Nr. 768995)**
**am: 12.12.2012**

Erstgutachter: PD. Dr. rer. nat. C. Wolters
Zweitgutachter: Prof. Dr. Ing. L. Leutelt

**Contents**

## Abstract

Brain activity can be recorded by electroencephalography (EEG) and magnetoencephalography (MEG). The acquired data can be used to localize the underlying sources of the currents in the brain tissue, a method called source localization. In epilepsy patients some of the recorded patterns can lead to the generators of seizures. Usually medical staff marks the specific patterns and this data often is used without any additional verification by non-clinical staff for further processing of the source localisation. Up to now in many groups the hand marking of the patterns has been taken as gold standard.

This thesis aims to find, evaluate and improve possible unexpected or unrecognized factors influencing the signal quality at the intersection between medical and methodological staff involved. The main factors influencing the signal quality are the precision of the marking of epileptiform discharges as well as the clustering of the spikes. This thesis shows that rather minor imprecisions as incorrect peak markings and mixed clustering cause a significant change in the dipole localisation of up to 3 cm shift. Also the influence of semi-automatic template search algorithms on the source localisation precision is evaluated. In addition we offer a Matlab tool to correct the data easily without profound clinical knowledge. Now it is possible to create reliable and precise data as a basis for the source reconstruction. This data can also be used to reasonably evaluate upcoming new and highly sophisticated head models.

## Acknowledgements

I want to thank everyone who made this thesis and my studies possible, especially:

- Carsten Wolters for introducing me to this field of research and providing me with the right literature and tools as well as for being advisor of this thesis,
- Ümit Aydin for supporting me with many ideas and detailed information about the localization process and for taking the time to read this thesis and to provide me with corrections and annotations,
- Christoph Kellinghaus and Stefan Rampp for sharing their clinical knowledge and for their support during the whole process,
- My wife and my daughter for their mental and patient support at all times and who make the studies and this thesis possible.

# 1. Introduction

This thesis is part of the master course in medical informatics of the University of Applied Science, Beuth Hochschule Berlin. This course provides profound contents about the implementations of informatics in the medical field. Resulting from the connection between profound medical knowledge and good experience in recording, evaluation, processing and visualization of medical data of different origins, graduates of this course will find perfect operating conditions in all areas of health care business.

Special aim of this course is the improvement of communication at the intersection of medical staff and methodologists (i.e. IT specialists, mathematics). In the course of my clinical training in the department of neurology I started to specialize in the field of epilepsy, which deals with the diagnosis, treatment and research of seizures and underlying conditions. Main diagnostic tools are the electroencephalogram (EEG) and magnetoencephalogram (MEG) and imaging of the brain with the aim of evaluating the seizure generating structures in the brain.

One approach to detect these generating structures is called EEG/ MEG source localization. Source localization uses non-invasively recorded electric field potentials (EEG) and magnetic field potentials of brain activity to calculate and determine the underlying generator in the brain structures. This procedure is called “inverse problem”. The localization of epileptiform discharges and field potentials from simultaneously recorded EEG and MEG data is part of a current project of the Institute for Biomagnetism and Biosignalanalysis Münster (PD Dr. rer. nat. Carsten Wolters) and the epilepsy centre Erlangen (Prof. Dr. med. H.Stefan) supported by the DFG (Deutsche Forschungsgemeinschaft).

This project is characterized by a high degree of interdisciplinarity which combines medical-epileptological knowledge with modern mathematical procedures of source analysis. Basic requirement for source reconstruction of epileptogenic potentials and fields is a signal with the highest possible signal to noise ratio. Sufficient signal to noise ratios are often only achieved by averaging different spikes. These spikes must derive from the same cluster with respect to time course and spatial resolution. In clinical practice all epileptiform discharges

are marked by a specially trained EEG/MEG reader. After visual analysis the signal is assigned to the electrode or sensor, where the maximum of the signal is recorded. Some commercial tools for signal processing provide a correlation algorithm to search for similar discharges with respect to temporal-spatial resolution.

Main aim of this master thesis is the definition, evaluation and improvement of possibly unexpected or unrecognized parameters influencing the goodness and precision of source localization from EEG/MEG data.

# 2. Methods

## 2.1. Basic principles

### 2.1.1. Epileptic seizures, epilepsy and clinical principles

About 40 million patients suffer from epilepsy as epidemiological studies estimate. This condition results in about 142.000 deaths per year, about 0.2% of all annual deaths (Global burden of Disease Study (GDB)). Numbers for Germany mostly refer to studies by Hart and Shorvon from the UK (Hart and Shorvon, 1995a, 1995b). About 0.5-1% of the general population (400.000 – 500.000 people) suffers from epilepsy with about 30.000 newly detected conditions per year (Brandt, Christian, 2008). Furthermore a lot of conditions like uncontrolled seizures, stigmata and discrimination result in impairments of daily life routine (Gaitatzis et al., 2004; Scambler, 2006).

An epileptic seizure is defined as “transient symptoms or clinical features of abnormal excessive and pathologically synchronized brain activity” (Wyllie et al., 2010, p. 3). This means that it comes to uncontrolled and hyperactive dysfunctions in groups of brain cells. Obvious symptoms are usually loss of consciousness and rhythmic or tonic cramps of muscles for up to several minutes. Besides these features some seizures might only be recognized by a transient mild impairment of consciousness or in characteristic epileptiform discharges in the EEG recording (Wyllie et al., 2010, p. 192).

The term epilepsy defines a disease with a number of criteria to be fulfilled. To meet the criteria usually more than one seizure with latency of more than 24h need to be recognized. The seizures must be unprovoked, so without an event

impairing the brain function like a trauma (Robert S. Fisher et al., 2005). A single epileptic seizure will not automatically lead to the diagnosis of epilepsy. About 5% of the general population will have a single epileptic seizure during lifetime without being diagnosed with epilepsy (Brandt, Christian, 2008).

The epilepsies can be divided in three main etiological groups. The first group contains the symptomatic epilepsies which result from a preceding impairment of the brain structure. The reasons for impairment might be congenital change in brain structure, strokes, trauma and infections of brain tissue. The second group of idiopathic epilepsies contains those which result from genetic predispositions and usually appear in childhood or early adolescence. All other epilepsies are classified as cryptogenic which means that the underlying reason in unknown. Many of the former cryptogenic epilepsies can nowadays be reclassified by newer imaging technics or more sophisticated genetic testing (Wyllie et al., 2010, p. 3).

Common feature of all epilepsies is the uncontrolled and synchronized neuronal activity spreading over different brain regions due to impaired inhibition mechanisms. Depending on the affected brain region, resulting symptoms can differ. Necessary information derive from an extensive medical history of the patient, third-party history, neurological and general examination, a reliable EEG recording and a high resolution brain imaging (Hirtz et al., 2000).

Treatment of seizures and epilepsy is aiming to gain seizure freedom. A curative treatment is not available and all therapeutic options are solely symptomatic up to now (Wyllie et al., 2010, p. 511). Different treatment options are life-style improvements, e.g. improvement of circadian rhythm, as well as medication. Epilepsy surgery can be an option as well after the generating structures in the brain are clearly identified and can be resected without creating lasting deficits. Medical treatment uses many different anticonvulsive drugs. By modulating the membrane potential of neuronal cells the disposition for seizures can be reduced. Mainly this is achieved by a modulation of the activity of ion channels in the membrane. Nevertheless about one third of all epilepsy patients are intractable. This means that after the correct diagnosis is made and

adequate treatment is administered no sufficient reduction in seizure frequency is reached (Wyllie et al., 2010, p. 511). In the group of newly diagnosed patients with epilepsy about 47% are seizure free after the first anticonvulsant drug. Another 10% will get seizure free after switching to another drug in mono-therapy. Only another 2.3% will reach seizure freedom after switching to a third drug in mono-therapy or in poly-therapy. These results lead to the conclusion that the chance of success will significantly decrease after the ineffective use of two anticonvulsants in mono-therapy (Brodie and Kwan, 2002; Kwan and Brodie, 2000, 2001; Wyllie et al., 2010, p. 812). Also after the introduction of new anticonvulsant agents within recent years these numbers remain mainly unchanged. Still about 30% of all patients will remain having intractable seizures (Callaghan et al., 2007; Luciano and Shorvon, 2007; Wyllie et al., 2010, p. 812).

In these cases epilepsy surgery provides the opportunity to resect the seizure generating structure after precise localization. This kind of therapy mainly provides an option for the first group of epilepsies which results from different types of brain tissue alterations. This group of epilepsy is also called “lesional” epilepsy. First resections of suspected lesions as generator for seizures are reported in 1886 by Victor Horsley (Horsley V, 1886; Vilensky, 2002). After resecting cortical structures significant reductions of epileptic seizures have been achieved and so the hypothesis of cortical generation has been created. This hypothesis has been strengthened by improved neurosurgical knowledge and more precise diagnostic tools. The term “epileptogenic zone” has been shaped and defined by Jean Talairach, Jean Bancaud and mainly by Hans O. Lüders (H. O. Lüders et al., 2006). This zone contains “the minimum amount of cortex tissue which needs to be resected (inactivated or disconnected) to reach seizure freedom) (H. O. Lüders et al., 2006; H. Lüders et al., 2008). The best case scenario will result in a complete and enduring seizure freedom without any lasting impairment after resection of a small amount of pathological brain tissue. So the mandatory basis for a successful, especially operative treatment of epilepsy is the precise definition and localization of the epileptogenic zone.

This zone is unique in each patient and in all cases it is a hypothetical construct. It derives from the results and localising information from different diagnostic methods (Wyllie et al., 2010, p. 825). Engel more precisely defines another region as subset of the epileptogenic zone. He describes the epileptogenic focus as the area of maximal electrophysiological interictal activity. This region is a dynamic spatiotemporal zone because interictal discharges can often move and shift within adjacent brain regions (Engel, 1996, 1996).

Recent studies reveal that the outcome of epilepsy surgery has been proven to be superior to medical treatment, especially in patients with lesional temporal lobe epilepsy (Engel, 2001; Engel et al., 2003; Jehi et al., 2009; Wiebe et al., 2001). Furthermore Engel states that the combination of surgery with medical treatment is four times as likely as medical treatment alone to achieve freedom from seizures" (Engel et al., 2003). Kuzniecky et al. show that epilepsy surgery can control seizures, improve quality of life and reduce costs of medical care (Kuzniecky and Devinsky, 2007). Even though the results of epilepsy surgery might be far better than the conservative treatments, this method is offered to only 2% to 3% of potential surgical candidates (Engel et al., 2003).

Since the precise definition of the epileptogenic focus and zone is still difficult and complex, current methods as brain imaging or EEG / MEG recordings and source reconstructions need to be improved. Aim of this thesis is the evaluation and improvement of parameters leading to the definition of the epileptogenic focus and zone. Special focus will be put on to the intersection between clinical and methodological pre-processing of the EEG and MEG data before it will be used for source localization procedures.

### 2.1.2. Principles of neuroanatomy and diagnostic tools

#### 2.1.2.1. Principles of neuroanatomy

In this chapter the basic structures of the brain, the neuro-anatomy and the generation of electric fields will be described.

In general, the nervous system can be divided in peripheral and central parts. The peripheral parts consist of afferent and efferent nerves connecting the

organs as muscles to the central nervous system. This central nervous system (CNS) can be roughly divided into brain stem with attached spinal cord, cerebellum and cerebrum. This is the main part of the human brain, consisting of two hemispheres and relevant for many voluntary and involuntary functions.

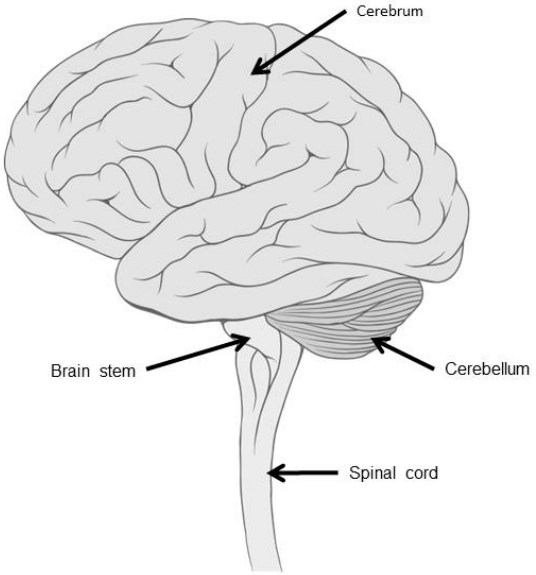


Figure 2.1: Human brain, taken from Wikimedia and modified, creative commons. Patrick J. Lynch, medical illustrator; C. Carl Jaffe, MD, cardiologist

As well it is focus of main interest for our studies, as the relevant discharges in epilepsy are generated in this part of the brain.

The cerebrum itself consists of an extensive surface which is folded and can be subdivided in different lobes. These lobes represent the brain regions the EEG topography is referring to.

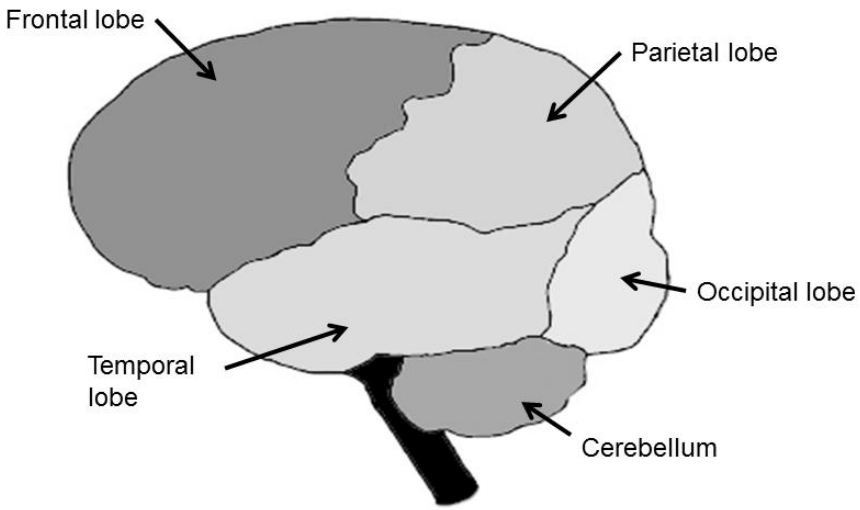


Figure 2.2: Brain lobes, taken from Wikimedia and modified, public domain

The histological architecture of the cerebrum is characterized by nerve cells, which are arranged in bundles and layers. All of these nerve cells have multiple interconnections directly to their neighbours as well as to distant parts of the brain and their target cells, like in muscle or sensory organs. The outer layer of the cerebrum is called the cerebral cortex or grey matter. This is a densely folded and about 6mm thick layer of altogether about $10^9$ to $10^{10}$different neurons, fibres and glia cells organised in layers containing different cell bodies or somata and dendrites as parts of the neuron. With respect to the basic principles of epilepsy and the basic function of the brain it is important to emphasize the parallel structure and highly interconnected organisation of these neurons.

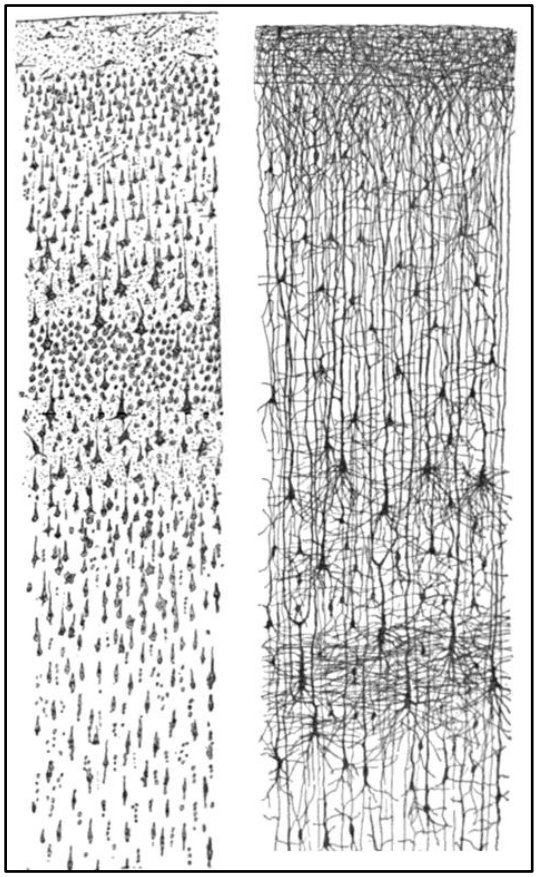

Figure 2.3: Drawing of cortical lamination; vertical cross-sections, with the surface of the cortex at the top. Left: motorcortex of human adult showing somata of neurons, right: cortex of human infant showing dendrites and axons. Modified drawing by Santiago Ramon y Cajal (1852-1934)

The underlying white matter mainly contains neuronal fibres and so called axons connecting the neurons in the cerebral cortex to distant region within the brain and target organs in the body.

Each neuron consists of a cell body, or soma, many dendrites and an axon. Information is exchanged between and transported within a neuron by electric currents. A cell receives the information by its dendrites, where other neurons are attached by connection sites, called synapses. The signal is transported by the axon and transferred to one or many other neurons. By the special interconnections and summation of inhibitory or excitatory signals, the information is altered and processed in the brain before it is sent to target organs like a muscle by an efferent axon. Neurons are surrounded by glia-cells,

which support the structure of the neurons but also can have electrochemical interconnections. Without being part of direct signal processing, which is done by neuronal cells, glia cells are an important factor supporting the signal processing.

To create and transport a signal within neurons, the basic histologic structure of the neuron needs to be explained. The wall of the axon is built as an about 8nm thick double layer semipermeable membrane which contains many highly selective channels and transporters for different substrates as ions. These ions, mainly potassium (K+), sodium (Na+) and chloride (Cl-) are electrochemically charged. By different mechanism a resting potential of the cell is created which can be measured as a potential of about -50 and -80mV between inside and outside of the membrane for pyramidal cell. This potential is built up by electrical and concentration gradients created by diffusion and ion pumps. There is about ten times more sodium in the extracellular and twenty times more potassium in the intracellular compartments than on the opposite side respectively. By the fact that the positive potassium ions can cross the membranes unimpaired by selective channels they follow the concentration gradient and cause a relative negativity in the intracellular compartment. The sodium ions try to follow the concentration and electrical gradient into the cell but cannot cross the membrane in resting state. Additionally the Na+/K+ pump transfers potassium into and sodium out of the cell keeping up the concentration gradient. As soon as the concentration and electrical gradients are at equilibrium, the movement of ions stops. The potential which can be measured is called the resting potential. The basic features are shown in Figure 2.4.

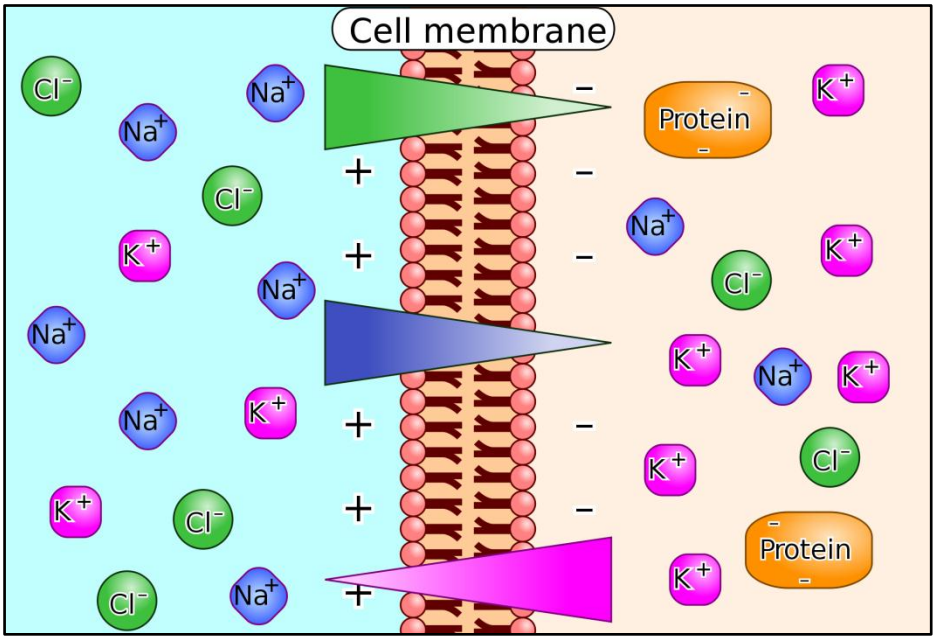


Figure 2.4: Resting potential of cell resulting from concentration and electrical gradient. Taken from Wikimedia creative commons, created by Biezl.

Signals in neurons are processed and transported by quick shifts of the membrane potential. In the dendrites several excitatory and inhibitory neurons connect to the neuron of interest by synapses. At the synapse, small potential shifts in the membrane of the postsynaptic region are caused and are called Excitatory Post Synaptic Potentials (EPSP). Also signals from inhibitory neurons can be processed and will cause a hyperpolarisation of the postsynaptic membrane, called Inhibitory Post Synaptic Potentials (IPSP). By summation of these signals over time and space a significant change of the membrane potential can occur. As soon as the increase of the resting potential reaches a threshold of -55mV, sodium channels will open and cause a short depolarisation by the influx of Na+ following the concentration and electrical gradient. Shortly afterward, potassium channels will open as well and the membrane will return to its resting potential again since potassium ions will leave the cell driven by the concentration gradient. The sum of all these potential shifts and extracellular compensatory ion shifts can be partly registered on the scalp by EEG or by the MEG as seen in figure 2.41.

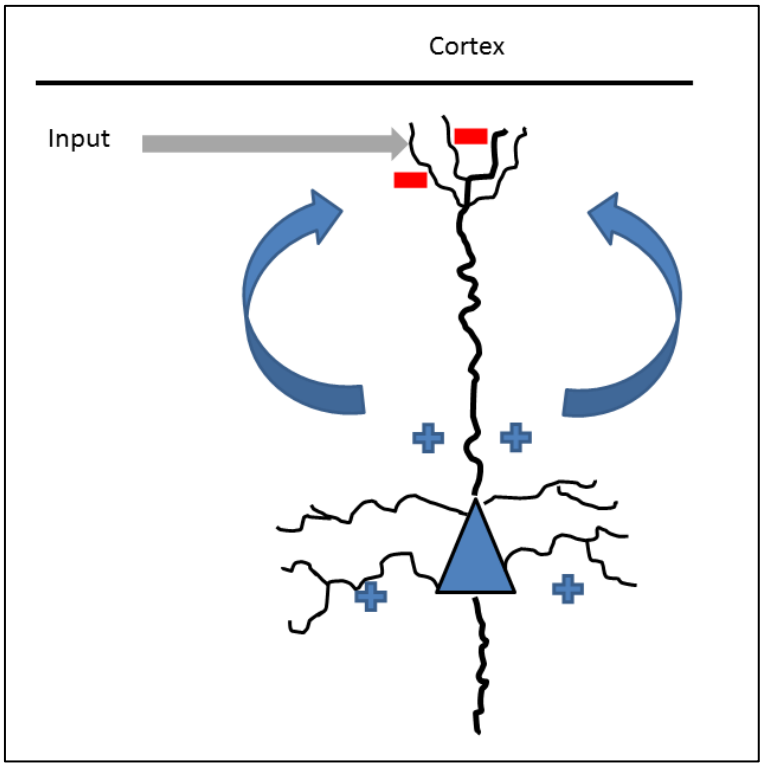


Figure 2.41: Dipole resulting from postsynaptic field potentials. The excitatory input at the apical dendrites causes a local negativity with ion shift from deeper layers. The EEG above the cortex records a negative potential. Own drawing, modified from Zschocke, Klinische Enzephalographie.

The positions of the neuronal networks in relation to the recording electrodes are basic features to understand the recording of the extracellular potentials (Deetjen P et al., n.d.; Speckmann, Erwin-Josef, 1986; Wyllie et al., 2010, p. 63).

In summary information in neurons is transferred and coded in short membrane potential changes which are transferred to other neurons by so called synapses (Speckmann, Erwin-Josef, 1986; Wyllie et al., 2010, p. 60). By the special arrangement and connection of excitatory and inhibitory neurons neuronal networks are created. These are able to encode, enhance or delete signals and so alter the information. By the kind of neuronal network, different functional parts of the brain are characterised. In a healthy brain the inhibitory interconnections between parallel neuronal networks can stop uncontrolled spreading of synchronised neuronal activity to near or distant neuronal networks

(Zschocke S and Hansen HC, 2011, p. 161). By failure of these inhibitory networks, epileptic discharges can influence surrounding networks and the epileptic activity can spread. In normal state, the brain activity is mainly unsynchronized and shows unspecific rather slow potential shifts in the EEG.

#### 2.1.2.2. Electroencephalography (EEG)

In clinical routine diagnostic commonly scalp EEG of 20-30 min is recorded. With respect to the intended clinical hypothesis provocation methods like hyperventilation or flicker light can be used to stimulate the patient. In principle, the recorded data will be printed on paper or nowadays usually digitally saved. This recording is evaluated and reported by a reader, usually a neurologist or neurophysiologist. During EEG reading the single channels are visualised on a computer screen and can be selected so that all possible bipolar or referential montages can be displayed as needed. Basic features of the report will describe background activity, frequency and so called normal variants. Furthermore pathological features will be described as regional slowing or appearance of epileptiform discharges (see also 2.1.2.1). All is summarised in the report.

To record an EEG, electrodes will be placed in a standardised order onto the scalp with electrically conductive paste. The placement is done by the “international 10-20 electrode system “, Figure 2.5. Fixed standard position will be marked on the skin and in relation the position of the electrode will be calculated. For routine EEG the averaged spatial resolution and precision is sufficient. For source reconstruction recordings, electrode numbers should be increased and the exact localisation should be recorded (Wyllie et al., 2010, p. 76).

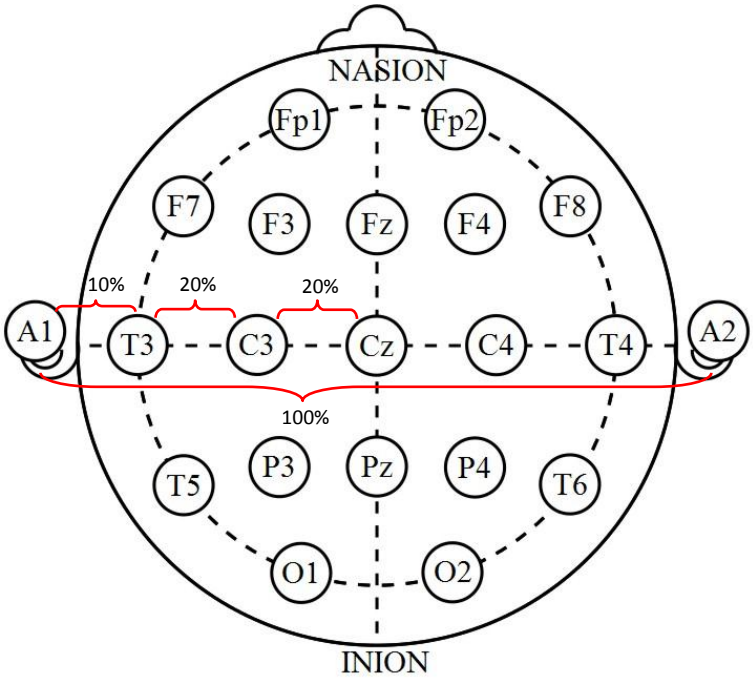


Figure 2.5: EEG electrode placement in the international 10/20 system. Taken from wikimedia, public domain and modified

For the recording of the brain potentials an amplification of the currents is necessary. This is done with the help of differential amplifiers. The differential amplifier returns the amplified subtraction of two channels.

$$\mathbf{V_{output}(t) = G \times [V_{input1}(t) - V_{input2}(t)]}$$

$V_{output}$: Potential at amplifier output
G : Gain
$V_{input1}$ : Potential at amplifier input 1
$V_{input2}$ : Potential at amplifier input 2

By calculation of the subtraction, only the differences of the two channels at a given time-point will be presented. Since artefacts mostly affect both input channels they will be subtracted and not displayed (common mode rejection). The important constraint of this method is the lack of information about the polarity at both inputs of the amplifier once the signal has been processed.

Especially when used in bipolar montages only the relation of the amplitude is displayed.

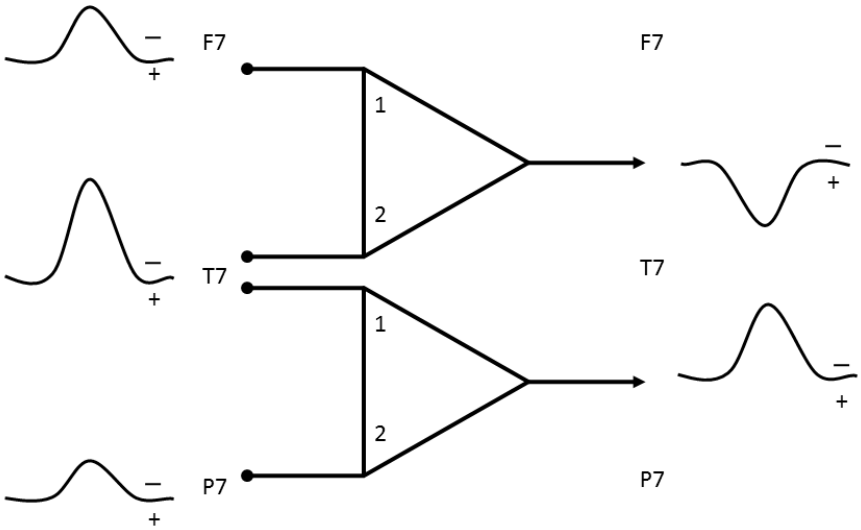


Figure 2.6: EEG differential amplifier showing the processing of three electrodes and the resulting waveform. F7 at input 1 is more positive than T7 at input 2 → + F7 - ( - T7) = + F7 + T7 = + F7/T7 → positive deflection, T7 at input 1 is more negative than P7 at input 2 → - T7 - ( + P7) = - T7 – P7 = - T7/P7 → negative deflection, own drawing.

After amplifying the calculated channels will be displayed onto a screen in standardised order, called montages. By selectively connecting different electrodes or groups, bipolar or referential montages are created.

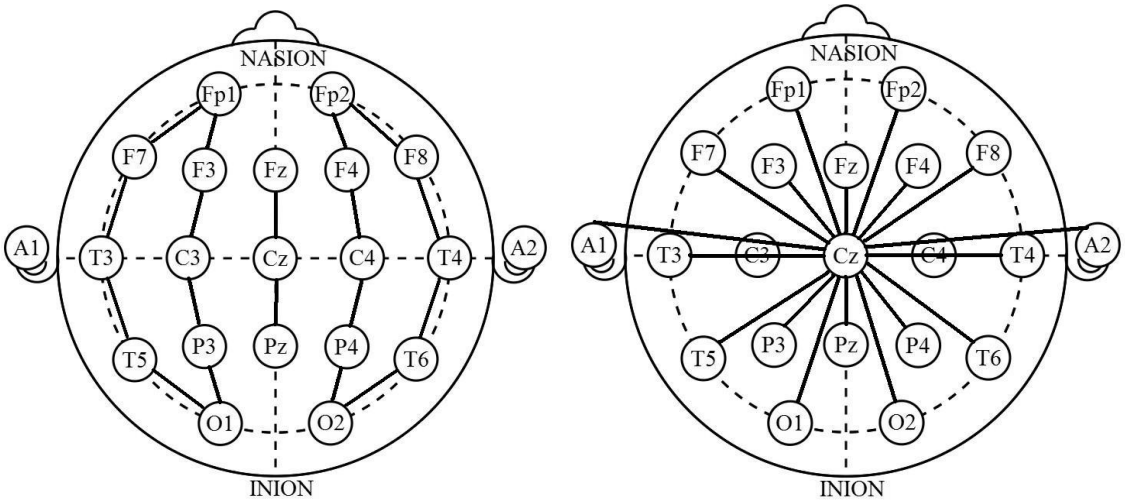


Figure 2.7: Bipolar longitudinal montage (left) and referential montage to Cz (right) marked by thick black lines. Taken from wikimedia, public domain and modified.

Bipolar montages usually display parallel longitudinal rows. Characteristic feature of longitudinal rows is the connection of the first electrode with input 1 and the next electrode with input 2.

Referential montages show the electrode of interest at input 1 which always is connected to the same or the same combination of reference electrodes at input 2. Two montages are schematically shown in figure 2.7.

The EEG is capable to record radial potentials in relation to the electrode since tangential sources are usually cancelled out.

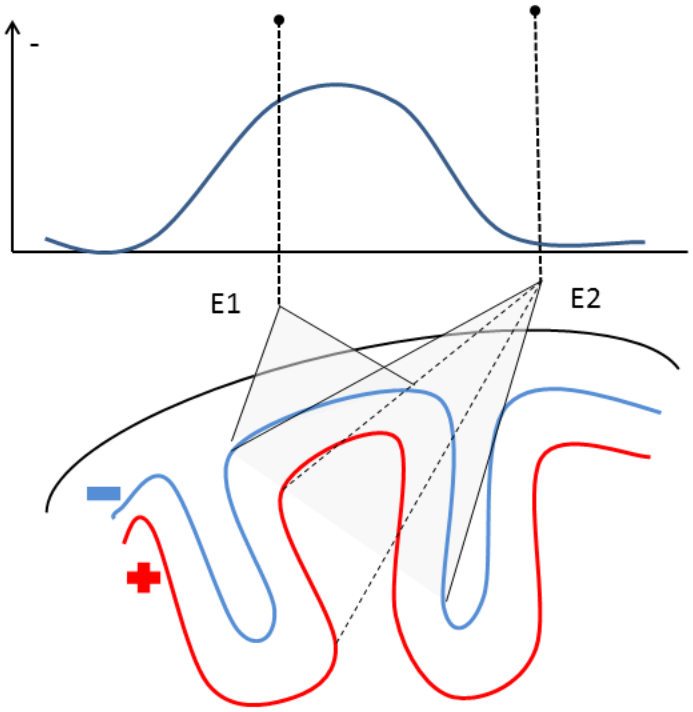


Figure 2.8: Tangential recording of EEG electrodes. E1 records the negative convexity of the cortex only (blue), E2 sees both negative and positive (red) areas which cancel out. The peak corresponds to the centre of the negative source (Modified from CCF lecture)

In contrast to the MEG (see below) tangential sources are recorded only to some part and only then, when radial parts of the potential fields are recorded by a rather distant electrode.

## Basic principles and definition of epileptiform discharges (ED)

When epileptiform activity occurs in the brain specific changes in the field potentials of the membrane potentials can be recorded. These specific patterns are called epileptiform discharges (ED). Based on the high degree of synchronisation of the underlying neuronal activity these field potentials are higher in amplitude than the normal background activity (Speckmann, Erwin-Josef, 1986, pp. 75, 97, 98). By summation, the anatomical orientation of the neurons (radially orientated pyramidal cells in the cortical layer) and the

characteristics of the potential shifts in the extracellular compartment, mostly the negative pole of the electric dipole can be recorded by the nearest EEG scalp electrode (Wyllie et al., 2010, p. 95; Zschocke S and Hansen HC, 2011, p. 8). In some conditions a real dipole can be recorded in routine EEG when the activated cortex area is recordable from two distant EEG electrodes. These dipoles usually are recorded in the central regions.

Often the positive pole is projected to the trunk where it cannot be picked due to lack of electrodes in this region. On the other hand the positive pole is projected to an electrode on the opposite side of the brain. There it can only be picked up as a far field potential where it has lost its sharp configuration and is covered by the noise. Only in case of averaging similar epileptiform discharges it can be made visible by increasing the signal to noise ratio for the positive pole as well (see figure 3.24)
Epileptiform discharges can be grouped in spikes, spike wave complexes, polyspikes or sharp waves. The grouping is solely descriptive by morphology. Especially in the case of the distinction between spikes and sharp wave it is not based on any pathophysiological correlate.

**Spike:** A potential showing a bi- or triphasic waveform and a sharp negative peak, with a characteristic duration of 20-70ms. The measurement of latency is subject to discussion and no valid definition is to be found. Some lecturers (i.e. from Cleveland Clinic Foundation, Ohio, USA) claim that the spike is measured at midpoint between the baseline and the peak of the spike, whereas this definition is arbitrary. The potential sticks clearly out of the background activity at common registration speed and display settings. The first slope to negative peak is steeper than the second slope after negative peak. The amplitude varies and is not subject to the definition. Often a Spike is followed by an aftercoming slow wave (see Spike-Wave-Complex) (J Gotman and Gloor, 1976; Jean Gotman, 1999; Noachtar et al., 2005).

**Sharp wave:** Similar waveform and characteristics as spike. In difference the peak is less sharp configured and the latency longer (70-200ms). A sharp wave usually is followed by an aftercoming slow wave (See figure 2.8).

**Sharp- or Spike-Wave-Complex:** Combination of a Spike or a Sharp-Wave and an aftercoming slow wave with negative peak. Can occur uniquely or repetitive.

**Poly-Spike-Complex:** Series of spikes containing repetitive zero crossings and associated aftercoming slow wave, also called Poly-Spike-Wave-Complex.

**Sharp-transient:** Sharply configured waveform not clearly meeting all criteria of an epileptiform discharge. Usually marked for further considerations but not rated as epileptiform event.

In summary the following criteria apply for all epileptiform discharges:

- Slope to negative peak is steeper than slope after negative peak
- Signal clearly sticks out of the background in usual reading conditions
- Aftercoming slow waves may follow, mainly with negative dominating polarity
- The signal is clearly affecting more than one electrode and shows a physiological field distribution
- Can be associated with rhythmic delta slowing in same region
- Can be associated with asymmetry of background activity, amplitude reduction in same region.

(Noachtar et al., 2005; Wyllie et al., 2010, p. 94; Zschocke S and Hansen HC, 2011)

All epileptiform discharges represent electrical dipoles, which are short, synchronous potential fields with a negative as well as positive maximum and a spatial orientation at a given time point. For deep generators it is often not

possible to record both poles in the EEG. This is due to different reasons stated below:

- One visible pole is usually near to scull and has a predominantly radial component. This pole is recorded in the EEG with high amplitude and a sharp waveform as signs of a near field potential. Often this pole has a negative deflection
- The opposite pole often projects into deep brain structures or the trunk. This pole is usually registered by a distant electrode with low amplitude and a broad waveform as signs of a far field potential. This pole often is of a positive deflection.
- The opposite pole amplitude (far field) usually is lower than noise level, often only detectable after averaging
- Alteration of signal quality by volume conduction at distant electrodes
- Maximum of near field pole outside the electrode range (mostly below)

If an ED is recognised and meets the given criteria, it will be marked in the data. This follows the clinical convention that it should be marked at the peak of the signal in the channel of the highest amplitude in a referential montage as seen in the lower channels of Figure 2.8.

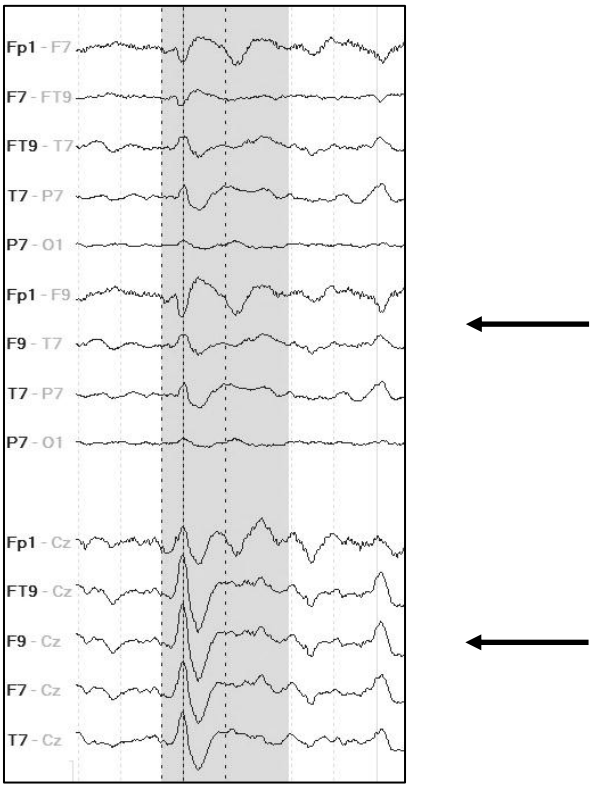


Figure 2.81: Sharp wave regional F9, seen in bipolar montage and referential montage to Cz. Negativity is up by convention (figure taken from data processing).

This maximum peak of amplitude in the referential montage as well as a negative phase reversal in a bipolar montage marks the position with the maximum negativity and therefore the regional maximum of the ED.

**Interictal Spikes** are epileptiform discharges recorded in seizure free intervals. After Lüders, these ED define the irritative zone and can be considered as very focal seizures not spreading to other cortex regions. Only seldom these discharges are accompanied by clinical symptoms if eloquent cortex is affected (H. O. Lüders et al., 2006). Zschocke explains potentials recorded in the EEG by fast changing focus in selective cortex layers caused by ion shifts and the postsynaptic potentials. By this a small positive peak is followed by the main negative peak. This negative peak is caused by the sum of synchronised paroxysmal cell depolarisations of the big synchronised and radial orientated pyramidal cell (Zschocke S and Hansen HC, 2011, p. 160).

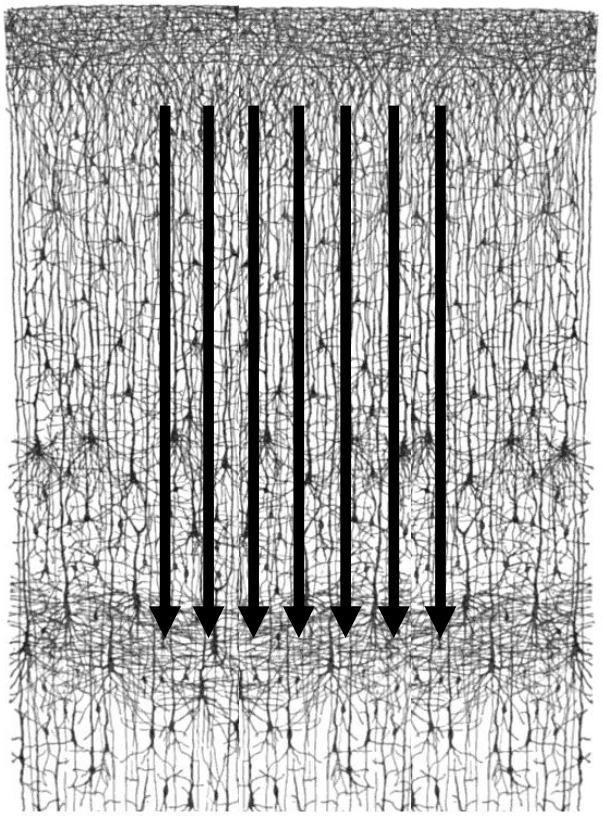

Figure 2.9: Schematic representation of the parallel organised activated neurons in the cortical layer. Taken from Wikimedia, modified drawing by Santiago Ramon y Cajal (1852-1934)

To record and display such a potential, about 600 to 800 synchronously activated neurons are necessary and an activated cortex patch of 6cm² minimum size (Lehmenkühler et al., 1991). In other studies, activated cortex patches of 10-20 cm² are stated, whereas in these studies insulating cortex grids had been placed between the cortex and the recording electrodes (Tao, Baldwin, Hawes-Ebersole, et al., 2007; Tao, Baldwin, Ray, et al., 2007). In recent years also a much smaller amount of activated neurons is discussed, so that a number of 300 neurons in a cortex area of just a few mm are needed to produce recordable spikes (Albowitz et al., 1998; C. . Elger and E.-J Speckmann, 1983; Gorji et al., 2006; Rüdiger Köhling et al., 2000; Schomer and Silva, 2011).

Special focus will be put on these interictal spikes since this subgroup of epileptiform discharges represents the epileptogenic zone and is of special interest for the source localisation (H. O. Lüders et al., 2006). Because of the described pathophysiology the peak of the signal is the marker of the highest synchronicity and represents the highest number of simultaneously activated neurons. Furthermore the beginning of the signal represents the starting point but mostly is covered in the noise. With respect to source localisation it needs to be taken into account that the dipole position may change between the first positive peak (beginning of the signal) and the negative peak as feature of highest synchronicity (J S Ebersole and Wade, 1991). Despite this many publications actually suggest to make use of the spike localisation at the negative peak as an estimate of the irritative zone (Shiro Chitoku et al., 1999; Ayako Ochi, Hiroshi Otsubo, Sharma, et al., 2001; Ayako Ochi, Hiroshi Otsubo, Shiro Chitoku, et al., 2001; H. Otsubo et al., 2001; Hiroshi Otsubo et al., 2001; Sato et al., 1991; H Yoshinaga et al., 1999). These aspects will be discussed and evaluated as parameters for the data pre-processing.

#### 2.1.2.3. Magnetoencephalography (MEG)

With the help of magnetoencephalography (MEG) the magnetic field changes induced by the human brain can be recorded noninvasively and directly (Hämäläinen et al., 1993; Y. C. Okada et al., 1984; Y. Okada et al., 1999; Samuel J. Williamson et al., 1991). It can detect magnetic fields in the range of femtotesla ($10^{-15}$ Tesla) as long as artefacts from external magnetic sources like the earth's magnetic field ( about 50 µT), field from electric wiring (<10µT) or urban environmental noise like a bypassing lorry ($10^{8}$fT) are cancelled out. This usually can be reached by creating a shielded room, where the measurement is taking place and by a special setup of recording sensors positioned over the scalp. Measurement sensors are close to the skin, reference sensors are positioned in some distance. By this arrangement of the sensors, called squids (super conducting quantum interference device) the EMG is able to actively cancel out magnetic fields not deriving from the underlying brain structures (Lau et al., 2008). Under optimal circumstances temporal resolution of less than a

millisecond and spatial resolution of less than a millimetre can be attained (Brenner et al., 1975; Hämäläinen et al., 1993; R. Hari et al., 1988; Y. C. Okada et al., 1984; Y. Okada et al., 1999; Romani et al., 1982). First MEG recordings have been made by David Cohen (D Cohen and Cuffin, 1983; David Cohen and Givler, 1972) with a single channel magnetometer.

Whole head MEGs can record more than 300 sensors at a time. The recording is reference free, no montages are necessary. With respect to source localisation and the importance of combining different methods like EEG and MEG, it is important to strengthen the facts that MEG is mainly sensitive to tangential dipoles and mainly neglects the radial component of the dipole vector since electrical and magnetic fields are complementary to each other. With respect to epilepsy research this means that there are epileptic spikes which might only captured by MEG or vice versa only by the EEG. It also means tha mostly superficial neocortical generators with sufficient tangential orientated component are captured by the MEG (Iwasaki et al., 2005; Harumi Yoshinaga et al., 2002). MEG recordings primarily measure intracellular currents which are induced by the synaptic potentials since the magnetic field of the extracellular volume currents mainly tends to cancel out (Barth et al., 1986; D Cohen and Cuffin, 1983).

Usually a recording lasts a few minutes, where the subject needs to remain still to avoid errors in spatial registration. Because of the complex technology MEG is much more expensive than scalp EEG and the expertise for MEG analysis and interpretation is less well established.

As stated above the brain is capable to create dipoles during signal processing. In case of an epileptic discharge a large number of synchronised and parallel organised neurons will be activated. In this dipole the electric current will flow over a rather short distance from local positivity to local negativity. The induced magnetic field created by the dipole is characterized in strength and orientation and follows the right hand rule (figure 2.10).

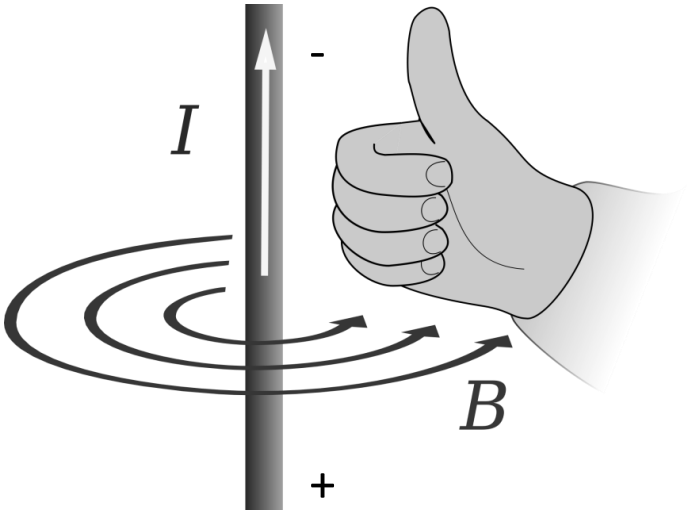


Figure 2.10: Right hand rule is a physics principle applied to electric current passing through a straight wire, resulting in a magnetic field. The thumb points in the direction of the conventional current (from positive to negative) and the fingers in the direction of the magnetic field. Taken from Creative commons, Wikimedia

Dipolar models are based on the assumption that a small number of current sources as multiple dipolar neurons or sheets of dipoles in the brain can model surface measurements. After Biot-Savart's Law, the general equation for the magnetic field strength, the falloff of the magnetic field is quadratic with the distance to the dipole. Furthermore, the deeper the source, the more radial is its orientation, which additionally weakens its fields outside the head. However, since the definition of radial and tangential is only valid in a spherical conductor, the situation gets more complex in realistic heads (C.H. Wolters et al., 2006).
MEG is able to contribute new aspects to epilepsy research and the outcome of epilepsy surgery. Patients undergoing epilepsy surgery with MEG recording in the presurgical evaluation were more likely to become seizure free after 6 months (Knowlton et al., 2008).

#### 2.1.2.4. Other diagnostic tools in epilepsy evaluation

During pre-surgical epilepsy evaluation and to some part in the routine diagnostic different diagnostic tools are used to analyse the origin of the

epileptic discharges or to find underlying diseases. With the help of **magnetic-resonance-imaging (MRI)**, internal structures of the brain can be visualized in detail. With improving techniques and scanners, better images with high resolutions can be produced and even small tissue alteration can be detected. The **positron-emission-tomography (PET)** and the **single-photon emission computed tomography (SPECT)** are nuclear medicine imaging techniques which create pictures of functional processes in the body or brain. After radiation emitting tracers (radionuclides) are administered to the patient their accumulated concentration will be measured in a three dimensional picture and show areas of higher or lower metabolism in specific regions.

Besides the routine EEG and the MEG, specific epilepsy centres will use **video-EEG monitoring** to capture several days of recording EEG and expected seizures. These data is co-registered and recorded features can be evaluated in EEG and video monitoring at the same time in order to define seizure semiology. In addition in specific cases invasive EEG monitoring will be used to implant grids of electrodes or intra-cortical electrodes to record epileptic discharges as near as possible to the suspected generator of the epileptic seizures.

Before epilepsy surgery is taking place, **neuropsychological tests** and **functional imaging (Wada /fMRI)** will be done to define eloquent cortex and to avoid lasting impairments for the patient after surgery.

### 2.1.3. Data processing and software applications

During the evaluation of the recorded data mainly two software packages were used which will be described in the following passages.

#### 2.1.3.1. Curry Neuroimaging suite 7.02 SBA

This commercial tool is a package for EEG acquisition, analysis, image data processing and source reconstruction. It is distributed by the Compumedics USA Inc.. At the IBB the current version 7.02 SBA was installed with the packages signal processing, basic source analysis and advanced source analysis. It was used as a comprehensive tool to combine MEG and EEG data

with imaging data for source reconstruction. It has implemented different algorithms for source localisation. After the data was recorded with the CTF Scanner (see below) it was loaded to Curry for pre-processing. All readers used the current Curry user interface to mark the epileptic discharges.

#### 2.1.3.2. Matlab R2010a

Matlab is a commercial tool for numerical computing and a fourth generation programming language. The name derives from a contraction of “Matrix Laboratory”. It is developed and distributed by the company MathWorks. Matlab uses matrix manipulations, plotting of functions and data. During the evaluation Matlab R2010a Student was used. In general, Matlab uses variables and can manipulate arrays of one dimension (vectors), two dimensions (matrices) or more dimensions. The software application is using the Matlab code which is directly typed into the Command window or can be executed by text files containing Matlab code or functions. These text files are called Scripts when they contain a sequence of Matlab statements. Functions make use of their own local variables. Functions need to be called from the Command Window, a script or another function and they need a defined set of input arguments. After calculation in the function, all local variables are lost and output arguments returned to the workspace. These scripts and functions are created in a separate editor and can be run at once. Even though Matlab can basically deal with classes the syntax and calling conventions differ significantly from other programming languages. For the data evaluation during the project, Matlab was used for data processing.

During our data evaluation a number of scripts and functions were created allowing specific data analysis and manipulations as stated extensively below.

## 2.2. Diagnostic procedure and evaluation

All sets with co-registered MEG and EEG data derive from the DFG study and were recorded at the Institute for Biomagnetism and Biosignalanalysis at the University of Münster. All recording procedures had been approved by the ethic committee and the DFG in advance.

For all recordings a VSM Medtech Ltd., Omega 2005 whole head MEG was used. It has 275 channel gradiometers, additionally 29 reference sensors for MEG- and 74 electrodes for EEG-recording as well as 6 channels for electro-oculo-graphy (EOG). The EEG is registered using a 74 equidistant electrode (Ag/AgCl) position cap, applying the international 10/10 system. During recording a sampling rate of 2400Hz was used to also allow analysis of fast ripples. For our purposes this data is processed with a 100Hz low pass filter to avoid aliasing and finally down-sampled to 300Hz.

For the thesis study 19 datasets from four patients were selected all recorded in the time between November 2011 and January 2012. Each recorded run lasts about 8 minutes and contains co-registered up to 304 sensors MEG and 74 electrodes EEG data. Subjects age ranged from 17 to 41 years, mean 27.5 years, gender equally distributed. All subjects have been diagnosed with epilepsy before and basic information from the health care record was provided.

### 2.2.1. Marking of epileptic discharges by clinical readers

All datasets have been read, evaluated and marked by 3 independent readers at different times between April 2012 and June 2012. For display and marking Curry Neuroimaging suite, version 7.03 SBA was used, distributed by the Compumedics USA Inc. (see 2.3.1). The 19 datasets were marked individually with the knowledge of the basic information from the health care records as cerebral imaging and common features of the individual seizures. For this study, primarily EEG data was read and marked. In a second evaluation, additional epileptic discharges in the MEG will be marked additionally.

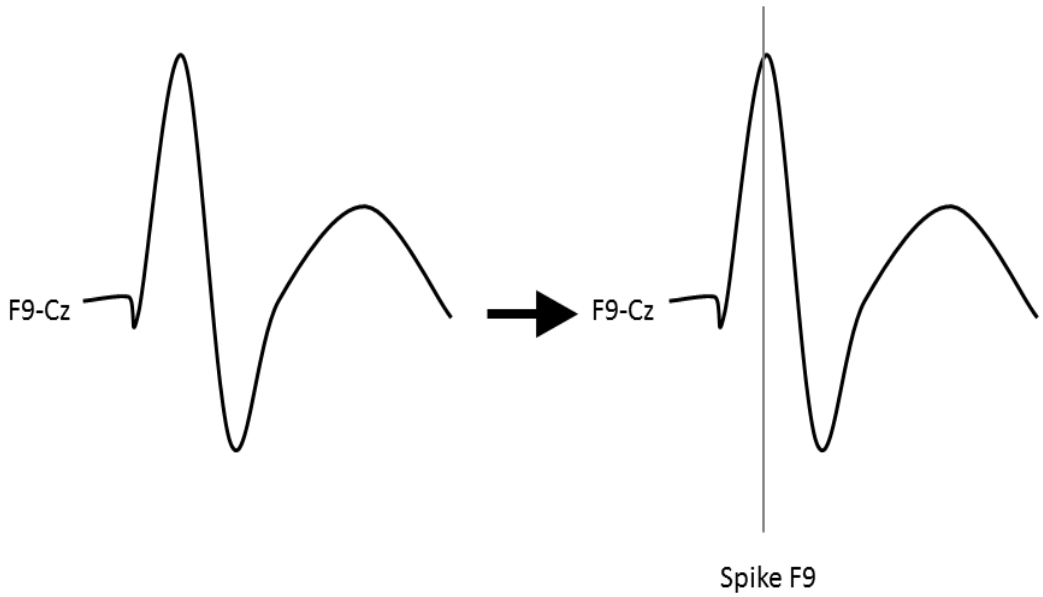


Figure 2.11: Marking of a spike in channel with maximum amplitude in reference montage. In this example the negative peak of the waveform in channel F9-Cz is selected.

The marking of the spike was done after general agreement on best clinical practice. For best evaluation and for comparison reasons, epileptic discharges should be marked at a genuine and in all cases clearly distinguishable position. As stated in 2.1.2.2 the highest synchronicity of the activated neurons will be at the negative peak of the signal. Even though latency, zero crossings and slopes will change from spike to spike, the only consistent position distinguishable from the background noise will be the negative peak. So it was expected that the marking at the position of the peak by hand will produce the gold standard of results for further processing.

All markings were assigned with an electrode name, stating the electrode with the highest amplitude in referential montage. This also was considered best clinical practice and was assumed to result in clearly defined clusters of epileptic discharges referring to their regional occurrence.

All results were saved in a program specific report file, readable by a text editor in the ASCII format. The relevant data for our further processing is the position

of the marker in number of samples and the assigned name given by the reader.

**Detection of epileptogenic discharges by automated algorithms**

Even though the main aim of this study does not deal with the question of computer aided de novo detection of epileptic discharges, a short summary on the topic will follow to give an overview over the issues in this field. In the past many publications have been made about ideas and advances of automatic detection algorithms for EEG or MEG data. First papers have been published by Gotman and Gloor in 1976 and 1977, proposing a decomposition of the waveforms to detect spikes automatically by computer software (J Gotman and Gloor, 1976). Many publications followed by Dümpelmann, Elger, Flanagan, Ji, Ossadtchi, Pang, just to mention a few of them (Dümpelmann and C. E. Elger, 1998, 1999; Flanagan et al., 2002; Ji et al., 2011; Ossadtchi et al., 2004; C. C. C. Pang et al., 2003). In most of the cases, precision and sensitivity are claimed to be better than hand marking procedures. Some of these algorithms were implemented in commercial analysing software almost none has been published for public domain use. Finally we were not able to implement any of these software codes for general de novo spike detection in common software packages. Commercial tools have not been evaluated.

In order to improve the detection of known spikes in a dataset, some software packages offer the function of a template search. As soon as an epileptic discharge has been defined by a clinical reader it can be used as a template for further automatic detection of matching epochs in the dataset. In the used feature offered by the software package Curry 7, amplitude and correlation criteria may be selected from 50% to 90% compliance. First the algorithm will search the data for an event matching the amplitude criteria. If this is set to 90%, the software will search in predefined channels for voltages that are at least 90% of the amplitude in the template. If this criterion is met, the correlation feature will compare the template with the new match. If correlation exceeds the predefined value, the match will be marked in a separate event-list.

## 2.3. Source localisation

Once EEG and MEG data has been obtained and evaluated the clinical reader is able to localise abnormalities to regions with a rather restricted precision only. The aim of source localisation is to determine the area of the brain where electric dipoles are generated from the recorded potentials or magnetic field on the scalp. In this so called **"inverse problem"** the localisation has to be estimated from the recorded data. In the **"forward problem"** the position of the generator is known and the field distribution at the area of interest can be uniquely calculated (Helmholtz, 1853; C. H. Wolters et al., 2008).

For every source localisation a first calculation of a **forward solution** is necessary. Even though this result can be calculated uniquely in theory, it is difficult to obtain since many inhomogeneities, the anisotropies of the brain and the surrounding tissue have to be taken into account. In the past and currently better head models are created to improve the approximation for a better calculation of these influencing factors. It is widely accepted e.g. that conductivity in the compartment of cerebrospinal fluid is much higher than in other compartments (Baumann et al., 1997). In general the inhomogeneities in resistivity affect the EEG electric field much more than the magnetic fields for MEG recordings (C.H. Wolters et al., 2006).

The **"inverse problem"** is a method to estimate backwards the intracerebral location and orientation of the underlying neuronal generator of an epileptiform discharge. Theoretically there are infinite numbers of possible correct answers. Therefore, depending on the prior information, different approaches to find the best solution for localising the generator have been made. Dipole fit methods are based on the assumption that a limited amount of current sources as multiple dipoles in the brain can adequately create surface measurements (Sheltraw and Coutsias, 2003, Wikipedia). Since without any priors no unique solution exists, the so-called restricted inverse solution was introduced where predefined assumptions about the current sources and the volume conductor are included in the algorithm (Stok et al., 1987).

The calculation of possible solutions is based on models created with the knowledge of brain activity. The three major models are sketched as follows.

The **dipole fit approach** is commonly used as single or multiple dipole models. On the basis of a registered magnetic field the best fitting dipole with its parameters location, orientation and strength is iteratively calculated. For the calculation a starting point, called initial guess is necessary.

The **linear model** uses the so called minimum norm estimation. A predefined set of known dipoles (1000 to 10000) with set positions and orientations is used. For a recorded magnetic field dipoles are calculated and compared. No initial guess is necessary as no bias by human interpretation is likely. A recent overview and comparison was recently discussed by Lucka et al (Lucka et al., 2012).

As **source model,** commonly the mathematical point-dipole is used. A magnetic field is represented by a single source and is characterized by strength, orientation and position. In the multiple ECD (equivalent dipole current dipole) the magnetic field is represented by multiple sources located in the brain compartment. It is commonly accepted and justified to use this model as long as neocortical generators assumed to be in the cerebral cortex are evaluated. As stated in the methods' section, the synchronized neuronal activity is generated at the apical dendrites of cortical pyramidal cells, which are anatomically organized in columns, perpendicularly orientated to the cerebral cortex (Barkley and Christoph Baumgartner, 2003). The spatial extend of this activated patch cannot be described by the point-dipole model since this model is an estimate of the centre of gravity of the source and represents the activity of a small collection of synchronised neurons (Grynszpan and Geselowitz, 1973).

For localisation, different head models are used. The **concentric sphere model** consists of simple spherical compartments representing roughly the main areas of the head. In the **boundary element model (BEM)** and the **finite element model (FEM)** more precise models of the brain topography, brain tissue and especially different conductivities are taken into account.

MEG and EEG source reconstruction might differ as stated above. A time lag between MEG and EEG spikes has been evaluated and discussed before in several publications (Bast et al., 2004; Merlet et al., 1997; Ekaterina Pataraia et al., 2005). One explanation for the asynchrony given by Merlet et al. is the

preferred sensitivity of the MEG to superficial tangential sources. The MEG signal may be larger in relation to the EEG signal, when the early neuronal activity is generated by rather tangential parts of the cortex. After propagation a larger and more radial orientated cortex patch can be activated resulting in a more dominant potential in the EEG recording. In later studies this effect has been recognized as well and a similar explanation was proposed (Ekaterina Pataraia et al., 2005).

With respect to source localisation in EEG, more constraints have to be considered. The electrical field is more distorted by volume conduction and more precise head models are necessary (Brette and Destexhe, 2012). The signal used for the calculation must be as clean and reliable as possible. Often the equivalent dipole model is used (C Baumgartner et al., 2000; J S Ebersole, 1997; Robert S. Fisher et al., 2005; Hiroshi Otsubo et al., 2001; Ekaterina Pataraia et al., 2005; Stefan et al., 2003, 2004; Harumi Yoshinaga et al., 2002). It is known that depending on the size of the activated cortex patch the equivalent dipole fit might be located in the underlying white matter. This estimated depth correlates with the extent of the activated cortical patch and the effective conductivity of the different brain compartments as well as from brain to scalp. (Lucka et al., 2012; Ramantani et al., 2006). Also the cortical activation might have been propagated to other regions during the time-course of the epileptic spike. In any case, the source localisation at the negative peak of the waveform represents only one specific position of the calculated dipole at this time point and might well differ from the onset of the epileptic discharge. As already discussed in the EEG chapter (2.1.2.2) many publications actually suggest to make use of the spike localisation at the negative peak as an estimate of the irritative zone (Shiro Chitoku et al., 1999, 2003; Hiroshi Otsubo et al., 2001; Sato et al., 1991; H Yoshinaga et al., 1999).

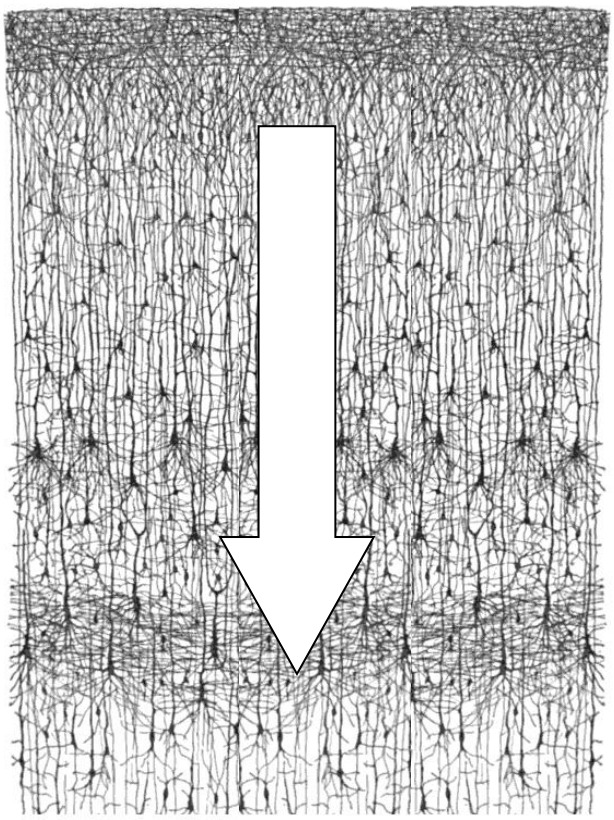

Figure 2.12: Schematic display of a calculated dipole in the cortex layer which does not represent a physical structure. Taken from Wikimedia, modified drawing by Santiago Ramon y Cajal (1852-1934)

Regarding the single equivalent dipole solution it needs to be strengthened that this dipole does not represent a physical structure in the brain. As stated before, it represents the centre of gravity of a volume of currents and might locate to a neighbouring structure depending on the size and shape of the volume of activated neuronal tissue (Barkley and Christoph Baumgartner, 2003; Lucka et al., 2012).

**Averaging** was discussed by Thickbroom et al in 1986 in order to use multiple similar spikes to reduce background noise (Thickbroom et al., 1986). After averaging and increasing the signal to noise ratio, other interesting parts of the waveform might get uncovered so that also earlier time- points might be evaluated (Thickbroom et al., 1986). During the averaging process different

sub-clusters of spikes are likely to be mixed and the signal therefore might be contaminated (Bast et al., 2004, 2006). In these studies template search algorithms have been used after defining spike clusters by spatio-temporal analysis and averaging some signals for the template.

In many publications about source localisation in EEG and MEG, no information is given about the exact way of marking the spike and the process of averaging (Shiro Chitoku et al., 2003; Harumi Yoshinaga et al., 2002). In some cases it is referred to the practices of the clinical readers taking different marking procedures into account for inter-rater reliabilities (Barkmeier et al., 2012). Here marking differences for the same spike of up to 120 ms are stated. This fact can be neglected as long as the study does not lead to source reconstruction. Since in averaging studies the marking at the same morphological feature of the epileptiform discharge is important, a closer look at the outcome and the precision of unaided markings needs to be taken.

For source reconstruction of interictal spikes the following parameters are necessary and should be taken into account:

- High signal to noise ratio
- Precise marking of the epileptiform discharge
- Averaging
- High correlation of similar spikes
- Clear clusters of identical spikes
- High number of spikes for averaging

**Recent procedures for data pre-processing and source localisation in summary**

The leading goal of this master thesis is to find, evaluate and improve possible unexpected or unrecognized factors influencing the signal quality at the intersection between medical and methodological staff involved.

Summarising the recent clinical practice, the workflow for localisation of epileptic generators worked as follows and was taken as gold standard.

- Recording of combined EEG / MEG data of selected subjects
- Filtering of the data to avoid aliasing and down sampling to 300Hz
- Reading and evaluation of the data by clinical readers
- **Marking of all epileptic discharges at the negative peak**
- **Clustering of all epileptic discharges to the respective electrode with maximum amplitude**
- **Averaging the resulting clusters without further evaluation of the spatial topography for source localisation**
- **No search for additional spikes possibly left out by clinical readers but still meeting the criteria**
- **No independent MEG marking** (*planned as independent evaluation in course of DFG project)
- No **standardised procedure** at intersection between clinical readers and further data processing

Factors for further evaluation and improvement in this thesis are marked in bold.

# 3. Results

In this chapter the identified factors influencing precision of source localisation will be evaluated and separately discussed.

While analysing the intersection between clinical reading and methodological processing of the data special emphasize was put on the demands for a good and reliable signal. As highly sophisticated and precise head models will be used in the further process of the DFG project, it was important to rule out any unexpected systematic errors during the pre-processing of the data especially at the mentioned intersection. Furthermore a standardized way was developed and implemented to evaluate and improve all future datasets for source reconstruction. In this chapter the detected influencing factors will be separately explained and evaluated as well as the main parts of the respective algorithm are discussed. The main scripts of the Matlab files are attached in the appendix as print out.

**Methods:** For all pre-processing procedures either the Curry 7.03 user interface with its implemented features was used as described or external calculations have been made with Matlab. For these calculations a standardized procedure was defined and used. In the Curry program, the respective run of the MEG / EEG recording was first loaded and the following parameters set:

- band pass filter: 1-70Hz
- notch filter 50Hz, harmonics
- constant baseline correction for EEG
- common average montages used in later source reconstruction for EEG

After visual inspection all channels with obvious artifacts were deselected, usually 2-3 channels. The selected dataset was exported to a .dat ASCII coded file, which could be opened easily by Matlab for further processing. When exported, three different files are created automatically (see Figure 3.2 for further details). The main file .dat contains the amplitude value for each sensor and electrode at every sample-point (300Hz). The data is organized in a matrix,

where columns are coding for the electrodes/sensors whereas the rows are coding the sample-points. Furthermore a .rs3 file is created which contains information about the spatial position of sensors and electrodes during recording in relation to the head. As well the assignment of the number and name of electrode to each column of the data file is set. These data are all stored in a folder for structured analysis.

## 3.1. Toolbox summary for data evaluation

During the evaluation of factors influencing signal-to-noise ratio and precision of source localisation from combined MEG/EEG recordings a number of supporting Matlab scripts were created, refined and combined for the pre-processing of the data. The main parts of the program code and the usage are described in the respective chapters of this thesis. In figure 3.1 the schematic organisation of the current methods of the toolbox is shown.

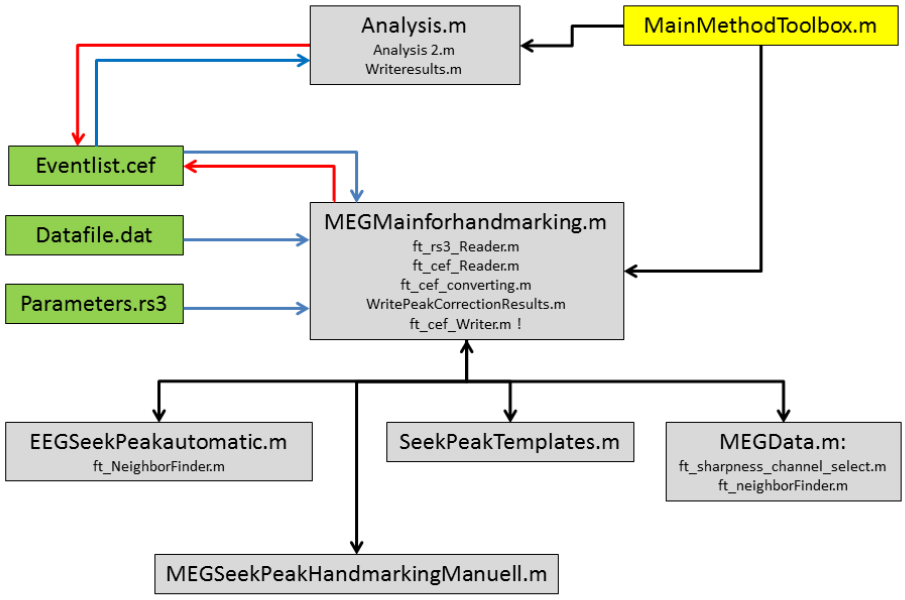


Figure 3.1: Matlab toolbox for data pre-processing. All preceding methods have been combined and reduced as much as possible to get an easy to use and to understand toolbox. In the diagram the basic processing of the methods is described. Green boxes = data files, grey boxes = Matlab methods and depending functions, yellow = Main Method to start, blue arrows = reading data, red arrows = writing data

**Main Matlab script "MEGMainForHandmarkings.m"**

All Matlab scripts and methods are created for general analysis of this kind of data and automatically realize all steps for importing the data and loading all necessary information from the given Curry files. All steps are interactively described and controlled by the user either with implemented Graphical User Interfaces (GUI) or in the command window. Only basic knowledge about the mechanisms of Matlab and the data structure is needed. As seen in appendix part 1, the main method of the Matlab scripts **"MainForHandmarkings.m"** imports the data using a graphic user interface (GUI) for individual selection of the datafile and writes these information to a central matrix called **"Teildaten"** (Step 1). In the next step (Step 2) all relevant information as electrodes' and sensors' names as well as positions are read from the assigned .rs3 file by a separate Matlab-function called **"rs3_reader.m"**. Important information as the current electrode settings, so the assignment of the column number to the respective electrode or sensor name is written into an excel file which can be opened separately for reference during processing of the data (Step 3).

Finally the event-list file (.cef) is read by a Matlab routine importing all relevant information from the hand markings of each individual reader (Step 4). This event-file holds the information about the position of the peak, an interval around this marking and a code for the kind of marking for each marking assigned. For example an event manual1 is assigned "200001", manual2 is assigned "200002" and so on. Additionally each reader needs to name it individually; usually the type of epileptiform discharge and electrode with amplitude maximum is stated (see Figure 2.11). In summary for each event, the time point of the marker in the dataset, the event code and name is stated.

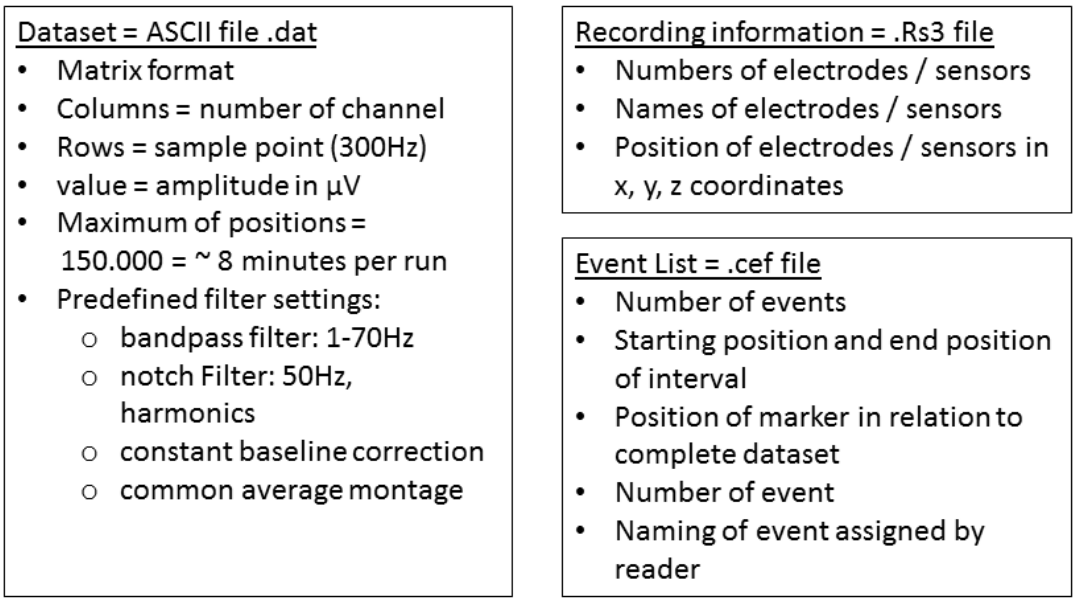


Figure 3.2: Summary of used files containing information relevant for current study

In Step 5 all events uniquely appearing in the event file are selected and the individually, not standardized naming by the reader is displayed. By documentation of the individual naming, the current event has to be assigned to its referring electrode of maximum amplitude for the Matlab matrix (figure 3.3). Following this, the events are separated in MEG and EEG events, since in some event-lists both modalities are marked simultaneously.

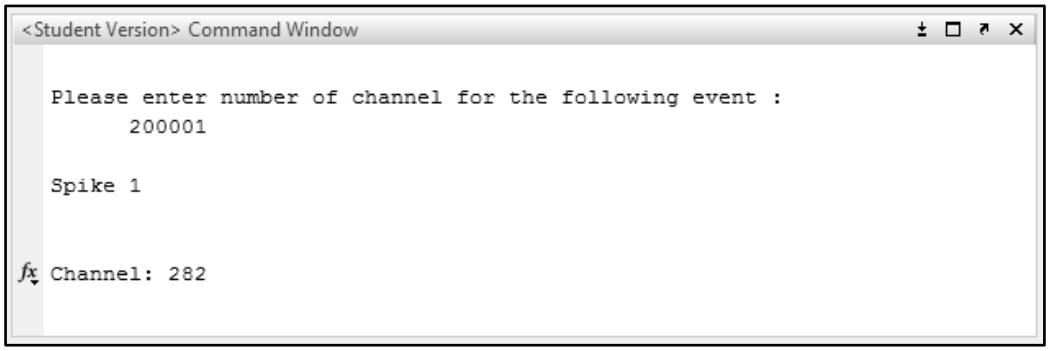


Figure 3.3: Example screenshot for an EEG event marked, information Spike 1 given by reader. Channel = input from User, channel number taken from current channel list

Step 6 asks the user to choose the method to run. In the current version, the following methods are available:

- EEGSeekPeakautomatic.m
- EEGSeekPeakManual.m
- SeekPeakTemplates.m
- MEGData.m (not discussed in this thesis)

After evaluation of the data by the specific sub-method selected, parameters are returned and processed by the method in order to save it back to the corrected .cef event-list. Additional log files about the changes and descriptive statistics are saved separately and automatically (Step 7).

## 3.2. Analysis and evaluation of hand markings

**Issue:**

To analyse the inter-rater variability of the interictal spike markings by all three readers, an automatic Matlab method was created and integrated into the main method. The aim was to create a tool for general use also for non-clinical staff and to deal easily with many event-lists to come during the on-going DFG project. With respect to source reconstruction purposes a tool was needed to combine the information of several reviewers to gain the maximum precision of the correctness of a spike.

For evaluating the inter-rater reliability we defined similar parameters as used in previous studies (Barkmeier et al., 2012; Brown et al., 2007; Dümpelmann and C. E. Elger, 1999). All reviewers were asked to mark the negative peak as the most prominent feature of the spike, but were free to use their best clinical procedure for marking. In opposition to the previous studies we defined a smaller time window of +/-15 sample-points (+/- 45ms) for matching results to avoid overlap and to be able to measure the primary precision for source reconstruction needed. The result of one reader was compared to the combined results of the two other reviewers. A **true positive** spike was defined as a spike, marked by at least one other reader as well. A **false positive** spike was defined

as a spike marked by the respective reader but not by any other reader and **false negative** spikes as a not marked spike by the respective reader but by all two other readers. From there the algorithm calculates the precision and the sensitivity for each run and reader separately and in relation to the other readers.

$$Sensitivity = \frac{true\ positives}{(true\ positives + false\ negatives)}$$

$$Precision = \frac{true\ positives}{(true\ positives + false\ positives)}$$

**Program code:**

The evaluation of the event-lists (.cef) created by Curry is realised by an algorithm implemented in the script files **"Analysis.m"** and **"Analysis2.m"**. It is called by the superior method **"MainMethodToolbox.m"** and guides the user through the data import and evaluation. At step 1 a flexible number of event-lists to compare can be loaded, whereas the current version is set to a maximum of 3 reviewers as needed for the study. All events are saved to separate but comparable matrices. In the next step 2 all event-lists are searched for uniquely existing events and during a question dialog each of these events needs to be assigned to the method, so either EEG or MEG, where it has been marked in. This is easily possible, since all assigned names by the reviewer are either documented or contain the kind of event in the name. This information is displayed during the assigning process as seen in figure 3.4.


Figure 3.4: Graphical user interface (GUI) for assigning the event to the method. In this case the event m1 (=200001) named Spike 1 F9 by the reviewer is assigned to EEG events.

Since there was no unified terminology agreed on, which made use of the names of Curry electrodes for example, there was no comfortable way to realise this automatically, but it could be easily implemented for further reviews of new datasets. Also it is possible to discard events if these events are marked artefacts or other events not for evaluation. In step 3 the dependent method **"analysis2.m"** is called for further evaluation. In this method it is possible to switch between the evaluation of either solely EEG or MEG data or both of it (step 4) and all unwanted events get deselected (step 5).

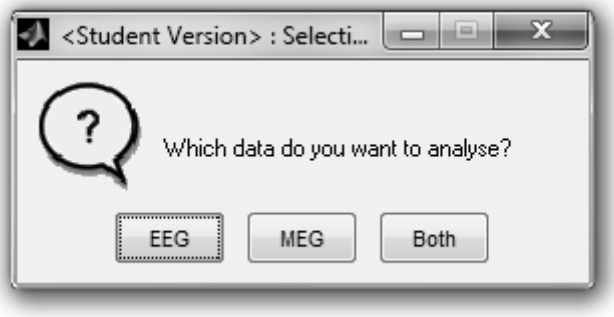


Figure 3.5: Graphical user interface (GUI) for choosing the kind of analysis to be applied to the data.

During step 6 the precision is calculated where each event of the respective event-list is compared to the others in the predefined range (called precision, set to 15 sample-points, 45ms during step 5). This matching list is evaluated during step 7 for intersections and finally the percentages and parameters for the descriptive analysis are set and calculated in step 8. The results are collected and written to a text file by the method **"writeresults.m"**. An example log file is attached in appendix 8.1.

**Results:**

A total of 57 event-lists have been analysed for this current study, resulting from 19 runs (of 4 patients) read by 3 reviewers. Reader 1 did not find and mark any EEG events in patient 3, run 2 and 3. Reader 2 did not mark any EEG events in patient 3, run 2, 3 and 4. Reader 3 did not mark any EEG events in patient 3, run 2, 3, 4 and patient 4, run 6 and 7. In total 1107 spikes have been marked by any of the reviewers separately which includes all overlapping results. Of these, 754 spikes were marked by at least one reader returning the sum of unique events in each of the sets displayed schematically in Table 3.1 and Table 3.2. A total of 85 events have been marked by all three reviewers. For reviewer 1 an overall weighted sensitivity of 60.03% and precision of 76.19% was calculated. For reviewer 2 the weighted sensitivity was 91.82% and precision 64.23%. Reviewer 3 gained a weighted sensitivity of 94.23% and precision of 44.42%. All results reflect the definition above regarding a spike as true if it is marked by at least two readers.

All these results can be calculated for MEG and EEG / MEG events additionally, as the method is created to deal with this information as well. For the current study only the EEG results were important, but it needs to be emphasized that the MEG calculation as well as combined MEG/EEG calculation is possible, though.

| EEG | Span 15 | unique spikes in run | Reader 1 Total EEG Spikes by reader | % by >=2 readers | % by 3 readers | Sensitivity | weight | Precision | weight |
|---|---|---|---|---|---|---|---|---|---|
| subject 1 | run5 | 63 | 3 | 66,67% | 0,00% | 22,22% | 0,67 | 66,67% | 2,00 |
| | run6 | 123 | 25 | 88,00% | 64,00% | 39,29% | 9,82 | 88,00% | 22,00 |
| | run7 | 107 | 20 | 100,00% | 75,00% | 58,82% | 11,76 | 100,00% | 20,00 |
| | run8 | 194 | 51 | 84,31% | 74,51% | 39,39% | 20,09 | 84,31% | 43,00 |
| | | | | | | | | | |
| subject 2 | run2 | 78 | 5 | 40,00% | 20,00% | 50,00% | 2,50 | 40,00% | 2,00 |
| | run3 | 28 | 2 | 100,00% | 0,00% | 33,33% | 0,67 | 100,00% | 2,00 |
| | run4 | 44 | 3 | 100,00% | 33,33% | 42,86% | 1,29 | 100,00% | 3,00 |
| | run5 | 41 | 11 | 63,64% | 27,27% | 77,78% | 8,56 | 63,64% | 7,00 |
| | run6 | 23 | 5 | 40,00% | 0,00% | 100,00% | 5,00 | 40,00% | 2,00 |
| | | | | | | | | | |
| subject 3 | run2 | 0 | 0 | - | - | - | - | - | |
| | run3 | 0 | 0 | - | - | - | - | - | |
| | run4 | 2 | 2 | 0,00% | 0,00% | 0,00% | 0,00 | 0,00% | 0,00 |
| | run5 | 2 | 2 | 50,00% | 0,00% | 100,00% | 2,00 | 50,00% | 1,00 |
| | run6 | 3 | 1 | 100,00% | 100,00% | 50,00% | 0,50 | 100,00% | 1,00 |
| | | | | | | | | | |
| subject 4 | run3 | 14 | 10 | 50,00% | 30,00% | 100,00% | 10,00 | 50,00% | 5,00 |
| | run4 | 19 | 17 | 64,71% | 23,53% | 100,00% | 17,00 | 64,71% | 11,00 |
| | run5 | 8 | 6 | 83,33% | 33,33% | 100,00% | 6,00 | 83,33% | 5,00 |
| | run6 | 2 | 2 | 50,00% | 0,00% | 100,00% | 2,00 | 50,00% | 1,00 |
| | run7 | 3 | 3 | 33,33% | 0,00% | 100,00% | 3,00 | 33,33% | 1,00 |
| | | | | | | | | | |
| | All | 754 | | | | | | | |
| | 1107 | | 168 | | | 65,51% | | 65,53% | |
| | | | weighted | | | 60,03% | | 76,19% | |

| EEG | Span 15 | unique spikes in run | Reader 2 Total EEG Spikes by reader | % by >=2 readers | % by 3 readers | Sensitivity | weight | Precision | weight |
|---|---|---|---|---|---|---|---|---|---|
| subject 1 | run5 | 63 | 11 | 63,64% | 0,00% | 77,78% | 8,56 | 63,64% | 7,00 |
| | run6 | 123 | 61 | 81,97% | 26,23% | 89,29% | 54,46 | 81,97% | 50,00 |
| | run7 | 107 | 37 | 83,78% | 40,54% | 91,18% | 33,74 | 83,78% | 31,00 |
| | run8 | 194 | 119 | 92,44% | 31,93% | 95,65% | 113,83 | 92,44% | 110,00 |
| | | | | | | | | | |
| subject 2 | run2 | 78 | 54 | 7,41% | 1,85% | 100,00% | 54,00 | 7,41% | 4,00 |
| | run3 | 28 | 25 | 24,00% | 0,00% | 100,00% | 25,00 | 24,00% | 6,00 |
| | run4 | 44 | 17 | 29,41% | 5,88% | 62,50% | 10,63 | 29,41% | 5,00 |
| | run5 | 41 | 21 | 38,10% | 14,29% | 88,89% | 18,67 | 38,10% | 8,00 |
| | run6 | 23 | 8 | 12,50% | 0,00% | 50,00% | 4,00 | 12,50% | 1,00 |
| | | | | | | | | | |
| subject 3 | run2 | 0 | 0 | - | - | - | - | - | - |
| | run3 | 0 | 0 | - | - | - | - | - | - |
| | run4 | 2 | 0 | - | - | - | - | - | - |
| | run5 | 2 | 1 | 100,00% | 100,00% | 100,00% | 1,00 | 100,00% | 1,00 |
| | run6 | 3 | 2 | 100,00% | 50,00% | 100,00% | 2,00 | 100,00% | 2,00 |
| | | | | | | | | | |
| subject 4 | run3 | 14 | 9 | 55,56% | 33,33% | 100,00% | 9,00 | 55,56% | 5,00 |
| | run4 | 19 | 13 | 84,62% | 30,77% | 100,00% | 13,00 | 84,62% | 11,00 |
| | run5 | 8 | 3 | 100,00% | 66,67% | 60,00% | 1,80 | 100,00% | 3,00 |
| | run6 | 2 | 1 | 100,00% | 0,00% | 100,00% | 1,00 | 100,00% | 1,00 |
| | run7 | 3 | 1 | 100,00% | 0,00% | 100,00% | 1,00 | 100,00% | 1,00 |
| | | | | | | | | | |
| | All | 754 | | | | | | | |
| | 1107 | | 383 | | | 88,46% | | 67,09% | |
| | | | | | | 91,82% | | 64,23% | |

| EEG | Span 15 | unique spikes in run | Reader 3 Total EEG Spikes by reader | % by >=2 readers | % by 3 readers | Sensitivity | weight | Precision | weight |
|---|---|---|---|---|---|---|---|---|---|
| subject 1 | run5 | 63 | 58 | 15,52% | 0,00% | 100,00% | 58,00 | 15,52% | 9,00 |
| | run6 | 123 | 108 | 50,93% | 14,82% | 100,00% | 108,00 | 50,93% | 55,00 |
| | run7 | 107 | 99 | 32,32% | 15,15% | 94,12% | 93,18 | 32,32% | 32,00 |
| | run8 | 194 | 177 | 64,97% | 21,47% | 100,00% | 177,00 | 64,97% | 115,00 |
| | | | | | | | | | |
| subject 2 | run2 | 78 | 24 | 12,50% | 4,17% | 75,00% | 18,00 | 12,50% | 3,00 |
| | run3 | 28 | 7 | 57,14% | 0,00% | 66,67% | 4,67 | 57,14% | 4,00 |
| | run4 | 44 | 33 | 24,24% | 3,03% | 100,00% | 33,00 | 24,24% | 8,00 |
| | run5 | 41 | 21 | 28,57% | 14,29% | 66,67% | 14,00 | 28,57% | 6,00 |
| | run6 | 23 | 12 | 8,33% | 0,00% | 50,00% | 6,00 | 8,33% | 1,00 |
| | | | | | | | | | |
| subject 3 | run2 | 0 | 0 | - | - | - | - | - | - |
| | run3 | 0 | 0 | - | - | - | - | - | - |
| | run4 | 2 | 0 | - | - | - | - | - | - |
| | run5 | 2 | 1 | 100,00% | 100,00% | 100,00% | 1,00 | 100,00% | 1,00 |
| | run6 | 3 | 3 | 66,67% | 33,33% | 100,00% | 3,00 | 66,67% | 2,00 |
| | | | | | | | | | |
| subject 4 | run3 | 14 | 3 | 100,00% | 100,00% | 60,00% | 1,80 | 100,00% | 3,00 |
| | run4 | 19 | 4 | 100,00% | 100,00% | 36,36% | 1,45 | 100,00% | 4,00 |
| | run5 | 8 | 6 | 66,67% | 33,33% | 80,00% | 4,80 | 66,67% | 4,00 |
| | run6 | 2 | 0 | - | - | - | - | - | - |
| | run7 | 3 | 0 | - | - | - | - | - | - |
| | | | | | | | | | |
| | All | 754 | | | | | | | |
| | 1107 | | 556 | | | 80,63% | | 51,99% | |
| | | | | | | 94,23% | | 44,42% | |

Table 3.1: Analysis of sensitivity and precision for each reader and all subjects

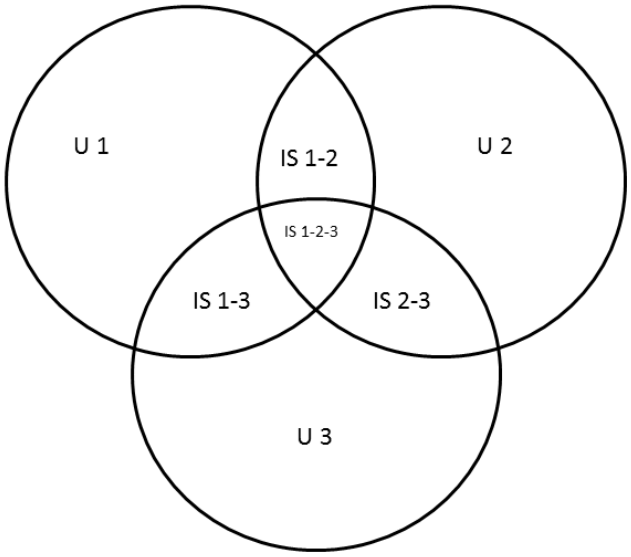


Figure 3.6: Venn diagram; set of reviewer results. U = set of unique results, IS = set of intersection between two or three reviewers

| EEG | Span 15 | unique spikes in run | U1 | U2 | U3 | $U_{total}$ | IS $1_{total}$ | $IS_{total}$ | IS 1-2 | IS 1-3 | IS 2-3 | IS 1-2-3 |
|---|---|---|---|---|---|---|---|---|---|---|---|---|
| subject 1 | run5 | 63 | 1 | 4 | 49 | 54 | 9 | 9 | 0 | 2 | 7 | 0 |
| | run6 | 123 | 3 | 11 | 53 | 67 | 40 | 88 | 16 | 22 | 50 | 16 |
| | run7 | 107 | 0 | 6 | 67 | 73 | 19 | 64 | 17 | 18 | 29 | 15 |
| | run8 | 194 | 8 | 9 | 62 | 79 | 77 | 191 | 38 | 43 | 110 | 38 |
| | | | | | | | | | | | | |
| subject 2 | run2 | 78 | 3 | 50 | 21 | 74 | 3 | 6 | 2 | 1 | 3 | 1 |
| | run3 | 28 | 0 | 19 | 3 | 22 | 6 | 6 | 2 | 0 | 4 | 0 |
| | run4 | 44 | 0 | 12 | 25 | 37 | 6 | 9 | 1 | 3 | 5 | 1 |
| | run5 | 41 | 4 | 13 | 15 | 32 | 6 | 15 | 6 | 4 | 5 | 3 |
| | run6 | 23 | 3 | 7 | 11 | 21 | 2 | 2 | 1 | 1 | 0 | 0 |
| | | | | | | | | | | | | |
| subject 3 | run2 | 0 | 0 | 0 | 0 | 0 | 0 | 0 | 0 | 0 | 0 | 0 |
| | run3 | 0 | 0 | 0 | 0 | 0 | 0 | 0 | 0 | 0 | 0 | 0 |
| | run4 | 2 | 2 | 0 | 0 | 2 | 0 | 0 | 0 | 0 | 0 | 0 |
| | run5 | 2 | 1 | 0 | 0 | 1 | 0 | 3 | 1 | 1 | 1 | 1 |
| | run6 | 3 | 0 | 0 | 1 | 1 | 1 | 4 | 1 | 1 | 2 | 1 |
| | | | | | | | | | | | | |
| subject 4 | run3 | 14 | 5 | 4 | 0 | 9 | 2 | 11 | 5 | 3 | 3 | 3 |
| | run4 | 19 | 6 | 2 | 0 | 8 | 7 | 19 | 11 | 4 | 4 | 4 |
| | run5 | 8 | 1 | 0 | 2 | 3 | 3 | 9 | 3 | 4 | 2 | 2 |
| | run6 | 2 | 1 | 0 | 0 | 1 | 1 | 1 | 1 | 0 | 0 | 0 |
| | run7 | 3 | 2 | 0 | 0 | 2 | 1 | 1 | 1 | 0 | 0 | 0 |

Table 3.2: Results of calculation by method “Analysis.m”

Legend of table 3.2:

| | |
|---|---|
| Unique spikes in run: | all unique spikes in all event-lists |
| Total reviewer 1: | T1 = U1 + IS_1_2 + IS_1_3 – IS_1_2_3 |
| Total reviewer 2: | T2 = U2 + IS_1_2 + IS_2_3 – IS_1_2_3 |
| Total reviewer 3: | T3 = U3 + IS_1_3 + IS_2_3 – IS_1_2_3 |
| Unique total ($U_{total}$): | U1 + U2 + U3 |
| Total events: | ($U_{total}$+2*(IS_1_2+ IS_1_3 + IS_2_3))-3*IS_1_2_3 = T1+T2+T3 |
| $U_{total}$: | total number of unique events per run without any intersection |
| IS $1_{total}$: | total number of events in intersection with only one other set |

**Discussion:**

The results as shown in Table 3.1 represent a mean sensitivity of 78.2% and mean precision of 61.46%, considering a spike as true when marked by at least 2 reviewers. Using weighted numbers there is not much change in the values. These results mainly match (Black et al., 2000; Dümpelmann and C. E. Elger, 1999; Webber et al., 1993) or exceed (Barkmeier et al., 2012) the outcomes of

some of the earlier inter-rater reliability studies. This might be due to the fact that in advance the criteria for epileptic discharges were well defined. Surprisingly the all match result is rather low with only 85 events of 754 unique spikes (11.3%) which might be due to the fact that one of the reviewers used a rather conservative style of marking. No MEG results have been evaluated in detail since no independent marking was available at the time of the study.

As shown in the Venn diagram displaying all sets of events marked by all three reviewers each subset of interest can be easily calculated by the Matlab script. The number of events in each of these subsets is shown in table 3.2 and explained in the accompanying legend. Even though a true positive spike usually is defined as marked by two of three readers, also specific event lists can be easily created containing all events marked by all three readers, in this case 85 events.

The Matlab scripts for the analysis easily allow the user to import and evaluate new event lists quickly in a standardised way and no further calculation for the matching studies will be necessary as soon as the MEG data will be included in the evaluation.

### 3.3. Correction of hand markings to the peak

**Issue:**

As stated in the preceding chapters, for source localisation a clear and reliable signal with a high signal to noise ratio is needed. Since in clinical routine diagnostic the report is made on descriptive evaluation of an EEG or MEG recording, the marking of an epileptic discharge is only relevant for retrospective re-evaluation. Once averaging is included in the process, the precision of the marking is relevant to gain the maximum information from the signal. As shown in Figure 3.7, an incorrect marking in the vicinity but not exactly at the peak will result in a biased averaged signal.

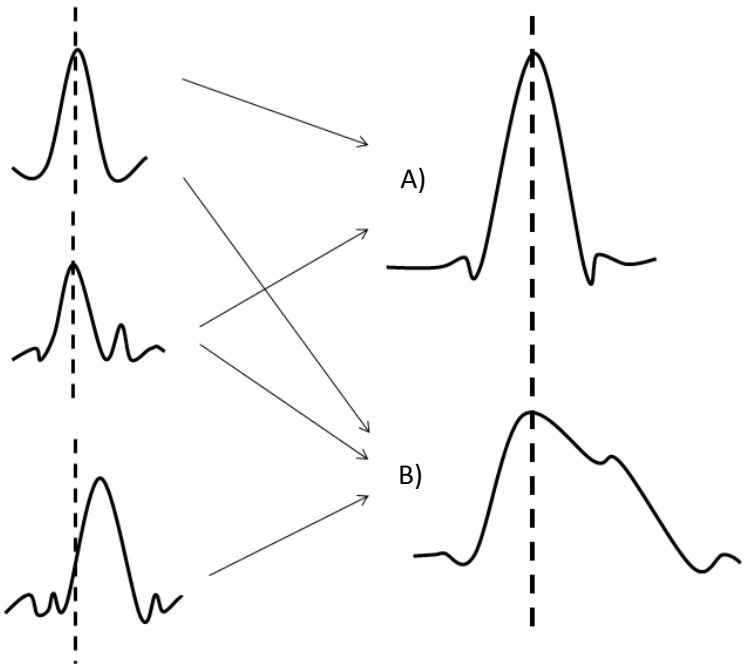


Figure 3.7: Schematic effect of imprecise marking on average result. A) Two optimally marked peaks result in an increased signal to noise ratio, B) imprecise markings results in a lower peak amplitude and changed waveform loosing information about the epileptic discharge.

The effect in the outcome has not been evaluated yet. But from the information known we expect the signal to noise ratio to decrease since different spatial information about the epileptic discharge at different stages of propagation are

mixed. The aim is to evaluate the precision of the marking of best clinical practice and to find a procedure to process the signal in order to get the best and reliable information from it for source localisation.

**Program code**:

In order to analyse the hand markings for the accuracy of selecting the exact negative peak, the dataset was loaded to Matlab as stated in the general section above.

Appendix 3 shows the program code **"EEGSeekPeakautomatic.m"** and the relevant steps.

**"EEGSeekPeakautomatic.m"** automatically finds the most negative peak in the vicinity of a given marker as well as in the neighbouring electrodes. For each event it selects the channel of the hand marked maximum electrode to start from (Step 1). For reasons described later, it calculates the nearest surrounding electrodes by the function **"Neighbourfinder.m"** and searches for a local minimum which represents the maximum negative amplitude of the epileptiform discharge.

The result as the exact sample point at the most negative electrode (black circle in figure 3.8) can be displayed in relation to former markers and the information is saved into the event file format. At the same time it analyses the difference of sample-points to the hand marking. In step 2 the amplitude difference resulting from this imprecise marking is calculated as every sample point next to the peak results in lower amplitude of the respective peak as seen in Figure 3.7 and Figure 3.9 (gain of amplitude = Amplitude'). The method **"NeighborFinder.m"** uses the information of the sensor position in the 3D space and calculates the nearest electrodes next to the main electrode. The number of electrodes in the vicinity can be selected in advance. A high number will result in a higher chance yielding the most negative channel but will also increase the risk of detecting artefacts. The current calculations were done with a number of 5, searching the first degree neighbours for the maximum negativity and the main electrode in the centre.

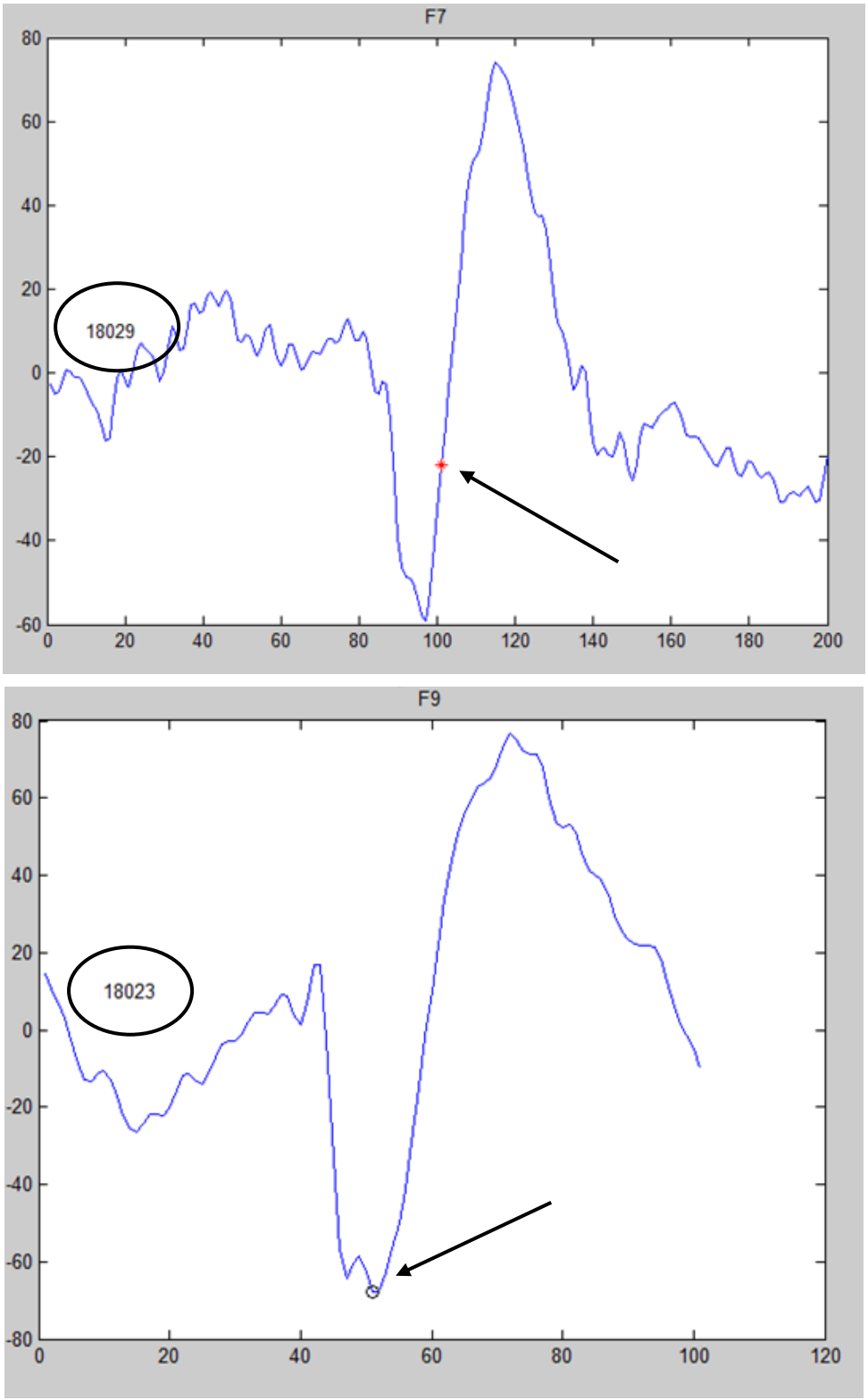


Figure 3.8: Results from Matlab: Peak correction (different time intervals), setting the marker (black arrow) to the most negative position of the most negative channel (F7 to F9) and returning number of sample point (black circle). Note different scaling.

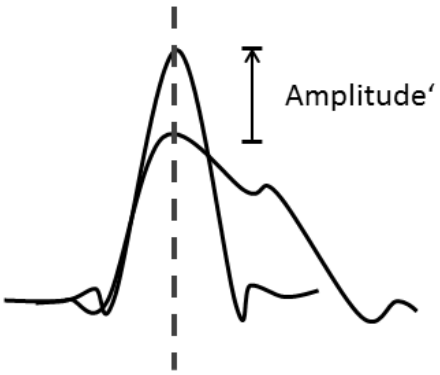


Figure 3.9: Gain of amplitude calculated in Step2, method “SeekPeakautomatic.m”

The percentage of amplitude gain is calculated by the following formula:

$$Amplitude'\ percentage = \frac{amplitude\ new - amplitude\ old}{amplitude\ new}$$

Figure 3.10: Formula to calculate percentage of amplitude gain in relation to new maximum amplitude at negative peak.

In step 3 finally MEG events and those events without a reliable peak within a given range are excluded and the descriptive statistic for the results is calculated. Afterwards the script refers back to the main method for data saving and writing log files. An example log file is attached in the appendix 8.2.
In **summary** this method changes the marker to the maximum negativity of a peak at the most negative electrode in the vicinity of the original hand marking. The output states the change in absolute sample-points and the amplitude change within the new, most negative channel caused by the imprecise marking.

**Results:**

The results were calculated and saved in a separate log file as shown in appendix.

A total of 4 patients and 19 runs have been marked by three readers respectively. Altogether 1107 epileptiform discharges have been marked. Of these, four events were excluded during analysis. In total 883 events have been corrected to the nearest peak of the most negative channel of the original or the surrounding electrodes. Weighted to the individual numbers of events in each run it results in a mean of 84.15% of changed events (range of 0% -100% in all event groups), overall changed events 79.77%. Absolute mean deviation from the negative peak was 6.85ms (2.06 sample-points), standard deviation 4.54ms (1.36 sample-points). With respect to amplitude the results for all 19 recordings are as follows: Maximum amplitude gain was 197.63µV, minimum amplitude gain 0µV and mean amplitude gain 7.25µV (standard deviation 7.12µV). With respect to new maximum negative amplitude it results in a weighted mean percentage of 32.94% (standard deviation 69.79%) of amplitude gain. Since the correction is made to the best position, statistical evaluation is negligible. These results are shown in Table 3.3.

Next pages: Table 3.3 containing all results for peak correction and the resulting amplitude change for each run by each reviewer.

| EEG | Span 10 | | Total EEG Spikes | Events | | | | | Time in ms | | | | Amplitude in µV | | | | | | |
|---|---|---|---|---|---|---|---|---|---|---|---|---|---|---|---|---|---|---|---|
| | | | by reader | excl. | corr. | | % corr. | weight | Max. deviation | Min.deviation | abs. Mean | abs. Std. | Min. deviation | Abs.Mean | Abs.Std. | percentage | weight | percentage std. | weight |
| patient 1 | run5 | reader1 | 3 | 1 | 2 | | 100,00% | 3 | 3,33 | -9,99 | 6,66 | 4,7093 | -22,895 | 11,9725 | 15,4467 | 11,32% | 0,33963 | 15,19% | 0,45567 |
| | | reader2 | 11 | 0 | 9 | | 71,82% | 7,89998 | 3,33 | -13,32 | 4,8436 | 4,0412 | -66,648 | 9,9688 | 19,2106 | 8,17% | 0,899118 | 13,76% | 1,51305 |
| | | reader3 | 58 | 1 | 42 | | 73,68% | 42,73672 | 13,32 | -9,99 | 3,9726 | 3,2964 | -33,95 | 3,1103 | 5,6403 | 4,47% | 2,59173 | 8,71% | 5,052786 |
| | run6 | reader1 | 25 | 0 | 22 | | 88,00% | 22 | 29,97 | -29,97 | 14,2524 | 10,8553 | -63,71 | 15,9837 | 17,7505 | 7,25% | 1,81155 | 119,36% | 29,84 |
| | | reader2 | 61 | 0 | 55 | | 90,16% | 55,00004 | 13,32 | -23,31 | 6,933 | 4,9502 | -197,633 | 12,799 | 26,393 | 12,72% | 7,76042 | 17,51% | 10,67805 |
| | | reader3 | 108 | 0 | 84 | | 77,78% | 84,00024 | 9,99 | -16,65 | 4,5017 | 3,8715 | -28,04 | 4,7238 | 5,9332 | 5,93% | 6,402348 | 8,03% | 8,667648 |
| | run7 | reader1 | 20 | 0 | 20 | | 100,00% | 20 | 23,31 | -29,97 | 12,321 | 6,926 | -67,488 | 22,1988 | 18,9452 | 21,07% | 4,2144 | 15,87% | 3,1732 |
| | | reader2 | 37 | 1 | 31 | | 86,11% | 31,86107 | 9,99 | -13,32 | 6,3825 | 4,0881 | -24,54 | 6,042 | 5,9632 | 5,38% | 1,992339 | 4,40% | 1,628148 |
| | | reader3 | 99 | 0 | 78 | | 78,79% | 78,00012 | 16,65 | -23,31 | 4,6755 | 4,4858 | -29,519 | 3,8046 | 5,5025 | 5,55% | 5,496084 | 15,84% | 15,68061 |
| | run8 | reader1 | 51 | 0 | 44 | | 86,28% | 44,00025 | 26,64 | -26,64 | 9,4024 | 7,701 | -116,958 | 22,2786 | 26,81 | 21,03% | 10,72275 | 26,27% | 13,3977 |
| | | reader2 | 119 | 0 | 88 | | 73,95% | 88,0005 | 13,32 | -23,31 | 4,3094 | 3,8861 | -39,989 | 5,387 | 7,5691 | 5,38% | 6,399106 | 7,85% | 9,337335 |
| | | reader3 | 177 | 0 | 133 | | 75,14% | 132,99957 | 16,65 | -16,65 | 4,7975 | 4,1823 | -48,563 | 6,1343 | 8,7987 | 6,86% | 12,146094 | 10,03% | 17,76018 |
| | | | | | | | | | | | | | | | | | | | |
| | Sum | | 769 | 3 | 608 | Mean | 83,48% | | | | 6,92 | 5,25 | | 10,37 | 13,66 | 9,59% | | 21,90% | |
| | | | | | | Mean* | 79,26% | | | | | | | | | 7,90% | | 15,24% | |
| | | | | | | | | | | | | | | | | | | | |
| patient 2 | run2 | reader1 | 5 | 0 | 5 | | 100,00% | 5 | 9,99 | -6,66 | 5,994 | 2,7861 | -18,526 | 9,366 | 8,2781 | 25,75% | 1,2877 | 25,85% | 1,2927 |
| | | reader2 | 54 | 1 | 43 | | 81,13% | 43,81128 | 16,95 | -19,98 | 5,5291 | 4,8408 | -20,461 | 2,8378 | 3,7767 | 8,08% | 4,361094 | 11,98% | 6,4665 |
| | | reader3 | 24 | 0 | 17 | | 70,83% | 16,99992 | 9,99 | -9,99 | 4,0237 | 3,5377 | -11,563 | 3,3945 | 4,1325 | 10,38% | 2,49192 | 15,08% | 3,61872 |
| | run3 | reader1 | 2 | 0 | 2 | | 100,00% | 2 | 13,32 | 6,66 | 9,99 | 4,7093 | -7,392 | 6,23 | 1,6433 | 13,92% | 0,27832 | 4,92% | 0,098444 |
| | | reader2 | 25 | 0 | 19 | | 76,00% | 19 | 13,32 | -13,32 | 4,7952 | 4,199 | -14,239 | 1,9711 | 3,1939 | 5,19% | 1,297275 | 9,33% | 2,3331 |
| | | reader3 | 7 | 0 | 5 | | 71,43% | 5,00003 | 3,33 | -9,99 | 3,8057 | 3,5599 | -3,804 | 1,2277 | 1,5282 | 2,71% | 0,189959 | 3,47% | 0,24297 |
| | run4 | reader1 | 3 | 0 | 3 | | 100,00% | 3 | 9,99 | -6,66 | 7,77 | 1,9226 | -21,162 | 11,332 | 9,9192 | 20,63% | 0,61875 | 16,19% | 0,48555 |
| | | reader2 | 17 | 0 | 15 | | 88,24% | 14,99995 | 13,32 | -16,65 | 5,8765 | 4,6396 | -16,7282 | 3,3503 | 4,9363 | 10,98% | 1,86575 | 23,36% | 3,97154 |
| | | reader3 | 33 | 0 | 27 | | 81,82% | 26,99994 | 9,99 | -19,98 | 4,44 | 3,9635 | -17,456 | 2,9726 | 4,2477 | 8,41% | 2,77662 | 15,72% | 5,18727 |
| | run5 | reader1 | 11 | 0 | 8 | | 72,73% | 7,99997 | 13,32 | -13,32 | 6,0545 | 5,3318 | -25,206 | 5,9131 | 8,7057 | 16,89% | 1,8579 | 22,73% | 2,5003 |
| | | reader2 | 21 | 0 | 19 | | 90,48% | 18,99996 | 13,32 | -16,65 | 5,3914 | 4,2744 | -23,1625 | 4,4296 | 6,6082 | 14,14% | 2,96982 | 23,55% | 4,94634 |
| | | reader3 | 21 | 0 | 17 | | 80,95% | 16,99992 | 6,66 | -13,32 | 4,7571 | 3,4238 | -4,4 | 1,6427 | 1,3311 | 5,77% | 1,211553 | 5,25% | 1,10334 |
| | run6 | reader1 | 5 | 0 | 4 | | 80,00% | 4 | 9,99 | -3,33 | 3,996 | 3,6478 | -7,0365 | 2,0073 | 2,8951 | 10,92% | 0,54615 | 17,88% | 0,89375 |
| | | reader2 | 8 | 0 | 5 | | 62,50% | 5 | 0 | -6,66 | 3,33 | 3,083 | -4,684 | 1,4657 | 1,8522 | 3,02% | 0,24172 | 3,87% | 0,309272 |
| | | reader3 | 12 | 0 | 8 | | 66,67% | 8,00004 | 6,66 | -13,32 | 4,1625 | 4,0474 | -6,045 | 1,8537 | 1,9954 | 6,70% | 0,803436 | 6,46% | 0,774648 |
| | | | | | | | | | | | | | | | | | | | |
| | Sum | | 248 | 1 | 197 | Mean | 81,52% | | | | 5,33 | 3,86 | | 4,00 | 4,34 | 10,90% | | 13,71% | |
| | | | | | | Mean* | 79,76% | | | | | | | | | 9,19% | | 13,80% | |

| EEG | Span 10 | | Total EEG Spikes | Events | | | | | Time in ms | | | | Amplitude in µV | | | | | | |
|---|---|---|---|---|---|---|---|---|---|---|---|---|---|---|---|---|---|---|---|
| | | | by reader | excl. | corr. | | % corr. | weight | Max. deviation | Min.deviation | abs. Mean | abs. Std. | Min. deviation | Abs.Mean | Abs.Std. | percentage | weight | percentage std. | weight |
| patient 3 | run2 | reader1 | 0 | 0 | 0 | | - | - | - | - | - | - | - | - | - | - | - | - | - |
| | | reader2 | 0 | 0 | 0 | | - | - | - | - | - | - | - | - | - | - | - | - | - |
| | | reader3 | 0 | 0 | 0 | | - | - | - | - | - | - | - | - | - | - | - | - | - |
| | run3 | reader1 | 0 | 0 | 0 | | - | - | - | - | - | - | - | - | - | - | - | - | - |
| | | reader2 | 0 | 0 | 0 | | - | - | - | - | - | - | - | - | - | - | - | - | - |
| | | reader3 | 0 | 0 | 0 | | - | - | - | - | - | - | - | - | - | - | - | - | - |
| | run4 | reader1 | 2 | 0 | 2 | | 100,00% | 2 | -3,33 | -29,97 | 16,65 | 18,8373 | -15,6308 | 8,3734 | 10,2635 | 50,38% | 1,00768 | 62,85% | 1,25696 |
| | | reader2 | 0 | 0 | 0 | | - | - | - | - | - | - | - | - | - | - | - | - | - |
| | | reader3 | 0 | 0 | 0 | | - | - | - | - | - | - | - | - | - | - | - | - | - |
| | run5 | reader1 | 2 | 0 | 2 | | 100,00% | 2 | 13,32 | -6,66 | 9,99 | 4,7093 | -8,736 | 6,1085 | 3,7158 | 22,82% | 0,45634 | 12,08% | 0,24168 |
| | | reader2 | 1 | 0 | 1 | | 100,00% | 1 | 3,33 | 3,33 | 3,33 | 0 | -1,004 | 1,004 | 0 | 3,60% | 0,036043 | 0,00% | |
| | | reader3 | 1 | 0 | 1 | | 100,00% | 1 | 6,66 | 6,66 | 6,66 | 0 | -3,779 | 3,779 | 0 | 13,56% | 0,13556 | 0,00% | |
| | run6 | reader1 | 1 | 0 | 1 | | 100,00% | 1 | -13,32 | -13,32 | 13,32 | 0 | -28,7732 | 28,7732 | 0 | 96,83% | 0,96827 | 0,00% | |
| | | reader2 | 2 | 0 | 2 | | 100,00% | 2 | 6,66 | -19,98 | 13,32 | 9,4187 | -41,277 | 22,177 | 27,0115 | 79,08% | 1,5815 | 84,63% | 1,692626 |
| | | reader3 | 3 | 0 | 2 | | 66,67% | 2,00001 | 3,33 | -3,33 | 2,22 | 1,9226 | -1,713 | 1,0283 | 0,90674 | 6,77% | 0,203178 | 6,07% | 0,182214 |
| | | | | | | | | | | | | | | | | | | | |
| | Sum | | 12 | 0 | 11 | Mean | 95,24% | | | | 9,36 | 4,98 | | 10,18 | 5,99 | 39,01% | | 23,66% | |
| | | | | | | Mean* | 91,67% | | | | | | | | | 36,57% | | 28,11% | |
| | | | | | | | | | | | | | | | | | | | |
| patient 4 | run3 | reader1 | 10 | 0 | 9 | | 90,00% | 9 | 13,32 | -26,64 | 9,657 | 7,7621 | -16,3852 | 7,0094 | 5,6017 | 142,60% | 14,26 | 526,98% | 52,698 |
| | | reader2 | 9 | 0 | 6 | | 66,67% | 6,00003 | 3,33 | -3,33 | 2,22 | 1,665 | -3,827 | 1,032 | 1,3456 | 4,60% | 0,41436 | 7,40% | 0,666351 |
| | | reader3 | 3 | 0 | 3 | | 100,00% | 3 | 3,33 | -3,33 | 3,33 | 0 | -1,643 | 0,81167 | 0,74116 | 3,38% | 0,101487 | 4,22% | 0,126453 |
| | run4 | reader1 | 17 | 0 | 16 | | 94,12% | 16,00006 | 19,98 | -19,98 | 8,0312 | 6,1243 | -27,3308 | 5,2016 | 7,1369 | 109,09% | 18,5453 | 437,86% | 74,4362 |
| | | reader2 | 13 | 0 | 13 | | 100,00% | 13 | 16,65 | -6,66 | 6,4038 | 4,1817 | -10,558 | 2,3158 | 2,681 | 8,50% | 1,105559 | 29,94% | 3,89246 |
| | | reader3 | 4 | 0 | 4 | | 100,00% | 4 | 3,33 | -6,66 | 4,1625 | 1,665 | -2,116 | 1,5045 | 0,50843 | 310,72% | 12,4288 | 548,30% | 21,932 |
| | run5 | reader1 | 6 | 0 | 5 | | 83,33% | 4,99998 | 26,64 | -9,99 | 13,875 | 11,0276 | -40,911 | 18,7495 | 17,9224 | 55,53% | 3,33186 | 55,81% | 3,34866 |
| | | reader2 | 3 | 0 | 3 | | 100,00% | 3 | -3,33 | -9,99 | 6,66 | 3,33 | -6,798 | 4,144 | 2,3941 | 13,25% | 0,3975 | 9,42% | 0,282579 |
| | | reader3 | 6 | 0 | 4 | | 66,67% | 4,00002 | 9,99 | -6,66 | 3,885 | 3,8929 | -14,483 | 2,738 | 5,7634 | 7,34% | 0,440688 | 15,40% | 0,92376 |
| | run6 | reader1 | 2 | 0 | 1 | | 50,00% | 1 | 3,33 | 0 | 1,665 | 2,3547 | -0,489 | 0,2445 | 0,34578 | 0,93% | 0,018689 | 1,32% | 0,02643 |
| | | reader2 | 1 | 0 | 0 | | 0,00% | 0 | 0 | 0 | 0 | 0 | 0 | 0 | 0 | 0,00% | 0 | 0,00% | 0 |
| | | reader3 | 0 | 0 | 0 | | - | - | - | - | - | - | - | - | - | - | - | - | - |
| | run7 | reader1 | 3 | 0 | 2 | | 66,67% | 2,00001 | 19,98 | 0 | 12,21 | 10,7045 | -26,2881 | 10,0959 | 14,1647 | 325,19% | 9,7557 | 494,91% | 14,8473 |
| | | reader2 | 1 | 0 | 1 | | 100,00% | 1 | 3,33 | 3,33 | 3,33 | 0 | -3,927 | 3,927 | 0 | 12,07% | 0,12072 | 0,00% | 0 |
| | | reader3 | 0 | 0 | 0 | | - | - | - | - | - | - | - | - | - | - | - | - | - |
| | | | | | | | | | | | | | | | | | | | |
| | Sum | | 78 | 0 | 67 | Mean | 78,27% | | | | 5,80 | 4,05 | | 4,44 | 4,51 | 76,40% | | 163,97% | |
| | | | | | | Mean* | 85,90% | | | | | | | | | 78,10% | | 222,03% | |
| | | | | | | | | | | | | | | | | | | | |
| | All | | | | | | | | | | | | | | | | | | |
| | Sum | | 1107 | 0 | 883 | Mean | 84,62% | | | | 6,85 | 4,54 | | 7,25 | 7,12 | 33,98% | | 55,81% | |
| | | | | | | Mean* | 84,15% | | | | | | | | | 32,94% | | 69,79% | |

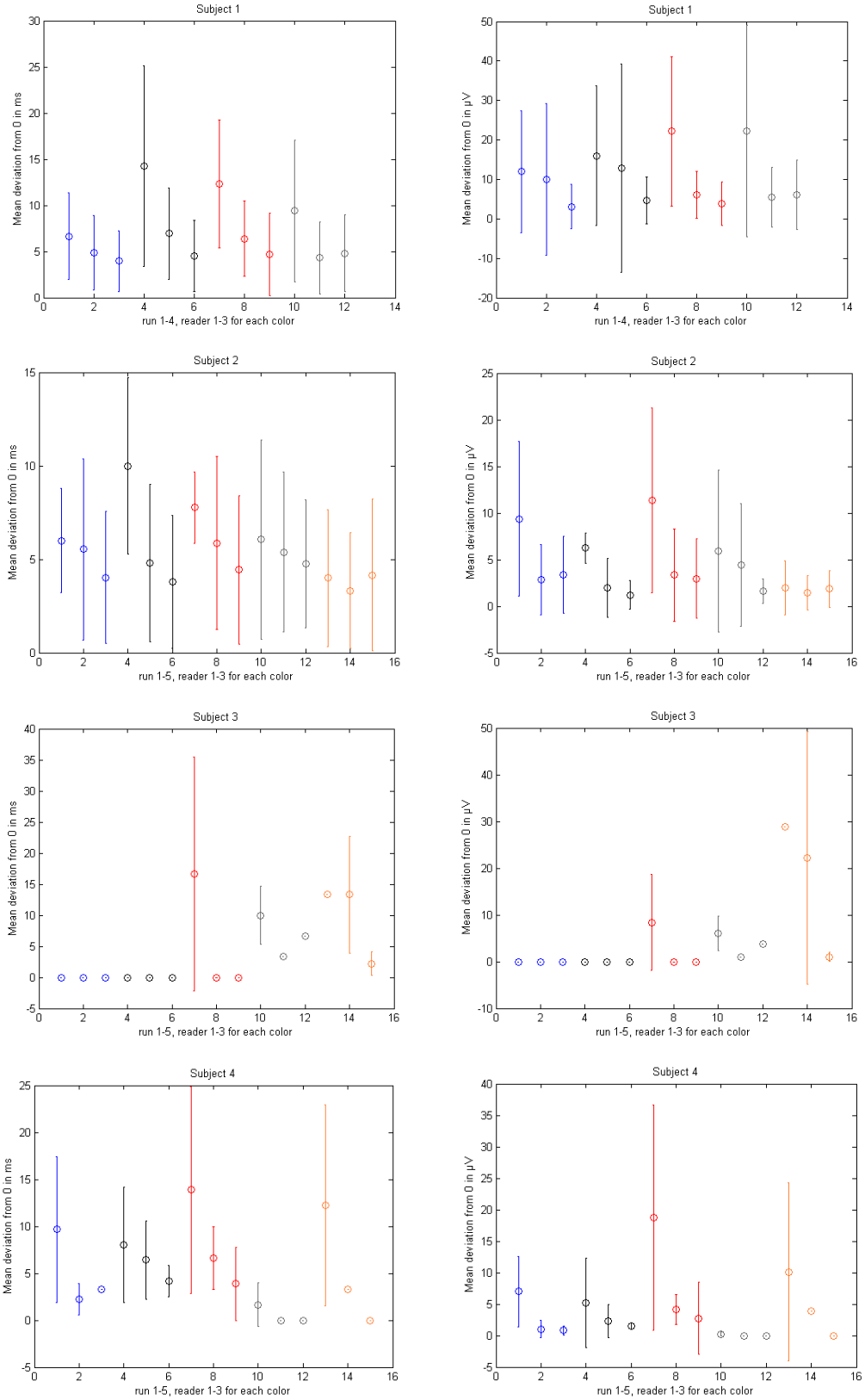


Figure 3.11: Mean and standard deviation of results for each reader, same run = same colour

**Dipole calculation procedure and results:**

The corrected data is averaged and saved as epoched file for semi-automatic overnight processing. Source localization along with the creation of the head models for the forward solution is performed using CURRY 7 software (Compumedics).

In this study we use two sets of T1 weighted MRI's to create the head model. The first T1 has gadolinium markers on Nasion, pre-auricular left and pre-auricular right. These position markers (fiducials) are later used to co-register the EEG and MEG sensors to the MRI. The second T1 is measured with a water selective sequence. This one is used for the segmentation of the skin, outer skull, inner skull and cortex. For the segmentation the skin, brain, cortex and white matter thresholds along with a seed slice are processed for each patient. The surfaces of segmented skin, outer skull and inner skull are then used to construct triangle meshes with 8, 7 and 5 mm resolution respectively. The conductivity value for the skin and brain is taken as 0.33 S/m, while the skull conductivity is taken as 0.0042 S/m. Finally a three layer Boundary element solution is calculated from this head model to be used in the inverse solution (M. Fuchs et al., 1998; Wagner M et al., 1997).

Before source reconstruction, the measurements have been pre-processed with a bandpass filter from 3 to 100 Hz along with a notch filter at 50Hz (and its harmonics). A signal free interval of 100ms preceding the epileptiform discharge is used for noise estimation. For source reconstruction moving dipole solutions with confidence ellipsoids are used. In this model the six parameters that determine the position and orientation are calculated separately for each time instance in a range of time. The optimal parameters are found by minimizing the residual variation and a nonlinear simplex algorithm is used in CURRY to calculate the location parameters (Manfred Fuchs et al., 1998).

During the dipole calculation the characteristic parameters are saved automatically into a table for further evaluation in Matlab. The saved parameters are:

- Name of the file and the data
- T = Time point of dipole fit (in relation to the marker = 0 ms)

- Signal to noise ratio used for dipole calculation at T
- Normalised residuals
- Original residuals
- Confidence ellipsoid
- Coordinates (x, y, z)
- Mean global field power (MGFP, as value of amplitude) of signal at T

The confidence ellipsoid is calculated by the formula (Fuchs et al, 2004):

$$v_k = \frac{4\pi N^3 s^{\frac{3}{2}}}{(3\ \sum_{kx}\sum_{ky}\sum_{kz})} = \frac{4\ \pi\ l_{kx} l_{ky} l_{kz}}{3}$$

k = dipole position
$v_k$ =confidence volume
N = mean noise level
$l_k$ = length of axes k
s = number of sensors

Without going into too many details of this calculation, there can be drawn two main facts from this equation. First the lengths of the ellipsoid axes $l_k$ are inversely proportional to the SNR and the ellipsoid volume is inversely proportional to the third power of the SNR. This means, the smaller the ellipsoid volume, the more reliable the dipole fit will be (Manfred Fuchs et al., 2004). After importing the results' table to Matlab a script is created for easy access to the events of interest by positive and negative constraints. By intersection and union of the gained matrices the intended subset of data for comparison reason is selected.

An example script file **"ResultsEvaluationEEGfromEEGmarkings.m"** is printed in the appendix. The data is separated into two groups to compare statistic calculation automatically. All descriptive parameters as minimum, maximum, mean, median, quantiles and standard deviation as well as variance are calculated. The respective boxplot is saved.

In total 87 averaged events in two groups are evaluated and the respective dipole fits are calculated. Even though we reach a number of n=87, normal distribution of the results cannot be proven. As seen in figure 3.12, the subtraction (SNR group2 – group1) differs from the normal distribution. Testing results also support the fact that normal distribution cannot be assumed. Therefore for all testing the distribution free Wilcoxon signed rank test is used. The respective results are shown and discussed separately in every subchapter.

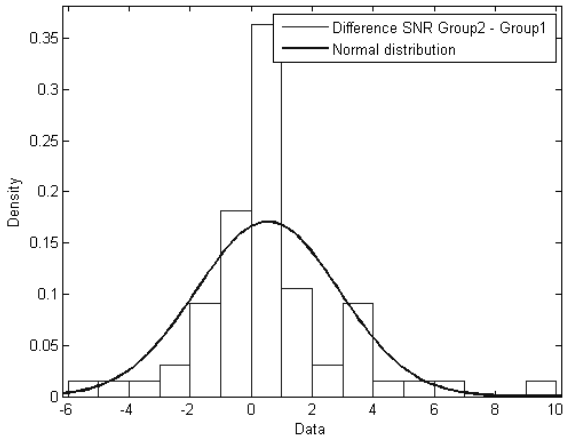


Figure 3.12: Histogram of differences of SNR (group2-group1) in comparison to normal distribution (example for EEG data, y-axis: frequency density of the interval, x-axis: discrete intervals (bins), with an area equal to the frequency of the observations in the interval. The total area of the histogram is equal to the number of data (source Wikipedia))

**Results:**

Dipole calculations are made for the EEG data and the MEG data separately. Since there might be a shift of the peaks in the two modalities as discussed before, each modality is evaluated separately and in relation to the other modality.

The following combinations are evaluated:

1. results at peak of EEG only for EEG
2. results at peak of MEG only for MEG
3. results of the EEG at the time instance of the MEG peak
4. results of the MEG at the time instance of the EEG peak

In all cases group1 represents the genuine hand markings as group 2 represents the peak corrected events without new clustering. The group events are completely identical in numbers and event types but differ in position of the marker at the peak as shown above. All groups are compared with respect to MGFP, SNR, normalized (norm) residuals, original residuals, confidence ellipsoids and shift of position as seen in table 3.4. The main findings are mentioned in the text.

**The following results apply to the dipole calculation at the EEG peak only for the EEG (1):**

| Results (1) n=87 | Group | MGFP | SNR | Normalized residual | Original residual | Ellipsoid Volume | shift |
|---|---|---|---|---|---|---|---|
| Maximum | 1 | 84,81 | 37,18 | 0,54 | 0,78 | 3616,23 | 0,00 |
| | 2 | 86,42 | 43,39 | 0,57 | 0,61 | 1434,05 | 125,93 |
| Mean | 1 | 20,04 | 8,08 | 0,25 | 0,29 | 165,28 | 0,00 |
| | 2 | 21,91 | 8,77 | 0,23 | 0,26 | 114,93 | 15,10 |
| Median | 1 | 13,79 | 6,17 | 0,24 | 0,26 | 28,27 | 0,00 |
| | 2 | 15,44 | 7,42 | 0,21 | 0,24 | 13,75 | 6,82 |
| Min | 1 | 3,11 | 1,67 | 0,07 | 0,11 | 0,11 | 0,00 |
| | 2 | 2,77 | 1,71 | 0,07 | 0,12 | 0,09 | 0,00 |
| Standard Deviation | 1 | 14,08 | 6,32 | 0,11 | 0,14 | 486,84 | 0,00 |
| | 2 | 15,43 | 6,37 | 0,10 | 0,12 | 284,27 | 21,64 |
| Variance | 1 | 19,83 | 39,90 | 0,01 | 0,02 | 237013,90 | 0,00 |
| | 2 | 23,80 | 40,53 | 0,01 | 0,01 | 80808,08 | 468,17 |
| p Wilcoxon signed rank | | < 0,0001 | 0,0039 | | | 0,0005 | |

Table 3.4: Descriptive statistics for EEG at EEG peak and all evaluated parameters, n=87 event groups.

The SNR increases in all statistic parameters (mean from 8.08 to 8.77) as shown in boxplot 3.13 and the table 3.4. This result is significant in the Wilcoxon signed rank test with p=0.0039. The MGFP as well increases highly significantly with p <0.0001 in the Wilcoxon signed rank test. The confidence ellipsoid decreases as expected, shown in boxplot 3.14 and table 3.4 as well with a significance of p=0.0005 in the Wilcoxon signed rank test. The peak correction causes a mean shift of the dipole position of 15.10 mm in the current calculation, shown in boxplot 3.14, as well highly significant (p<0.0001) in the Wilcoxon rank test (table 3.4a).

| Differences (1) | MGFP | SNR | Ellipsoid Volume | shift |
|---|---|---|---|---|
| Maximum | 8,64 | 9,16 | 950,78 | 125,93 |
| Mean | 2,19 | 0,69 | -50,35 | 15,10 |
| Median | 1,54 | 0,23 | -0,79 | 6,82 |
| Min | 0,28 | -5,76 | -2763,13 | 0,00 |
| Standard Deviation | 1,54 | 2,36 | 385,42 | 21,64 |
| Variance | 2,38 | 5,55 | 148547,11 | 468,17 |
| p Wilcoxon signed rank | < 0,0001 | 0,0039 | 0,0005 | < 0,0001 |

Table 3.4a: Differences and results of Wilcoxon signed rank test for the respective parameters

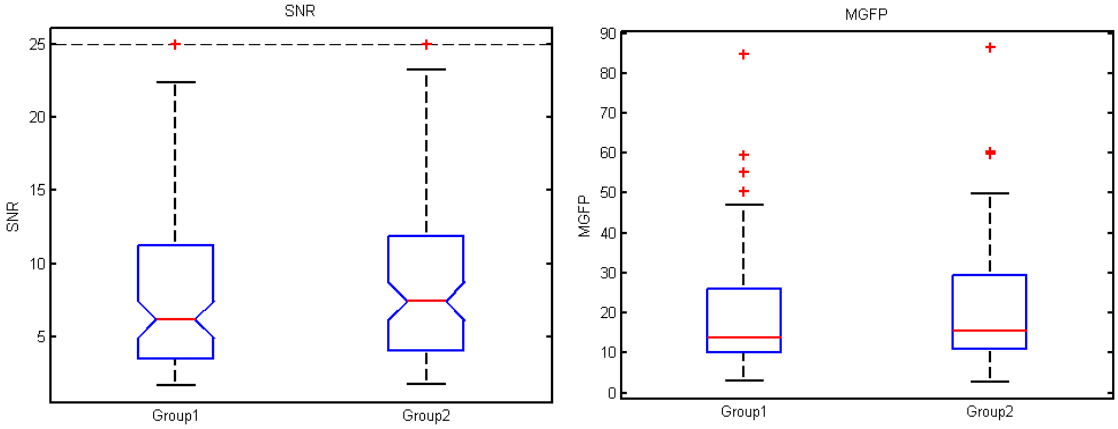


Figure 3.13: Boxplots for SNR and MGFP at EEG peak for EEG data (data limits set)

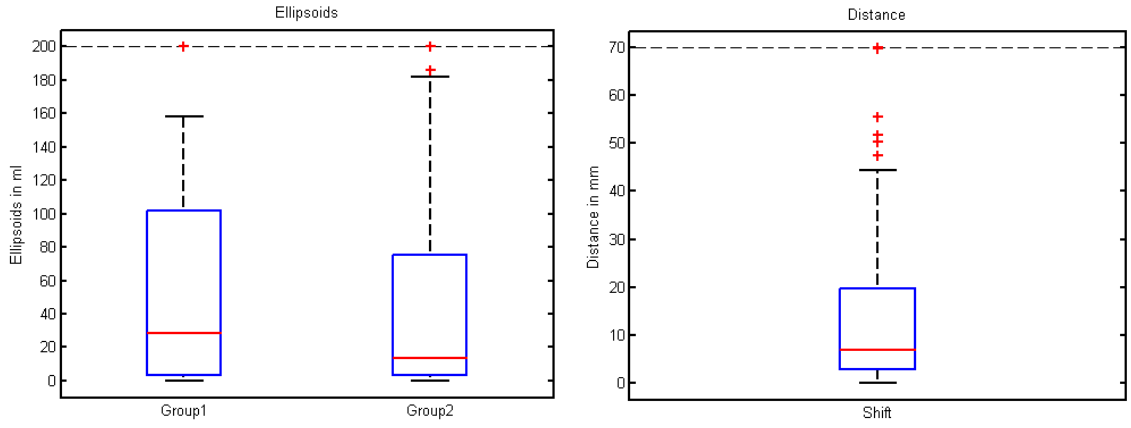


Figure 3.14: Boxplot for the confidence ellipsoid in ml and shift in position of dipole in mm (data limits set)

**The following results apply to the dipole calculation at the MEG peak only for the MEG (2):**

| Results (2), n=65 | Group | MGFP | SNR | Normalized residual | Original residual | Ellipsoid Volume | shift |
|---|---|---|---|---|---|---|---|
| Maximum | 1 | 68,11 | 17,46 | 0,61 | 0,80 | 231,65 | 0,00 |
| | 2 | 70,07 | 17,03 | 0,64 | 0,79 | 117,37 | 99,07 |
| Mean | 1 | 27,74 | 5,70 | 0,39 | 0,48 | 15,51 | 0,00 |
| | 2 | 27,58 | 5,83 | 0,39 | 0,48 | 9,02 | 28,89 |
| Median | 1 | 25,62 | 4,74 | 0,39 | 0,46 | 4,57 | 0,00 |
| | 2 | 25,08 | 5,09 | 0,38 | 0,46 | 2,45 | 17,86 |
| Min | 1 | 12,16 | 2,16 | 0,14 | 0,24 | 0,00 | 0,00 |
| | 2 | 12,07 | 1,99 | 0,16 | 0,22 | 0,00 | 0,00 |
| Standard Deviation | 1 | 12,37 | 3,43 | 0,10 | 0,14 | 36,11 | 0,00 |
| | 2 | 12,27 | 3,43 | 0,12 | 0,15 | 17,59 | 25,58 |
| Variance | 1 | 15,29 | 11,78 | 0,01 | 0,02 | 1304,09 | 0,00 |
| | 2 | 15,06 | 11,73 | 0,01 | 0,02 | 309,54 | 654,08 |
| p Wilcoxon signed rank | | 0,2528 | 0,1145 | | | 0,1467 | |

Table 3.5: Descriptive statistics for MEG at MEG peak and all evaluated parameters, n=65 event groups.

In this case there is no consistent trend of change of SNR and the confidence ellipsoid. The SNR maximum- and minimum values decrease slightly whereas mean and median increase. The confidence ellipsoid decreases in all parameters (figure 3.15 and table 3.5). The dipole positions shift by a mean of 28.89 mm as shown in boxplot 3.16. For none of the evaluated parameters a statistical significance is reached as expected and shown in table 3.5.
For the calculated differences of both groups only the shift of the dipole position reaches high significance ($p<0.0001$) in the Wilcoxon rank test (table 3.5a).

| Differences (2) | MGFP | SNR | Ellipsoid Volume | shift |
|---|---|---|---|---|
| Maximum | 2,33 | 2,37 | 117,18 | 99,07 |
| Mean | -0,02 | 0,14 | -6,49 | 28,89 |
| Median | 0,06 | 0,32 | -0,37 | 17,86 |
| Min | -1,95 | -2,83 | -194,16 | 0,00 |
| Standard Deviation | 0,65 | 0,94 | 35,24 | 25,58 |
| Variance | 0,42 | 0,87 | 1241,82 | 654,08 |
| p Wilcoxon signed rank | 0,2528 | 0,1145 | 0,1467 | <0,0001 |

Table 3.5a: Differences and results of Wilcoxon signed rank test for the respective parameters

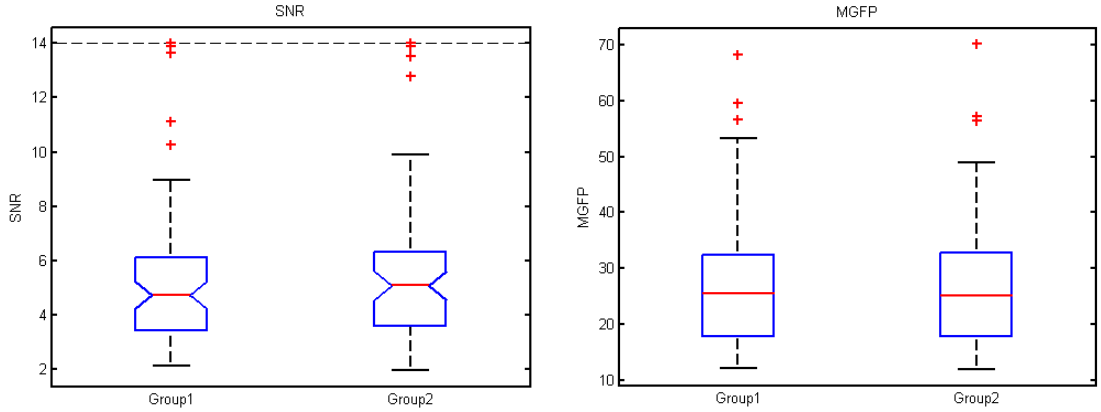


Figure 3.15: Boxplot for SNR and MGFP at MEG peak for MEG data (data limits set for SNR)

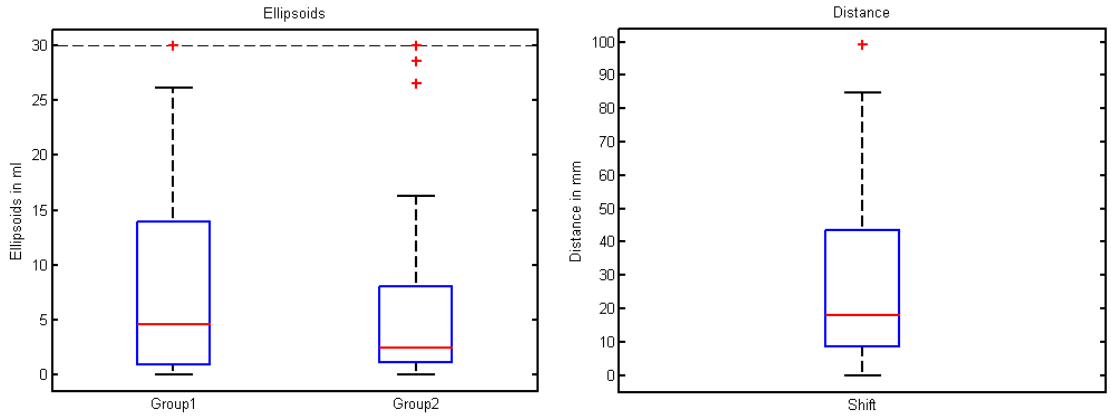


Figure 3.16: Boxplot for the confidence ellipsoid in ml and shift in position of dipole in mm (data limits set)

**The following results apply to the dipole calculation for EEG at time instance of the MEG peak (3):**

| Results (3), p=87 | Group | MGFP | SNR | Normalized residual | Original residual | Ellipsoid Volume | shift |
|---|---|---|---|---|---|---|---|
| Maximum | 1 | 47,40 | 33,35 | 0,59 | 0,79 | 5902,63 | 0,00 |
| | 2 | 46,78 | 39,75 | 0,63 | 0,77 | 2453,26 | 91,11 |
| Mean | 1 | 16,59 | 7,05 | 0,27 | 0,31 | 302,27 | 0,00 |
| | 2 | 17,46 | 7,28 | 0,27 | 0,31 | 218,12 | 20,07 |
| Median | 1 | 13,10 | 4,75 | 0,24 | 0,30 | 40,56 | 0,00 |
| | 2 | 14,30 | 5,51 | 0,24 | 0,28 | 23,54 | 7,99 |
| Min | 1 | 3,03 | 1,48 | 0,10 | 0,12 | 0,17 | 0,00 |
| | 2 | 2,77 | 1,64 | 0,08 | 0,12 | 0,11 | 0,00 |
| Standard Deviation | 1 | 10,78 | 6,08 | 0,11 | 0,14 | 765,62 | 0,00 |
| | 2 | 11,73 | 6,03 | 0,12 | 0,15 | 489,50 | 25,55 |
| Variance | 1 | 11,63 | 36,96 | 0,01 | 0,02 | 586176,11 | 0,00 |
| | 2 | 13,77 | 36,40 | 0,01 | 0,02 | 239611,76 | 652,69 |
| p Wilcoxon signed rank | | 0,6497 | 0,4333 | | | 0,1277 | |

Table 3.6: Descriptive statistics of dipole calculations for the EEG data at time instance of MEG peak, n=87 event groups.

The SNR and ellipsoid for the EEG dipole reconstructions at the time instance of the MEG peak improve as the SNR and MGFP parameters increase (figure 3.17 and table 3.6) and the mean confidence ellipsoids decrease (figure 3.18). The mean shift of the dipole position is 20.07 mm (figure 3.18). For none of the evaluated parameters a statistical significance is reached as expected and shown in table 3.6.

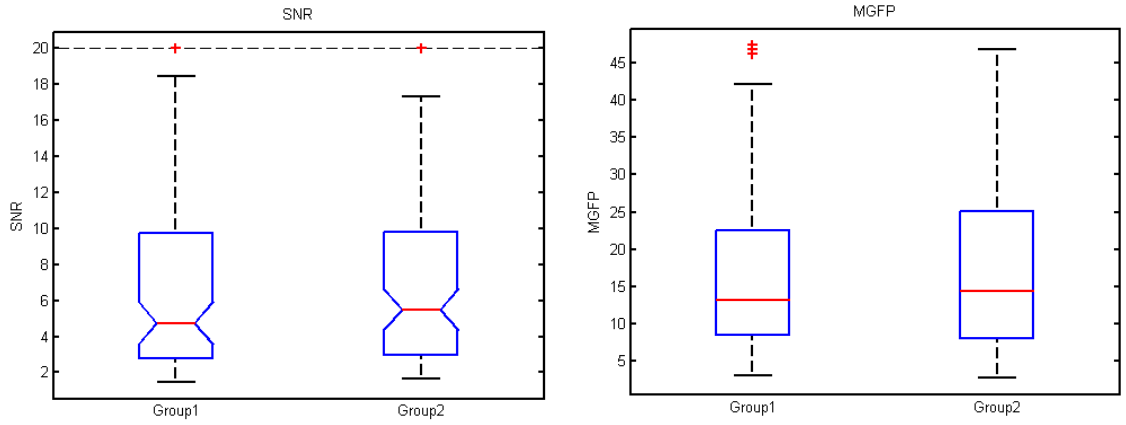


Figure 3.17: Boxplots for SNR and MGFP for EEG dipoles at MEG peak (data limit set for SNR)

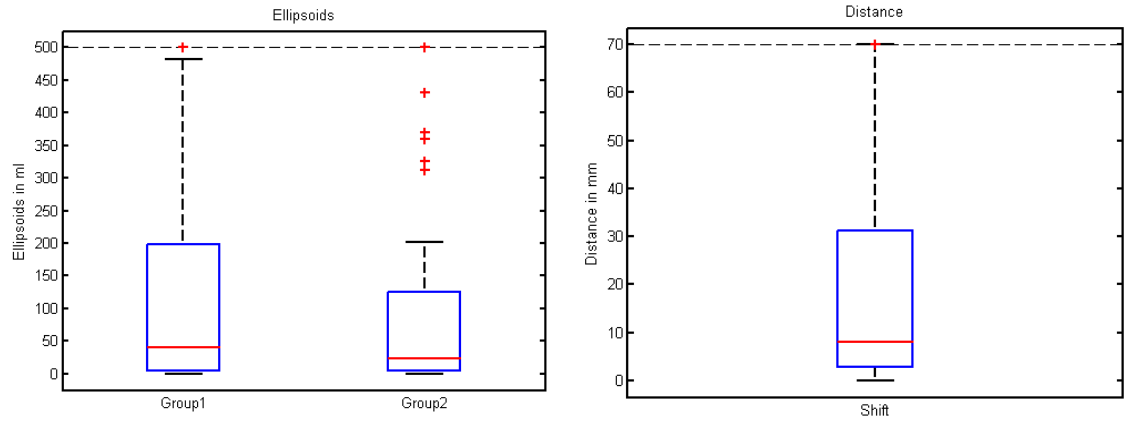


Figure 3.18: Boxplots for confidence ellipsoid in ml and shift in position of dipole in mm (data limits set)

For the calculated differences of both groups only the shift of the dipole position reaches high significance ($p<0.0001$) in the Wilcoxon rank test (table 3.6a).

| Differences (3) | MGFP | SNR | Ellipsoid Volume | shift |
|---|---|---|---|---|
| Maximum | 2,68 | 7,74 | 1480,42 | 91,11 |
| Mean | 0,09 | 0,24 | -84,15 | 20,07 |
| Median | 0,00 | 0,02 | -0,39 | 7,99 |
| Min | -2,78 | -14,55 | -4981,65 | 0,00 |
| Standard Deviation | 0,74 | 2,84 | 625,91 | 25,55 |
| Variance | 0,55 | 8,04 | 391769,33 | 652,69 |
| p Wilcoxon signed rank | 0,6497 | 0,4333 | 0,1277 | < 0,0001 |

Table 3.6a: Differences and results of Wilcoxon signed rank test for the respective parameters

**The following results apply to the dipole calculations for the MEG data at time instance of the EEG peak (4):**

| Results (4), n=87 | Group | MGFP | SNR | Normalized residual | Original residual | Ellipsoid Volume | shift |
|---|---|---|---|---|---|---|---|
| Maximum | 1 | 81,46 | 15,47 | 0,83 | 1,00 | 1021,14 | 0,00 |
| | 2 | 61,89 | 15,99 | 0,80 | 1,00 | 471,99 | 121,48 |
| Mean | 1 | 25,83 | 4,17 | 0,51 | 0,57 | 56,81 | 0,00 |
| | 2 | 25,45 | 4,32 | 0,50 | 0,56 | 26,21 | 23,62 |
| Median | 1 | 22,53 | 3,45 | 0,52 | 0,58 | 10,71 | 0,00 |
| | 2 | 23,19 | 3,48 | 0,50 | 0,56 | 8,38 | 13,41 |
| Min | 1 | 9,81 | 1,28 | 0,17 | 0,25 | 0,00 | 0,00 |
| | 2 | 7,27 | 1,54 | 0,16 | 0,22 | 0,00 | 0,00 |
| Standard Deviation | 1 | 13,52 | 2,81 | 0,16 | 0,17 | 148,65 | 0,00 |
| | 2 | 12,24 | 2,95 | 0,15 | 0,16 | 61,21 | 24,62 |
| Variance | 1 | 18,29 | 7,87 | 0,02 | 0,03 | 22097,62 | 0,00 |
| | 2 | 14,99 | 8,73 | 0,02 | 0,03 | 3746,29 | 605,99 |
| p Wilcoxon signed rank | | 0,2375 | 0,1123 | | | 0,0283 | |

Table 3.7: Descriptive statistics of dipole calculations for the MEG data at time instance of EEG peak, n=87 event groups.

The SNR and confidence ellipsoid for the MEG dipole reconstructions at the time instance of the EEG peak improve slightly as the SNR increases and the confidence ellipsoids decrease (figure 3.19 and 3.7). For none of the evaluated parameters a statistical significance is reached as expected and shown in table 3.7. The mean ellipsoid decreases from 56.81ml to 26.21ml and reaches significance level (p=0.0283). The dipole position shifts by a mean of 23.62 mm (figure 3.20) reaching high significance (p<0.0001) as shown in table 3.7a.

| Differences (4) | MGFP | SNR | Ellipsoid Volume | shift |
|---|---|---|---|---|
| Maximum | 1,05 | 2,93 | 469,37 | 121,48 |
| Mean | -0,04 | 0,15 | -30,60 | 23,62 |
| Median | 0,05 | 0,07 | -0,05 | 13,41 |
| Min | -2,38 | -2,53 | -961,19 | 0,00 |
| Standard Deviation | 0,57 | 0,97 | 152,52 | 24,62 |
| Variance | 0,33 | 0,95 | 23261,52 | 605,99 |
| p Wilcoxon rank test | 0,2375 | 0,1123 | 0,0283 | < 0,0001 |

Table 3.7a: Differences and results of Wilcoxon signed rank test for the respective parameters

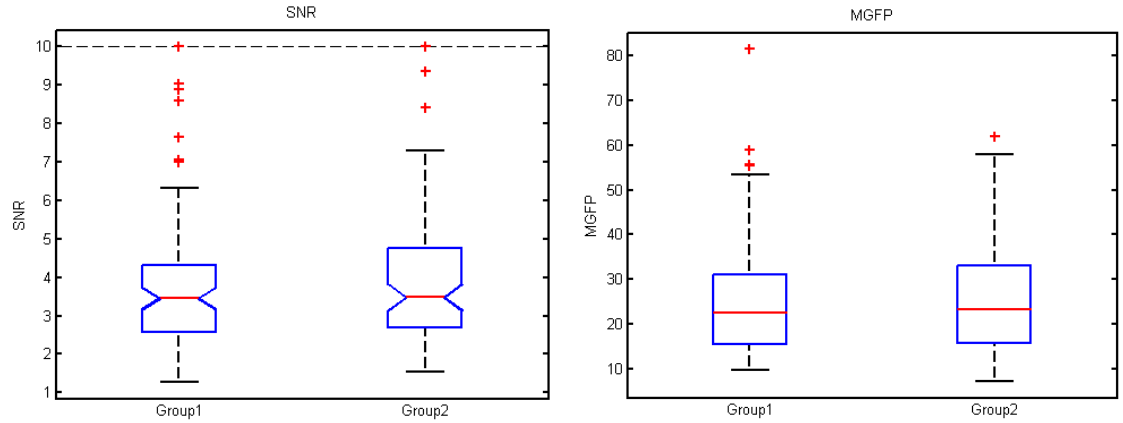


Figure 3.19: Boxplots for SNR and MGFP for MEG dipoles at EEG peak (data limit set for SNR)

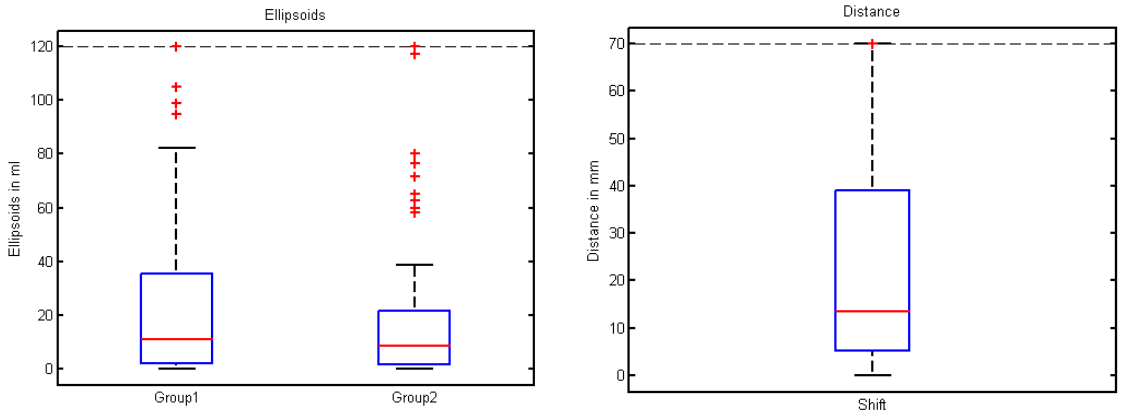


Figure 3.20: Boxplots for confidence ellipsoids in ml and shift in position of dipole in mm

**Discussion**:

In summary the results show that a high number of events are not marked at the correct position regarding the most negative electrode or the exact position of the marker next to the peak. Of 1107 epileptiform discharges in the EEG, a total of 883 (79.77%) have been corrected to the correct position with regard to channel and / or position. Only 224 events were regarded as correct markings. Even though there are features to correct the markers directly to the peak of the waveform (like in Curry 7), to our best knowledge no detailed analysis of these findings has been published before. The issue with these commercial tools is the fact that the marker usually is corrected to the maximum of the main global field power (MGFP) which does not always align with the peak of the maximum channel (see figure 3.21).

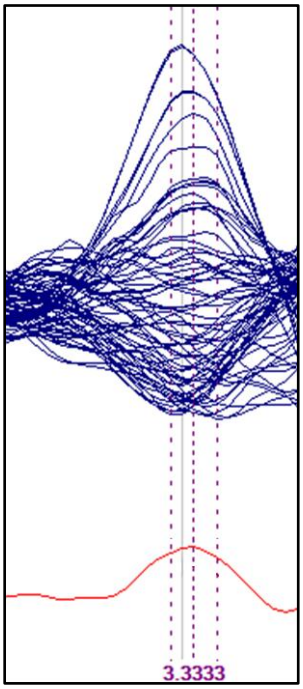


Figure 3.21: Shift of one SP (3,33ms) between negative peak of most negative electrode and MGFP for EEG (red line, averaging all channels). Picture taken from data processing

The MGFP is a generalized average of the common-average data representing the signal strength in all channels. To meet the criteria set up before to mark the EEG channel with the highest precision and at the best position, the Matlab tool was implemented and the impact on source reconstruction evaluated. Even though the individual corrections were little, there is an overall trend in almost all results. Especially with respect to the optimized EEG marking, the SNR and MGFP increase considerably and reach high statistical significance in the distribution free Wilcoxon signed rank test. The ellipsoid as a measurement of the reliability of the dipole fit result decreases as well significantly. All results for the other calculations (point 2-4) represent non optimized data since only the EEG peak was corrected for this study. As expected we see the most change in the EEG results.

Since the new datasets represent the optimal marking of the data with concern to our predefined best clinical practice we can measure the impact of the imprecision of the method commonly used up to now.

## 3.4. Correction of hand markings to new clusters

**Issue:**

Even though the aim of a high signal to noise ratio can be achieved by averaging as many spikes as possible the spatio-temporal distribution and the correct clustering of the spikes is an important factor. With respect to the EEG markings this is done by the assignment of the most negative electrode to the event marked. So clusters of similar spikes can be analysed. Even though only one (often the negative) pole of the event can be determined with high precision as stated before, this is the best clinical practice a human reviewer can make use of. In this chapter this clustering is evaluated with respect to its precision and the way it can be improved on the basis of the agreed clinical conditions. The aim is to purify the signal from biasing events and to improve SNR and localisation value even though the number of events averaged will decrease.

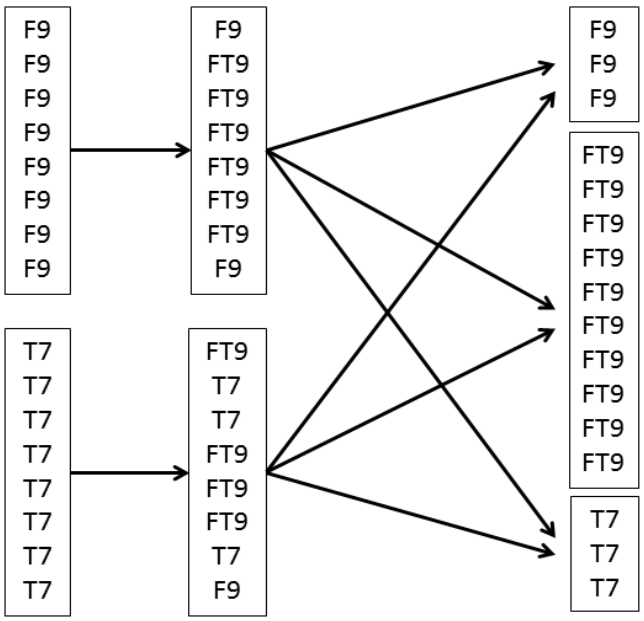


Figure 3.22: Example of original hand marked clusters (left) containing imprecise clustering (corrected in the middle) leading to a new clustering of the marked events resulting in a new main cluster.

**Program code:**

In fact the same program code as in 3.2 is used. Once the new maximum negativity is found the result is automatically saved into two different event lists. The first one includes just the peak corrected information, keeping the old naming of the event. These file names contain the abbreviation ” _PC_”. The structure is the same as in the original hand marking event list but contains the name of the new, most negative electrode. This process is seen in figure 3.22, left to middle. These files are saved for analysis as explained in 3.2.

For the current evaluation the clustering takes place according to the new name assigned as shown in figure 3.22, middle to right. These new clustered (NC) results are saved to a second event list containing the abbreviation “_PC_NC_”. More information on the algorithm used is stated in 3.2. All evaluations and calculations are carried out in the same way as in 3.2. The event lists are saved automatically and used for further processing. The resulting new clusters are averaged and saved for separate dipole calculations.

**Results:**

The following representative results show the calculations for all runs of subject 1. All those hand marked clusters are selected, which contain the highest number of events. In the second group the depending new clusters are selected, usually two clusters deriving from one old cluster. To give an overview of the results the descriptive parameters are calculated for each dataset and compared. Since the number of events n in one group differs and our aim is to increase the SNR with a lower number of more reliable signals, corrected SNR are displayed for comparison reasons. The correction is made by the following formula:

$$SNR\ corr = \frac{SNR}{\sqrt{n}}$$

The following table (3.8) shows the resulting descriptive parameters:

| Results GEN NC | Group | MGFP | SNR corr | SNR | Normalized residual | Original residual | Ellipsoid Volume | shift |
|---|---|---|---|---|---|---|---|---|
| Maximum | 1 | 31,42 | 5,11 | 37,18 | 0,32 | 0,30 | 28,27 | 0,00 |
| | 2 | 39,79 | 8,48 | 44,09 | 0,52 | 0,51 | 47,10 | 41,67 |
| Mean | 1 | 26,42 | 2,73 | 18,71 | 0,16 | 0,18 | 4,71 | 0,00 |
| | 2 | 28,18 | 4,26 | 18,60 | 0,16 | 0,19 | 5,55 | 12,87 |
| Median | 1 | 25,63 | 2,12 | 19,38 | 0,14 | 0,17 | 1,42 | 0,00 |
| | 2 | 28,38 | 4,01 | 15,58 | 0,16 | 0,16 | 1,40 | 8,87 |
| Min | 1 | 22,60 | 1,19 | 5,48 | 0,07 | 0,12 | 0,11 | 0,00 |
| | 2 | 14,37 | 1,50 | 2,59 | 0,04 | 0,10 | 0,13 | 4,65 |
| Standard Deviation | 1 | 3,06 | 1,35 | 9,12 | 0,08 | 0,06 | 8,56 | 0,00 |
| | 2 | 5,21 | 2,19 | 11,07 | 0,10 | 0,09 | 10,90 | 10,76 |
| Variance | 1 | 0,94 | 1,84 | 83,19 | 0,01 | 0,00 | 73,30 | 0,00 |
| | 2 | 2,72 | 4,79 | 122,59 | 0,01 | 0,01 | 118,73 | 115,88 |
| p Wilcoxon rank test | | 0,1309 | 0,0059 | 0,2754 | | | 1,0000 | |

Table 3.8: Descriptive statistics of dipole calculations for new clustered EEG data of subject 1.

In the direct comparison of the two groups there is a small decrease of the mean uncorrected SNR, which fails to reach significance level in the Wilcoxon signed rank test (p=0,2754). The result for the MGFP increases from 26.42 to 28.18 but also fails significance level (p=0.1309). The corrected SNR on the other hand increases its mean from 2.73 to 4.26 which reaches significance level (p=0.0059).

The increase of the mean ellipsoid by the new clustering (4.71 to 5.55) will be subject for further evaluation. The mean shift of the dipole position by the new clustering is 12.87 mm, which also reaches significance level (p=0.002).

| Differences GEN NC | MGFP | SNR corr | SNR | Ellipsoid Volume | shift |
|---|---|---|---|---|---|
| Maximum | 0,68 | 4,94 | 15,28 | 18,82 | 32,91 |
| Mean | 0,19 | 1,90 | 2,70 | 1,76 | 10,60 |
| Median | 0,25 | 1,91 | 1,26 | -0,01 | 6,81 |
| Min | -0,54 | -0,49 | -3,69 | -6,55 | 1,44 |
| Standard Deviation | 0,36 | 1,68 | 5,66 | 6,71 | 10,51 |
| Variance | 0,13 | 2,83 | 32,09 | 44,96 | 110,41 |
| p Wilcoxon signed rank | 0,1309 | 0,0059 | 0,2754 | 1,0000 | 0,0020 |

Table 3.8a: Differences and results of Wilcoxon signed rank test for the respective parameters

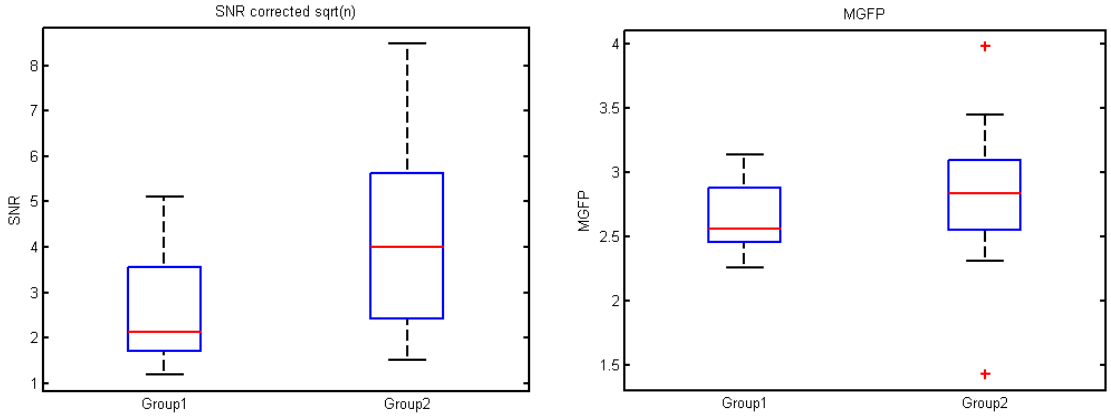


Figure 3.23: Boxplots of the corrected SNR (to number of events) as well as the uncorrected MGFP

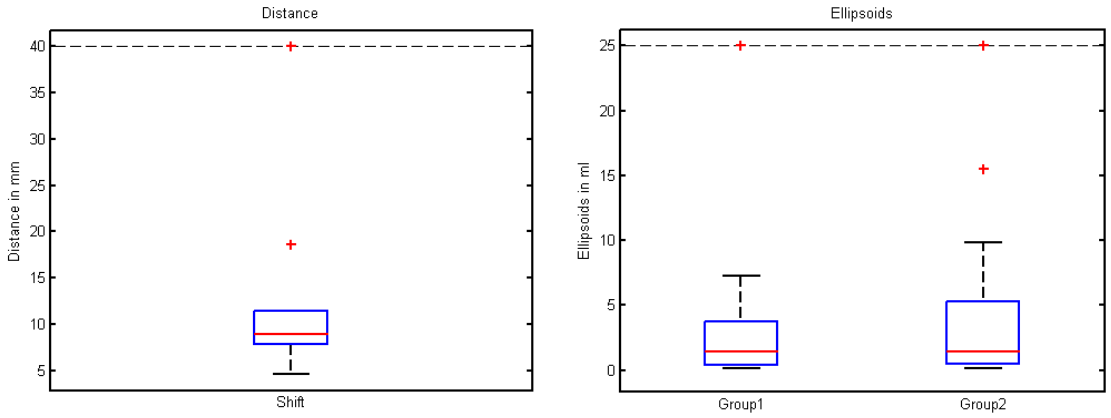


Figure 3.24: Boxplots of the dipole shift and the ellipsoids (data limits set)

Since the different clusters contain different amounts of averaged signals, the result of the SNR is corrected by the number of events included.

All results are made for the first degree electrode neighbours (n=5). As already shown in 3.2 a total of 79.77% of all markings have been changed. Since there is no unified naming of the original data, a specific evaluation of each event is not eligible.

## Discussion:

In summary this evaluation of the event lists shows that a high number of markings is not assigning the correct electrode of maximum negativity. By correction to the maximum negativity electrode in the vicinity of the marked electrode, new and more precise clusters of spikes are created for dipole

localisation. Even in the first degree neighbourhood these results lead to a purification of the clusters since biasing signals from other electrodes are removed from the averaging (see appendix 6.3). As shown in the example, the SNR itself decreases as the number of events is low. The increase of the confidence ellipsoids is due to this change, since the confidence volume is proportional to the 3$^{rd}$ power of noise. The event corrected SNR and the MGFP as value of amplitude increase significantly. This strengthens the hypothesis that the averaged signal is more precise than former one. By the correction of the signals the specificity of the localisation should improve. It is very likely that this effect is disguised by the larger effect of the decreasing SNR. In the end a final comment on this might only be possible with intracranial recordings or after surgery.

**Outlook:**

All calculations in 3.2 and 3.3 were made in a rather small neighbourhood of 5. For further analysis these results should be compared to second degree neighbourhood calculations (i.e. n=12-15) in order to increase the yield and to improve the precision of the clusters. Since only the number of neighbours needs to be changed in the **"NeighborFinder.m"** these results can be obtained easily.

## 3.5. Effects of the template search algorithm

Another option offered by the Curry program is the template matching. In this algorithm a template of a specific waveform is defined and all the data is searched for matching results.

Influencing parameters on the search are the amplitude difference and correlation, both can be selected between 50% and 90%. For example an amplitude setting of 80% results in matching events with amplitude of +/- 20% of the template value. For the use of this template search algorithm there are two underlying assumptions. The first assumption is that it helps to find all highly correlated events once a clear spike is marked by a clinical reviewer. This applies mostly to video monitoring units with long term EEG recordings as in that case only a rather short epoch needs to be evaluated by hand. If an epileptiform discharge was marked, the template search with high correlation parameters helps to find equal events in the rest of the data. For source reconstruction needs the second assumption could be more important. In case the data set contains many similar events deriving from the same spatio-temporal origin but does not reach exactly the criteria of clear epileptiform discharges the template search is able to find them as well. It needs to be evaluated if this information is reliable. Since noise can be reduced by including more epochs in the averaging process this might lead to an improved signal and source localisation. Again it needs to be taken into account that even if the SNR and source localisation parameters might improve with this technique the reliability of the calculated dipole might drop. The process must not mix signals from different spatio-temporal origin. Furthermore in current literature the localizing value of sharp transients not completely meeting the criteria of an epileptiform discharge remains undefined.

For the evaluation in this project the template matching process is carried out in a standardized way with parameters defined in advance. These are similar to other studies using a similar technique (Hamaneh et al., 2011). From the new clustered data (3.3.) an average waveform of each event is created. This is concatenated at the end of the original dataset.

From the averaged event the characteristic waveform is selected including the following parameters:

- offset of first negative slope from baseline
- negative and positive peak
- half of the after coming slow wave

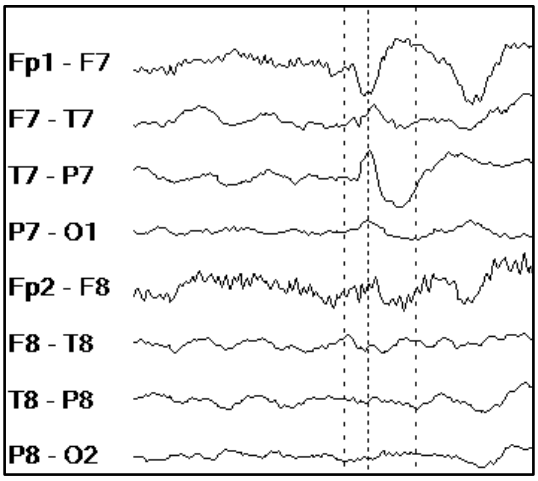


Figure 3.25: Selection of template in bipolar montage including negative and positive peak as well as half of the after coming slow wave. Picture taken and modified from data processing.

The parameters for the data are set as follows for the template search:

- channels with artefacts deselected
- baseline correction constant
- filter 1-70Hz
- 50Hz notch filter, harmonics

For the template search a subset of electrodes needs to be selected containing the most specific parts of the waveforms, so the peak with maximum amplitude. Since we are using averaged signals we are mostly able to select the known negative pole and the positive pole, as shown in the spatial maps.

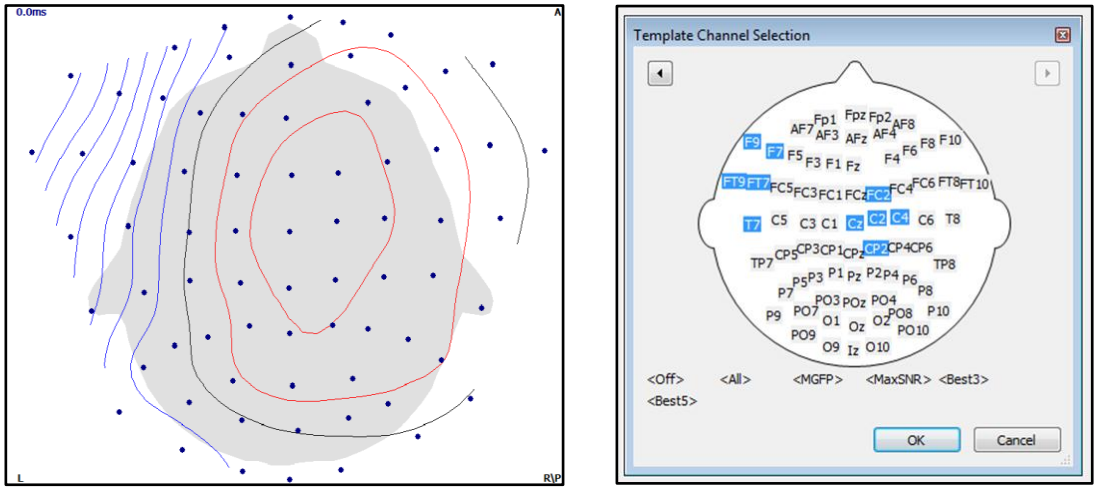


Figure 3.26: Template channel selection, electrodes around negative pole (FT9) and positive pole (C2) according to isopotential map (left). Pictures taken from data processing.

After running the template search algorithm all events matching at least 50% for amplitude and correlation are marked and saved into a new event-list. This can be altered online in the program by selecting the parameters of interest and the matching results (i.e. all events above 85% amplitude and 85% correlation) are displayed. The template algorithm is part of the commercial tool so no detailed information about the method is available.

For this study we chose a set of representative correlation (“C”) and amplitude (“A”) parameters.

- A85 / C85
- A65 / C65
- A85 / C65
- A65 / C85

**Issue:**

During processing of the data it became obvious that different averaging techniques lead to different and non-comparable results. For averaging defined epochs of the same length are used. In the Curry program with the predefined parameters this epoch is an interval of 700ms around the middle marker (200ms pre and 500ms post). For the hand marked events the middle marker is set to the negative peak so this position is unique in all averaged epochs. The templates search algorithm sets the middle marker to the beginning of the original template, which represents the offset of the slope. This means that the averaged signal from template search might contain different latencies from the offset to the peak which results in a biased peak configuration and spatio temporal resolution. Comparing different averaged epochs (n=3) by this method the noise value differed by up to 3.5% and the SNR value by up to 3% in both directions. Even though we did not test for significance, the averaged signals need to be corrected to evaluate the position of interest at the peak of the signal.

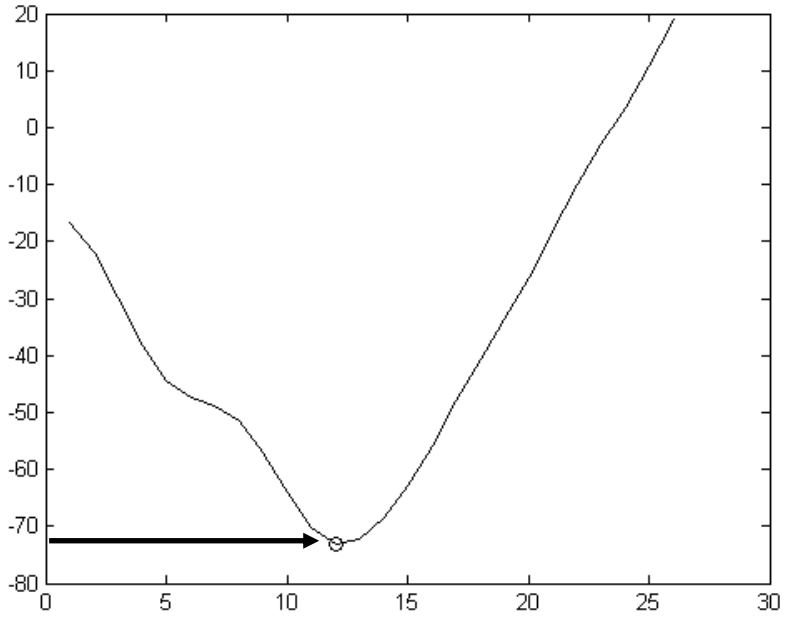


Figure 3.27: Automatic correction of marker from original position (SP 0) to most negative position (black circle).

**Program code:**

With the help of the Matlab script **"SeekPeakTemplates.m"** it is possible to correct the templates directly to the intended position. All markings containing the range 50%-100% for amplitude and correlation are saved in the event list by Curry.

The user starts the toolbox by **"MainMethodToolbox"** and selects the Peak correction and Template option (1). By the already discussed method **"MEGMainforhandmarkings.m"** all necessary files (.cef, .dat, .rs3) are loaded into the workspace. For evaluation a template search event list is selected. Afterwards the script **"SeekPeakTemplate.m"** is selected.

In step1 (as marked in the program code) the user is asked to input the most negative channel. Since we used corrected and newly clustered events for the template search, no **"neighborfinder.m**" was implemented any longer. The algorithm rather searches event by event for the negative peak in the already known channel to improve speed. This negative peak must be in a certain range after the middle marker of the interval, since the template search algorithm used to shift this marker from the peak to the beginning of the template as discussed in the preceding paragraph. This range was set to about 80msec in our study but can be altered as needed. Step 2 was implemented to catch errors if the event is too close to either end of the dataset. Step 3 calculates the maximum negativity and returns it to the superior method for further processing and automatic saving (figure 3.25).

For analysis up to 2500 events were loaded by one event list. This rules out any manual correction to the respective peak. Using the algorithm the automatic correction and saving takes less than 30 sec for each event list. Even though the actual correcting procedure is very fast, in total the generation of templates takes about 2 working days. This results from the definition and running of the template matching algorithm, the exporting and correction procedure as well as the following averaging and saving of the data as described. The dipole calculations usually take about 5 minutes by a semi-automatic procedure. After our studies, a new feature was implemented into the Curry algorithm. Now it is

possible to align the marker to the peak directly saving a lot of time during pre-processing.

**Results:**

The impact of the change in amplitude and correlation on the number of selected events is shown in figure 3.28.

| A / C | 85% | 65% |
|---|---|---|
| 85% | 3045 | 11907 |
| 65% | 7177 | 29843 |

Figure 3.28: Number of all events selected by different amplitude (A) and correlation (C) values for one subject

In this chapter only the results referring to the EEG peak will be discussed. All calculations have been done for subject 1. In all cases group1 represents the averaged results of the new clustered (see chapter 3.4) data and group2 its referring and averaged template matches.

**Amplitude 85% – Correlation 85%**

| Difference A85/C85, n=45 | Group | MGFP | SNR | Normalized residual | Original residual | Ellipsoid Volume | shift |
|---|---|---|---|---|---|---|---|
| Maximum | 1 | 60,45 | 44,09 | 0,48 | 0,52 | 773,50 | 0,00 |
| | 2 | 46,96 | 20,98 | 0,38 | 0,46 | 238,37 | 67,34 |
| Mean | 1 | 32,82 | 11,54 | 0,20 | 0,25 | 51,85 | 0,00 |
| | 2 | 28,46 | 9,91 | 0,20 | 0,24 | 21,36 | 24,11 |
| Median | 1 | 29,91 | 8,22 | 0,19 | 0,24 | 15,51 | 0,00 |
| | 2 | 26,82 | 8,95 | 0,19 | 0,22 | 8,18 | 23,12 |
| Min | 1 | 16,27 | 2,05 | 0,04 | 0,10 | 0,13 | 0,00 |
| | 2 | 16,38 | 2,38 | 0,09 | 0,13 | 0,71 | 5,60 |
| Standard Deviation | 1 | 9,51 | 9,59 | 0,09 | 0,10 | 125,73 | 0,00 |
| | 2 | 6,70 | 4,85 | 0,08 | 0,08 | 41,16 | 15,86 |
| Variance | 1 | 9,04 | 92,06 | 0,01 | 0,01 | 15808,62 | 0,00 |
| | 2 | 4,49 | 23,49 | 0,01 | 0,01 | 1693,98 | 251,62 |
| p Wilcoxon signed rank | | < 0,0001 | 0,8258 | | | 0,0428 | |

Table 3.9: Descriptive statistics of dipole calculations for template matches of subject 1 for amplitude 85% and correlation 85%

In table 3.9 the source reconstructions' results are displayed after the template search algorithm was applied with the parameters amplitude 85% and correlation 85%. A total of 3045 spikes are averaged. As shown in the table there is a decrease of the mean MGFP, mean SNR as well as the mean confidence ellipsoid volume. For the MGFP, the Wilcoxon signed rank test

reaches high significance (p<0.0001), whereas the SNR fails to reach significance (p=0.8258). The confidence ellipsoid reduction also reaches statistical significance (p=0.0428). The resulting mean shift of the dipole reconstruction is 24.11mm. As shown in table 3.9a this shift also reaches significance level (p<0.0001).

| Diff A85/C85, n=45 | MGFP | SNR | Ellipsoid Volume | shift |
|---|---|---|---|---|
| Maximum | 0,89 | 12,96 | 206,46 | 67,34 |
| Mean | -0,44 | -1,63 | -30,49 | 24,11 |
| Median | -0,37 | 1,04 | -3,78 | 23,12 |
| Min | -1,67 | -33,37 | -733,68 | 5,60 |
| Standard Deviation | 0,51 | 8,61 | 127,41 | 15,86 |
| Variance | 0,26 | 74,09 | 16234,42 | 251,62 |
| p Wilcoxon rank test | < 0,0001 | 0,8258 | 0,0428 | < 0,0001 |

Table 3.9a: Differences and results of Wilcoxon signed rank test for the respective parameters

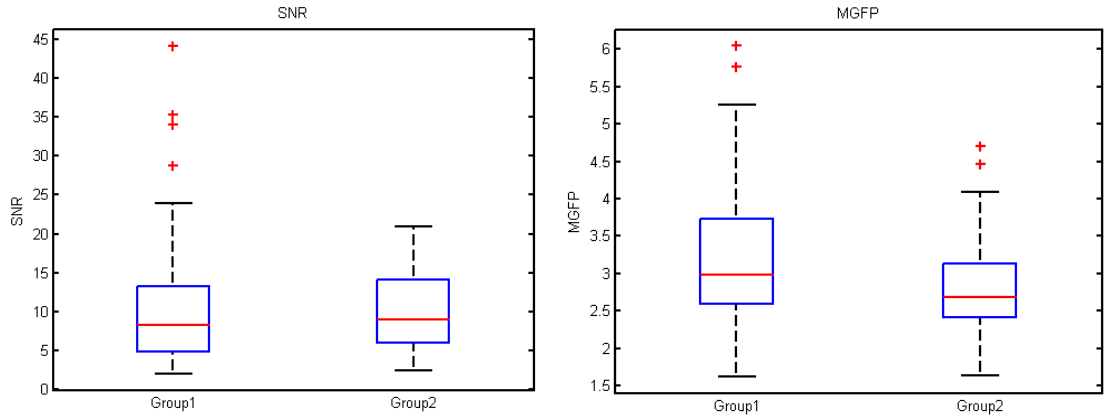


Figure 3.29: Boxplots for SNR and MGFP before and after template search for amplitude 85% and correlation 85%

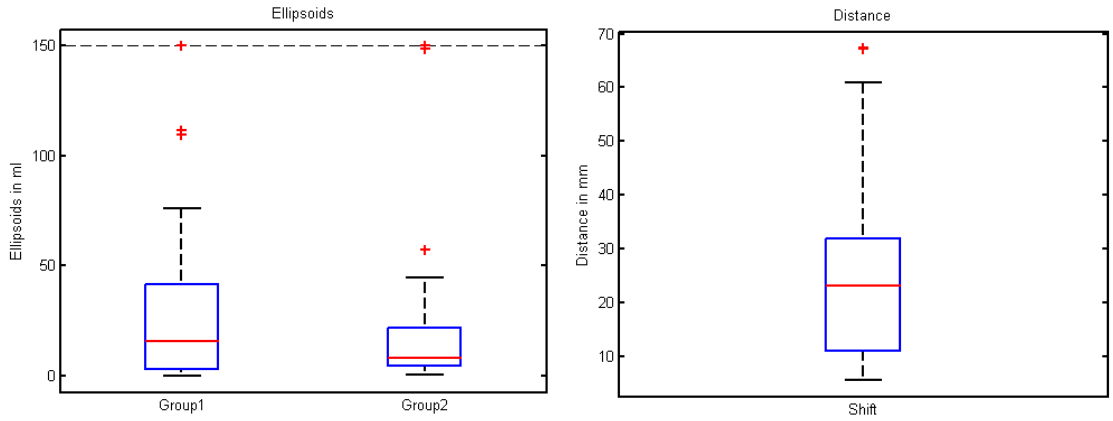


Figure 3.30: Boxplots for confidence ellipsoids and dipole location shift before and after template search for amplitude 85% and correlation 85%

## Amplitude 85% - Correlation 65%

| Templates A85/C65, n=45 | Group | MGFP | SNR | Normalized residual | Original residual | Ellipsoid Volume | shift |
|---|---|---|---|---|---|---|---|
| Maximum | 1 | 60,45 | 44,09 | 0,48 | 0,52 | 773,50 | 0,00 |
| | 2 | 45,98 | 35,70 | 0,34 | 0,43 | 37,72 | 67,82 |
| Mean | 1 | 32,82 | 11,54 | 0,20 | 0,25 | 51,85 | 0,00 |
| | 2 | 26,23 | 13,66 | 0,16 | 0,25 | 9,24 | 29,02 |
| Median | 1 | 29,91 | 8,22 | 0,19 | 0,24 | 15,51 | 0,00 |
| | 2 | 24,93 | 11,28 | 0,14 | 0,23 | 6,12 | 28,07 |
| Min | 1 | 16,27 | 2,05 | 0,04 | 0,10 | 0,13 | 0,00 |
| | 2 | 15,13 | 4,17 | 0,06 | 0,13 | 1,75 | 6,99 |
| Standard Deviation | 1 | 9,51 | 9,59 | 0,09 | 0,10 | 125,73 | 0,00 |
| | 2 | 6,73 | 7,75 | 0,07 | 0,08 | 8,88 | 12,74 |
| Variance | 1 | 9,04 | 92,06 | 0,01 | 0,01 | 15808,62 | 0,00 |
| | 2 | 4,52 | 60,13 | 0,00 | 0,01 | 78,77 | 162,20 |
| p Wilcoxon signed rank | | < 0,0001 | 0,0084 | | | 0,0001 | |

Table 3.10: Descriptive statistics of dipole calculations for template matches of subject 1 for amplitude 85% and correlation 65%.

In table 3.10 the source reconstructions' results are displayed after the template search algorithm was applied with the parameters amplitude 85% and correlation 65%. A total of 11907 spikes are averaged. As shown in the table the mean MGFP decreases whereas the mean SNR increases. The confidence ellipsoid volume decreases almost five fold. For all mentioned parameters, the Wilcoxon signed rank test reaches significance level (MGFP $p<0.0001$, SNR $p=0.0084$ and ellipsoids $p=0.0001$). The resulting mean shift of the dipole reconstruction is 29.07mm. As shown in table 3.10a this shift also reaches significance level ($p<0.0001$).

| Diff A85/C65, n= 45 | MGFP | SNR | Ellipsoid Volume | shift |
|---|---|---|---|---|
| Maximum | 0,48 | 17,68 | 16,02 | 67,82 |
| Mean | -0,66 | 2,12 | -42,61 | 29,02 |
| Median | -0,60 | 1,65 | -6,03 | 28,07 |
| Min | -1,80 | -21,64 | -741,61 | 6,99 |
| Standard Deviation | 0,48 | 7,98 | 121,05 | 12,74 |
| Variance | 0,23 | 63,61 | 14653,79 | 162,20 |
| p Wilcoxon rank test | < 0,0001 | 0,0084 | 0,0001 | < 0,0001 |

Table 3.10a: Differences and results of Wilcoxon signed rank test for the respective parameters

All changes of the parameters are shown in the following box plots.

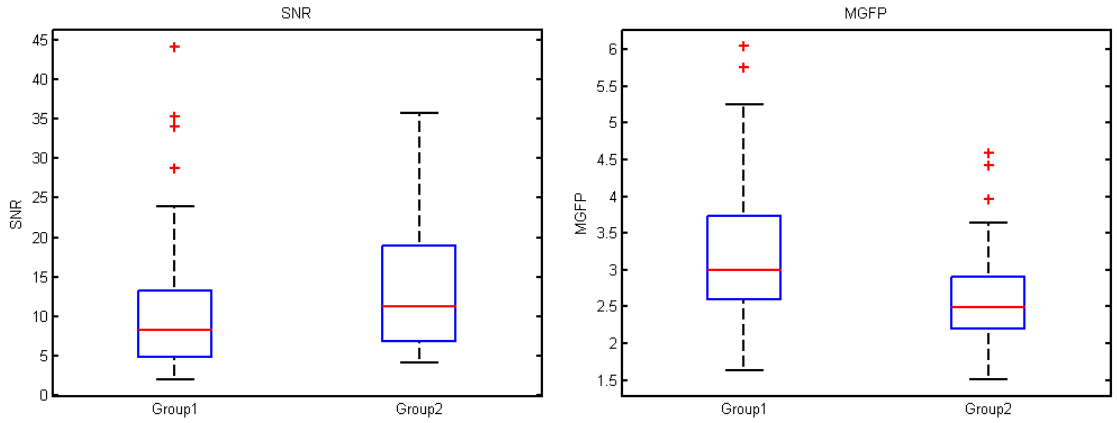


Figure 3.31: Boxplots for SNR and MGFP before and after template search for amplitude 85% and correlation 65%

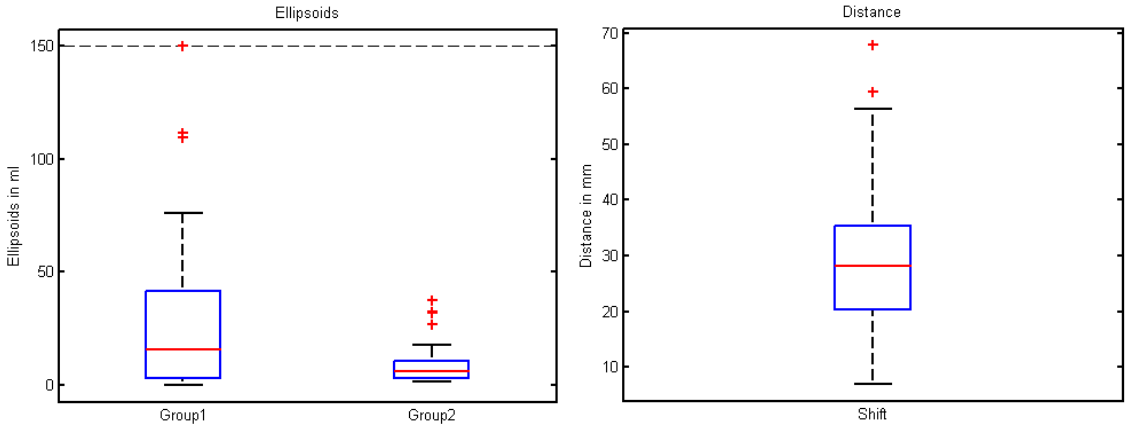


Figure 3.32: Boxplots for confidence ellipsoids and dipole location shift before and after template search for amplitude 85% and correlation 65%

## Amplitude 65% - Correlation 85%

| Template A65/C85, n=45 | Group | MGFP | SNR | Normalized residual | Original residual | Ellipsoid Volume | shift |
|---|---|---|---|---|---|---|---|
| Maximum | 1 | 60,45 | 44,09 | 0,48 | 0,52 | 773,50 | 0,00 |
| | 2 | 40,94 | 29,10 | 0,42 | 0,54 | 421,54 | 63,58 |
| Mean | 1 | 32,86 | 11,43 | 0,21 | 0,25 | 54,06 | 0,00 |
| | 2 | 27,23 | 11,21 | 0,20 | 0,23 | 23,37 | 22,83 |
| Median | 1 | 29,91 | 7,50 | 0,19 | 0,24 | 15,67 | 0,00 |
| | 2 | 25,90 | 10,27 | 0,18 | 0,20 | 6,05 | 18,61 |
| Min | 1 | 16,27 | 2,05 | 0,04 | 0,10 | 0,13 | 0,00 |
| | 2 | 16,13 | 2,47 | 0,08 | 0,12 | 0,48 | 6,04 |
| Standard Deviation | 1 | 9,46 | 9,66 | 0,10 | 0,09 | 125,87 | 0,00 |
| | 2 | 5,84 | 6,21 | 0,07 | 0,09 | 64,04 | 14,69 |
| Variance | 1 | 8,94 | 93,34 | 0,01 | 0,01 | 15844,08 | 0,00 |
| | 2 | 3,41 | 38,60 | 0,01 | 0,01 | 4100,77 | 215,84 |
| p Wilcoxon signed rank | | < 0,0001 | 0,3635 | | | 0,0165 | |

Table 3.11: Descriptive statistics of dipole calculations for template matches of subject 1 for amplitude 65% and correlation 85%.

In table 3.11 the source reconstructions' results are displayed after the template search algorithm was applied with the parameters amplitude 65% and correlation 85%. A total of 7177 spikes are averaged. As shown in the table the mean MGFP and the mean SNR decrease slightly. The confidence ellipsoid volume decreases by half. For the MGFP and the confidence ellipsoids, the Wilcoxon signed rank test reaches significance level (MGFP $p<0.0001$, ellipsoids $p=0.0165$). The SNR does not reach significance level ($p=0.3635$). The resulting mean shift of the dipole reconstruction is 22,83mm. As shown in table 3.11a this shift also reaches significance level ($p<0.0001$).

| Diff A65/C85, n= 45 | MGFP | SNR | Ellipsoid Volume | shift |
|---|---|---|---|---|
| Maximum | 1,48 | 15,19 | 310,98 | 63,58 |
| Mean | -0,56 | -0,22 | -30,69 | 22,83 |
| Median | -0,51 | 1,20 | -5,20 | 18,61 |
| Min | -2,27 | -25,66 | -748,11 | 6,04 |
| Standard Deviation | 0,64 | 7,87 | 133,54 | 14,69 |
| Variance | 0,41 | 61,93 | 17832,08 | 215,84 |
| p Wilcoxon rank test | < 0,0001 | 0,3635 | 0,0165 | < 0,0001 |

Table 3.11a: Differences and results of Wilcoxon signed rank test for the respective parameters

All changes of the parameters are shown in the following box plots.

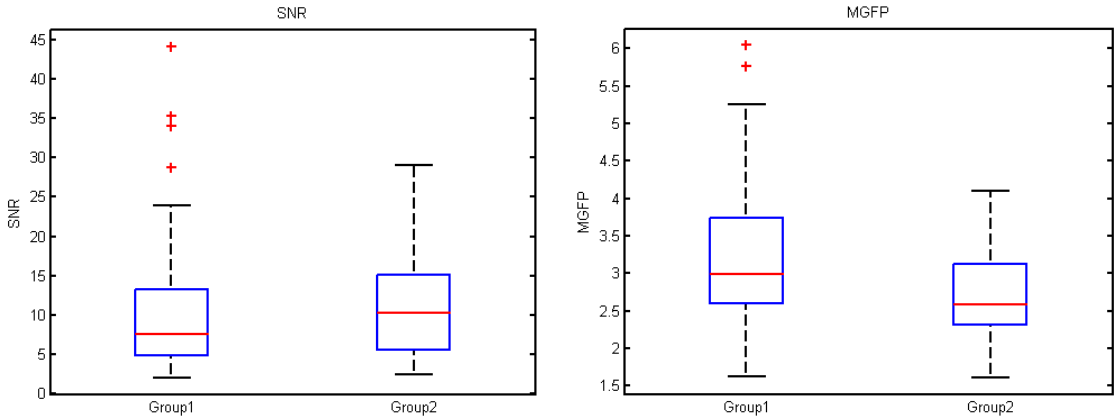


Figure 3.33: Boxplots for SNR and MGFP before and after template search for amplitude 65% and correlation 85%

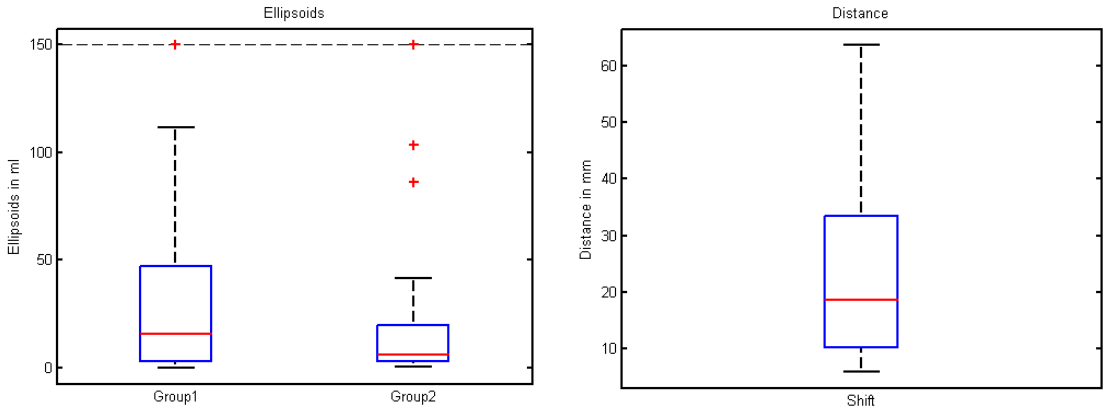


Figure 3.34: Boxplots for confidence ellipsoids and dipole location shift before and after template search for amplitude 65% and correlation 85%

## Amplitude 65% - Correlation 65%

| Templates A65/C65, n=45 | Group | MGFP | SNR | Normalized residual | Original residual | Ellipsoid Volume | shift |
|---|---|---|---|---|---|---|---|
| Maximum | 1 | 60,45 | 44,09 | 0,48 | 0,52 | 311,90 | 0,00 |
| | 2 | 39,10 | 51,95 | 0,37 | 0,49 | 28,18 | 62,37 |
| Mean | 1 | 33,29 | 11,66 | 0,21 | 0,25 | 31,81 | 0,00 |
| | 2 | 23,74 | 12,85 | 0,17 | 0,26 | 8,02 | 27,88 |
| Median | 1 | 30,70 | 8,22 | 0,19 | 0,25 | 15,43 | 0,00 |
| | 2 | 22,63 | 11,04 | 0,17 | 0,23 | 5,97 | 28,74 |
| Min | 1 | 16,27 | 2,05 | 0,04 | 0,10 | 0,13 | 0,00 |
| | 2 | 15,09 | 3,79 | 0,04 | 0,12 | 2,01 | 5,78 |
| Standard Deviation | 1 | 9,81 | 9,51 | 0,09 | 0,10 | 52,70 | 0,00 |
| | 2 | 5,44 | 7,91 | 0,07 | 0,09 | 6,77 | 11,21 |
| Variance | 1 | 9,61 | 90,42 | 0,01 | 0,01 | 2777,25 | 0,00 |
| | 2 | 2,96 | 62,50 | 0,00 | 0,01 | 45,86 | 125,73 |
| p Wilcoxon signed rank | | < 0,0001 | 0,0587 | | | 0,0003 | |

Table 3.12: Descriptive statistics of dipole calculations for template matches of subject 1 for amplitude 65% and correlation 65%.

In table 3.12 the source reconstructions' results are displayed after the template search algorithm was applied with the parameters amplitude 65% and correlation 65%. A total of 29843 spikes are averaged. As shown in the table the mean MGFP decreases slightly. The confidence ellipsoid volume decreases almost 3 quarters. The SNR slightly increases. For the MGFP and the confidence ellipsoids, the Wilcoxon signed rank test reaches significance level (MGFP $p<0.0001$, ellipsoids $p=0.0003$). The SNR closely does not reach significance level ($p=0.0587$). The resulting mean shift of the dipole reconstruction is 27.88mm. As shown in table 3.11a this shift also reaches significance level ($p<0.0001$).

| Diff A65/C65 | MGFP | SNR | Ellipsoid Volume | shift |
|---|---|---|---|---|
| Maximum | 0,16 | 16,68 | 7,66 | 62,37 |
| Mean | -0,96 | 1,19 | -23,78 | 27,88 |
| Median | -0,81 | 2,81 | -6,22 | 28,74 |
| Min | -2,50 | -27,75 | -303,49 | 5,78 |
| Standard Deviation | 0,54 | 8,60 | 51,34 | 11,21 |
| Variance | 0,29 | 74,05 | 2635,53 | 125,73 |
| p Wilcoxon rank test | < 0,0001 | 0,0587 | 0,0003 | < 0,0001 |

Table 3.12a: Differences and results of Wilcoxon signed rank test for the respective parameters

All changes of the parameters are shown in the following box plots.

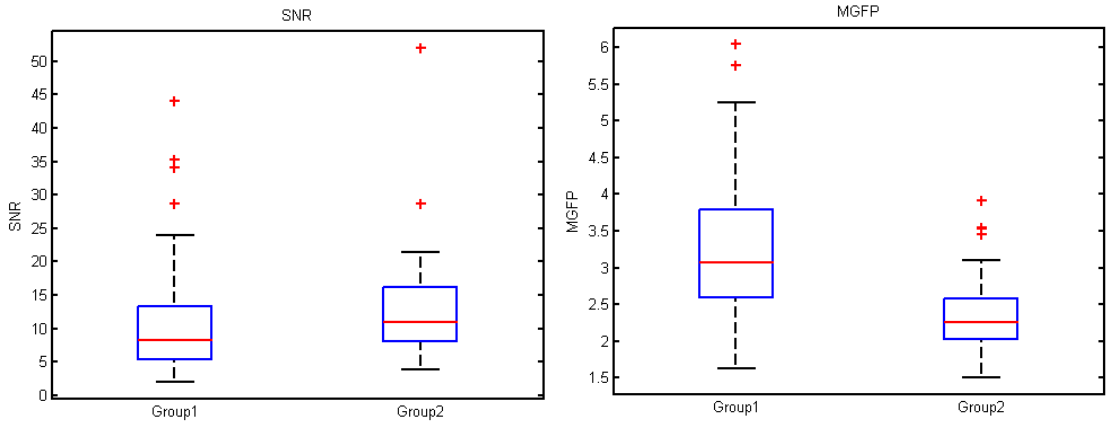


Figure 3.35: Boxplots for SNR and MGFP before and after template search for amplitude 65% and correlation 65%

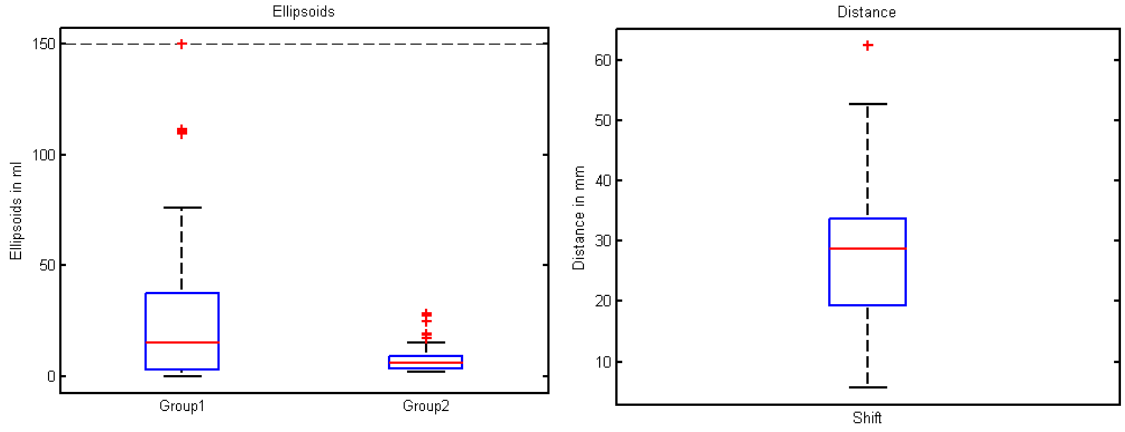


Figure 3.36: Boxplots for confidence ellipsoids and dipole location shift before and after template search for amplitude 65% and correlation 65%

**Discussion:**

By the template matching, correlating events are searched automatically by an algorithm once a characteristic waveform is selected by the user. In the current study this method is evaluated especially with respect to the impact on improving signal quality and the reliability of the dipole fit. For the evaluation corrected and newly clustered data is chosen of which an averaged signal was taken as template. The selected events marked by the used algorithm are corrected to the peak in order to compare it to the preceding data.

The results show effects on all evaluated parameters SNR, MGFP, confidence ellipsoids and dipole position.

With respect to SNR, in three of the four subsets there is an increase of the amplitude. Only in one subset, this increase is statistically significant. The SNR represents two parameters as it is calculated from the signal strength and the noise. The statistical significant subset includes signal with higher amplitudes. The other way round, widening the amplitude range does not result in an overall increase of the SNR. The same applies to the MGFP. In all subsets there is a significant decrease of the MGFP value. The template match includes also signals with lower amplitude according to the selected parameters. The noise decreases with every epoch we added for averaging since the noise is random and even the ones with small amplitude will reduce the noise in pre-trigger amplitude although they did not increase the MGFP. When the amplitude parameter is set to 65% this effect becomes very obvious. The MGFP represents the mean amplitude of the signal and so it is very likely that the decrease is the effect of the inclusion of the low amplitude signals. The confidence ellipsoid decreases significantly in all cases as parameter of the precision of the dipole localisation. The values of the mean decrease are rather similar, although the deviation of the value decreases with the number of included events. In all cases there is an effect on the dipole localisation which always differs after applying the template algorithm.

Since we simply used the template search algorithms without any constraints there are some aspects to be discussed. We have 60 * 8 seconds * 5 runs = 2400 seconds of measurement, and even in the case with A85/C85 it means one spike in every 780ms. For the A65/C65 it means one event every 80ms. This means that the spike events also includes other spikes in the time selected epoch range (700 ms) which will decrease the SNR since they might be included in the noise calculation interval.

Even though we assume that the corrections made to the data rule out biasing factors the definite impact on the source localisation cannot be judged solely from the dipole fitting results. As long as there is no precise information of the generating structure from intracranial recording or epilepsy surgery, these results cannot be proven.

In summary the most important fact is seen in the confidence ellipsoid, which decreases significantly with the increasing number of correlating events. The effects on MGFP and SNR are less since the inclusion of low amplitude signals seems to outweigh the reduction of the noise. In comparison to the earlier discussed peak correction and re-clustering the effects of the template algorithm on MGFP and SNR seem to be less.

The template search algorithm should also be used with care since the overlap of events might influence the calculation of the noise and bias the results.

## 4. Conclusions

This study aims to find, evaluate and improve possible unexpected or unrecognized factors influencing the signal quality at the intersection between medical and methodological staff involved. The main factors influencing the signal quality are the precision of the marking of epileptiform discharges as well as the clustering of the spikes. Both of these factors are known and both are major parameters of clinical practice used for decades. Unless very precise and pure data for further analysis and averaging is needed, little imprecision does not affect clinical decision in daily routine. At the intersection between clinical reviewer and further data processing, the precision of the marking usually cannot be verified. All later processing is relying on the quality of the data. In our case, the rather minor imprecisions as incorrect peak markings and mixed clustering cause a significant change in the dipole localisation of up to 3cm shift. This is shown extensively in the preceding chapters.

Since in the further process of improving source localisation, highly sophisticated head models with high precision will be used, these factors must be identified and ruled out in the pre-processing phase. Only by the usage of reliable and precise data the new head models can be evaluated reasonably.

In the end the peak correction and re-clustering procedures simply represent the best clinical practice. We are able to show the effect on the dipole localisation when this best clinical practice is not met unperceived. Also we offer a tool to correct the data easily without profound clinical knowledge.

Furthermore it was to evaluate the template matching algorithm for improving signal quality. As shown with subject 1, the impact on the signal quality itself does not show high significance. The effect of the inclusion of low correlation events seem to bias the averaged signal quality. Since the procedure of the algorithm is not known to us at this stage, all interpretations must be carried out carefully. The precision of the dipole localisation seems to increase with the number of events averaged as the confidence ellipsoids decreases significantly.
As in all cases the real position of the dipole remains unknown. All parameters and results presented only give evidence for the true activated neuronal patch in the brain.
For further evaluation of this study intracranial recordings nearer to the focus and the outcome of possible epilepsy surgery are necessary.

## 5. Glossary of terms

This glossary of terms refers to own descriptions as well as definitions taken from wikipedia.

| | |
|---|---|
| 10/20 System | Standardized placement of EEG electrodes in relation to fixed positions on every individual head |
| Afferent | All nerves transmitting information from receptor cells to the central nervous system |
| Amplification | The operation of an amplifier, a natural or artificial device intended to make a signal stronger. |
| Anisotropies | Anisotropy is the property of being directionally dependent, as opposed to isotropy, which implies identical properties in all directions |
| Anticonvulsive drugs | Medications supressing epileptic seizures |
| Axons | Parts of neurons for information transmission over distance |
| Band pass filter | Filter for bio-signals blocking frequencies above and below a certain threshold |
| Bipolar montage | Bipolar montages usually display parallel longitudinal rows. Characteristic feature of longitudinal rows is the connection of the first electrode with input 1 and the next electrode with input 2. |
| Brain stem | Part of the central nervous system connection the cerebrum with the spinal cord |

| | |
|---|---|
| CCF | Cleveland Clinic Foundation, Cleveland, Ohio, USA |
| Central nervous system | Parts of the nervous system containing the brain, cerebellum, brain stem and the myelon |
| Cerebellum | Part of the central nervous system providing functions like coordination |
| Cerebrospinal fluid | (CSF) is a clear colourless bodily fluid produced in the choroid plexus of the brain. It acts as a cushion or buffer for the cortex, providing a basic mechanical and immunological protection to the brain inside the skull and serves a vital function in cerebral auto-regulation of cerebral blood flow. |
| Concentration gradient | State of unequal concentration in two different compartments separated by a barrier |
| Conductivity | A measure of a material's ability to conduct an electric current |
| Confidence ellipsoid | A multi-dimensional generalization of a confidence interval. It is a set of points in an n-dimensional space, often represented as an ellipsoid around a point which is an estimated solution to a problem, although other shapes can occur. |
| Cortex | Outer layers of the brain containing several different kind of brain cells |
| Cortex grid | EEG electrodes fixed in a sheet of plastic for recording directly from the cerebral cortex |
| Dendrites | Part of neurons for interconnections with other neurons |

| | |
|---|---|
| Depolarisation | Breakdown of the resting potential |
| EEG | Electroencephalography, recording of brain activity by electrodes fixed to the scalp |
| Efferent | All nerves transmitting information from the central nervous system to cells of interest, i.e. muscle cells |
| Electro-oculo-graphy (EOG) | Recording of eye movements by electrodes |
| Eloquent cortex | Cortex area representing a loss function when disabled |
| Epilepsy | A common and diverse set of chronic neurological disorders characterized by seizures. |
| Equilibrium | *Diffusive equilibrium* is reached when the concentrations of the diffusing substance in the two compartments becomes equal. |
| Fast Ripples | High frequency oscillations as marker of seizure onset |
| Field potential | A particular class of electrophysiological signals, which is dominated by the electrical current flowing from all nearby dendritic synaptic activity within a volume of tissue |
| Glia cells | Cells surrounding the neurons not taking part in the direct transmission of information |
| Hemispheres | Left and right part of the cerebrum which is divided in half in the midline |
| Hyperpolarisation | Creation of a more negative resting potential than common |

| | |
|---|---|
| Hyperventilation | Fast breathing frequency |
| Ictal | State of presence of clinical and or EEG/MEG features of an epileptic seizure |
| Interictal | State of absence of clinical and or EEG/MEG features of an epileptic seizure |
| Inter-rater reliability | Differences and agreement of different reviewers reading the same set of data |
| Ion channels | Specific gates in the cell membrane for signal processing in the nervous system |
| Ion pumps | Parts of the cell membrane to shift ions from one side to the other in order to restore the membrane potential |
| MEG | Magnetoencephalogram, recording of brain activity by sensors placed over the scalp |
| Membrane potential | Difference in electrical potential between the interior and the exterior of a biological cell, basic feature of signal transmission in the nervous system |
| Metabolism | Metabolism is the set of chemical reactions that happen in the cells of living organisms to sustain life. |
| MGFP | Mean global field power |
| Neuron | Nerve cell taking part in transmission of information |
| Normal variants | Features in EEG similar to epileptiform discharges without consideration of an illness |

| | |
|---|---|
| Notch filter | Filter for bio-signals blocking a fairly small selection of frequencies (i.e. 50Hz) |
| Paroxysmal | Intermittent |
| Pathophysiology | Pathophysiology is the study of the changes of normal mechanical, physiological, and biochemical functions, either caused by a disease, or resulting from an abnormal syndrome |
| Peripheral nervous system | Nerves outside the brain, brain stem and the myelon |
| Pyramidal cell | Type of neuron found in areas of the brain including cerebral cortex, the hippocampus, and in the amygdala. |
| Radial | A radial pattern is one that appears to radiate from a point, like the spokes from the hub of a wheel |
| Referential montage | Referential montages show the electrode of interest at input 1 which always is connected to the same or the same combination of reference electrodes at input 2. |
| Residual | The residual of a sample is the difference between the sample and the *estimated* function value. |
| Resting membrane potential | The relatively static membrane potential of quiescent cells is called the resting membrane potential (or resting voltage), as opposed to the specific dynamic electrochemical phenomena called action potential and graded membrane potential. |

| | |
|---|---|
| Rhythmic delta slowing | Slowing of the background activity seen in EEG and MEG |
| Seizure semiology | Signs and features occurring during an epileptic seizure pointing to a potential generator or cause |
| Seizure | An epileptic seizure, occasionally referred to as a fit, is defined as a transient symptom of "abnormal excessive or synchronous neuronal activity in the brain |
| SNR | Signal to noise ratio |
| Source localisation | Mathematical calculation of the location of generators, where the recorded activity derives from |
| Spike | One of many characteristically epileptiform discharges recorded in EEG or MEG |
| Spinal cord | Part of the central nervous system connection the brain stem with the peripheral nerves, situated in the spine |
| Stroke | A stroke is the rapid loss of brain function(s) due to disturbance in the blood supply to the brain resulting in a brain defect |
| Synapse | Site of signal transmission between neurons |
| Synchronicity | Synchronicity is the experience of two or more events that are apparently causally unrelated or unlikely to occur together by chance, yet are experienced as occurring together in a meaningful manner |

| | |
|---|---|
| T1 Weighting | Special recording and presentation of acquired MRI pictures |
| Tangential | In geometry, the tangent line (or simply the tangent) to a plane curve at a given point is the straight line that "just touches" the curve at that point. As it passes through the point where the tangent line and the curve meet, called the point of tangency, the tangent line is "going in the same direction" as the curve |
| Template search | Algorithm for detection of similar events |
| Temporal lobe epilepsy | Epilepsy with a generator in the temporal lobe |
| Triangle mesh | Construct for cortex surface modelling by i.e. small triangles |
| Venn diagram | Venn diagrams or set diagrams are diagrams that show all possible logical relations between a finite collection of sets (aggregation of things). |
| Video monitoring unit | Place for recording EEG and video simultaneously for better description of seizure semiology and generator localisation |
| Wilcoxon signed rank rest | A non-parametric statistical hypothesis test used when comparing two related samples, matched samples, or repeated measurements on a single sample to assess whether their population mean ranks differ |

# 6. Appendix

## 6.1 Example of evaluation log file

```
15-Aug-2012 15:22:47.259
Subject: subject 1, run 8 ; Calculations for method: EEG
Total number of EEG spikes found by at least one reader: 194
Unique reviewer 1: 8
Unique reviewer 2: 9
Unique reviewer 3: 62
Intersection reviewer 1 and 2: 38
Intersection reviewer 1 and 3: 43
Intersection reviewer 2 and 3: 110
Intersection reviewer 1 and 2 and 3: 38
Precision for matches: SP +/- 15 = 45 ms
-----------------------------------------------
File information 1:
C:\Users\File1.cef

Total number of marked events: 59
Marked artefacts: 1
Total number of valid events: 58
Discarded events because of EEG analysis: 7
Number of EEG Events analysed: 51

Number of events and annotations:
200001      37       1  Spike 1
200002       4       1  Spike 2
200003       3       1  Spike 3
200004       7       1  Spike 4
200005       3       2  MEG Spike 1
200006       4       2  MEG Spike 2
200007       1       0  Start

Number of events in Event-list1:
0  8
1  5
2  38

Percentage of markings by one or more other raters: 0.84314
Percentage of markings by two other raters: 0.7451
True positives: 43
False positives: 8
False negatives: 72
Sensitivity: 0.37391
Precision: 0.84314
-----------------------------------------------
File information 2:
C:\Users\File2.cef

Total number of marked events: 119
Marked artefacts: 0
Total number of valid events: 119
Discarded events because of EEG analysis: 0
Number of EEG Events analysed: 119
```

```
Number of events and annotations:
200001     110       1  Spike 1 F9
200004       9       1  Spike 4 Fz
Number of events in Event-list2:
0  9
1  72
2  38

Percentage of markings by one or more other raters: 0.92437
Percentage of markings by two other raters: 0.31933
True positives: 110
False positives: 9
False negatives: 5
Sensitivity: 0.95652
Precision: 0.92437
------------------------------------------------
File information 3:
C:\Users\File3.cef

Total number of marked events: 177
Marked artefacts: 0
Total number of valid events: 177
Discarded events because of EEG analysis: 0
Number of EEG Events analysed: 177

Number of events and annotations:
200001     164       1  Spike (F9)
200002       2       1  Spike (P7)
200003      11       1  Spike (Fz)

Number of events in Event-list3:
0  62
1  77
2  38

Percentage of markings by one or more other raters: 0.64972
Percentage of markings by two other raters: 0.21469
True positives: 115
False positives: 62
False negatives: 0
Sensitivity: 1
Precision: 0.64972
```

## 6.2 Example of peak correction log file

```
03-Aug-2012 13:0:46.01

Event_File1.cef
-->
newcluster_Event_File1.cef

-----------------------------------------------

Total Events (EEG and MEG): 59
MEG Events: 8
EEG Events: 51
Excluded Events (no peak in range): 0
Number of analysed EEG Events: 51
Changed EEG Events: Total: 44 Percentage: 0.86275

-----------------------------------------------

SamplePoint (SP) Calculations:
Maximum deviation: 8 SP == 26.64ms
Minimum deviation: -8 SP == -26.64ms
Abs. mean: 2.8235 SP == 9.4024ms
Abs. standard deviation: 2.3126 SP == 7.701ms
Mean: -0.43137 SP == -1.4365ms
Standard deviation: 3.6456 SP == 12.1398ms

-----------------------------------------------

Amplitude Calculations:
Amplitude Minimum deviation: -116.958µV
Amplitude Abs. mean: 22.2786µV
Amplitude Abs. standard deviation: 26.81µV
Amplitude mean percentage to maximum amplitude : 0.21024
Amplitude standard deviation of percentage to maximum amplitude :
0.2627
```

## 6.3 Examples of topographies and localization

In the following examples the topographies and the resulting localization of averaged signals before and after correction and re-clustering are shown.

a) Averaged cluster of spikes marked at electrode F9 without correction, the corresponding topography (right). Pictures taken from data processing.

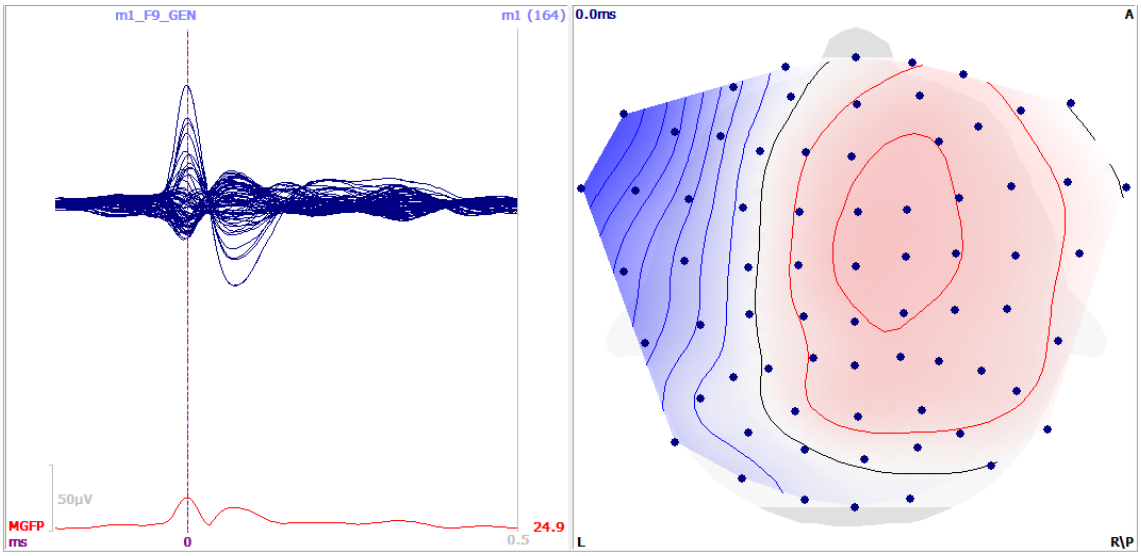


b) Averaged cluster of spikes marked at electrode F9 after correction, the corresponding topography (right). Pictures taken from data processing.

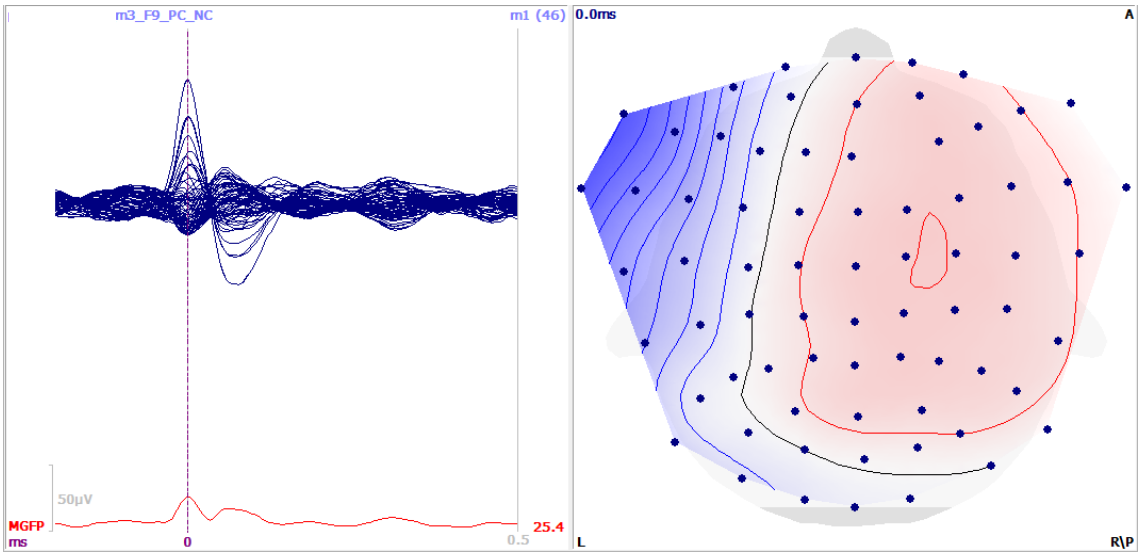

## 7. List of tables and figures

## 8. Bibliography

Albowitz B, Kuhnt U, Köhling R, Lücke A, Straub H, Speckmann E.-J, et al. Spatio-temporal distribution of epileptiform activity in slices from human neocortex: recordings with voltage-sensitive dyes. Epilepsy Research 1998; 32: 224–232.

Barkley GL, Baumgartner Christoph. MEG and EEG in epilepsy. J Clin Neurophysiol 2003; 20: 163–178.

Barkmeier DT, Shah AK, Flanagan D, Atkinson MD, Agarwal R, Fuerst DR, et al. High inter-reviewer variability of spike detection on intracranial EEG addressed by an automated multi-channel algorithm. Clin Neurophysiol 2012; 123: 1088–1095.

Barth DS, Sutherling W, Beatty J. Intracellular currents of interictal penicillin spikes: evidence from neuromagnetic mapping. Brain Res. 1986; 368: 36–48.

Bast T, Boppel T, Rupp A, Harting I, Hoechstetter K, Fauser S, et al. Noninvasive Source Localization of Interictal EEG Spikes: Effects of Signal-to-Noise Ratio and Averaging. Journal of Clinical Neurophysiology 2006; 23: 487–497.

Bast T, Oezkan O, Rona S, Stippich C, Seitz A, Rupp A, et al. EEG and MEG Source Analysis of Single and Averaged Interictal Spikes Reveals Intrinsic Epileptogenicity in Focal Cortical Dysplasia. Epilepsia 2004; 45: 621–631.

Baumann SB, Wozny DR, Kelly SK, Meno FM. The electrical conductivity of human cerebrospinal fluid at body temperature. IEEE Transactions on Biomedical Engineering 1997; 44: 220 –223.

Baumgartner C, Pataraia E, Lindinger G, Deecke L. Neuromagnetic recordings in temporal lobe epilepsy. J Clin Neurophysiol 2000; 17: 177–189.

Black MA, Jones RD, Carroll GJ, Dingle AA, Donaldson IM, Parkin PJ. Real-time Detection of Epileptiform Activity in the EEG: A Blinded Clinical Trial. Clin EEG Neurosci 2000; 31: 122–130.

Brandt, Christian. Epilepsien in Zahlen. 2008

Brenner D, Williamson S, Kaufman L. Visually evoked magnetic fields of the human brain. Science 1975; 190: 480–482.

Brette R, Destexhe A. Handbook of Neural Activity Measurement. 1st ed. Cambridge University Press; 2012.

Brodie MJ, Kwan P. Staged approach to epilepsy management. Neurology 2002; 58: S2–8.

Brown MW, Porter BE, Dlugos DJ, Keating J, Gardner AB, Storm PB, et al. Comparison of novel computer detectors and human performance for spike detection in intracranial EEG. Clinical Neurophysiology 2007; 118: 1744–1752.

Callaghan BC, Anand K, Hesdorffer D, Hauser WA, French JA. Likelihood of seizure remission in an adult population with refractory epilepsy. Annals of Neurology 2007; 62: 382–389.

Chitoku Shiro, Hoshida Tohru, Hirabayashi H, Sakaki T. Usefulness of the Dipole Tracing Method with a Scalp-Skull-Brain Head Model: Relationship between the Epileptic Focus and Equivalent Current Dipole Locations. Stereotactic and Functional Neurosurgery 1999; 73: 95–97.

Chitoku Shiro, Otsubo Hiroshi, Ichimura T, Saigusa T, Ochi Ayako, Shirasawa A, et al. Characteristics of dipoles in clustered individual spikes and averaged spikes. Brain and Development 2003; 25: 14–21.

Cohen D, Cuffin BN. Demonstration of useful differences between magnetoencephalogram and electroencephalogram. Electroencephalogr Clin Neurophysiol 1983; 56: 38–51.

Cohen David, Givler E. Magnetomyography: magnetic fields around the human body produced by skeletal muscles. Applied Physics Letters 1972; 21: 114 –116.

Compumedics. CURRY 7 Neuroimaging Suite: Current Reconstruction and Imaging [Internet]. Neuroscan; Available from: http://www.neuroscan.com/curry7.cfm

Deetjen P, Speckmann E, Hescheler J. Physiologie [Internet]. [cited 2012 May 7] Available from: http://www.buecher.de/shop/buecher/physiologie/deetjen-p-speckmann-e-j-hescheler-j-deetjen-peter-speckmann-erwin-j-hescheler-juergen/products_products/detail/prod_id/12902768/

Dümpelmann M, Elger CE. Automatic detection of epileptiform spikes in the electrocorticogram: a comparison of two algorithms. Seizure 1998; 7: 145–152.

Dümpelmann M, Elger CE. Visual and automatic investigation of epileptiform spikes in intracranial EEG recordings. Epilepsia 1999; 40: 275–285.

Ebersole J S, Wade PB. Spike voltage topography identifies two types of frontotemporal epileptic foci. Neurology 1991; 41: 1425–1433.

Ebersole J S. Defining epileptogenic foci: past, present, future. J Clin Neurophysiol 1997; 14: 470–483.

Elger C., Speckmann E.-J. Penicillin-induced epileptic foci in the motor cortex: Vertical inhibition. Electroencephalography and Clinical Neurophysiology 1983; 56: 604–622.

Engel J, Wiebe S, French J, Sperling M, Williamson P, Spencer D, et al. Practice Parameter: Temporal Lobe and Localized Neocortical Resections for Epilepsy. Epilepsia 2003; 44: 741–751.

Engel J. Surgery for Seizures. New England Journal of Medicine 1996; 334: 647–653.

Engel J. Finally, a Randomized, Controlled Trial of Epilepsy Surgery. New England Journal of Medicine 2001; 345: 365–367.

Fisher Robert S., Boas W van E, Blume W, Elger C, Genton P, Lee P, et al. Epileptic Seizures and Epilepsy: Definitions Proposed by the International League Against Epilepsy (ILAE) and the International Bureau for Epilepsy (IBE). Epilepsia 2005; 46: 470–472.

Flanagan D, Agarwal R, Gotman Jean. Computer-aided Spatial Classification of Epileptic Spikes. [Miscellaneous Article]. Journal of Clinical Neurophysiology March 2002 2002; 19: 125–135.

Fuchs M., Drenckhahn R., Wischmann H, Wagner M. An improved boundary element method for realistic volume-conductor modeling. IEEE Transactions on Biomedical Engineering 1998; 45: 980 –997.

Fuchs Manfred, Wagner Michael, Kastner J. Confidence limits of dipole source reconstruction results. Clinical Neurophysiology 2004; 115: 1442–1451.

Fuchs Manfred, Wagner Michael, Wischmann H-A, Köhler T, Theißen A, Drenckhahn Ralf, et al. Improving source reconstructions by combining bioelectric and biomagnetic data. Electroencephalography and Clinical Neurophysiology 1998; 107: 93–111.

Gaitatzis A, Carroll K, Majeed A, Sander JW. The Epidemiology of the Comorbidity of Epilepsy in the General Population. Epilepsia 2004; 45: 1613–1622.

Gorji A, Stemmer N, Rambeck B, Jürgens U, May T, Pannek HW, et al. Neocortical Microenvironment in Patients with Intractable Epilepsy: Potassium and Chloride Concentrations. Epilepsia 2006; 47: 297–310.

Gotman J, Gloor P. Automatic recognition and quantification of interictal epileptic activity in the human scalp EEG. Electroencephalography and Clinical Neurophysiology 1976; 41: 513–529.

Gotman Jean. Automatic Detection of Seizures and Spikes. Journal of Clinical Neurophysiology Inpatient 1999; 16: 130–140.

Grynszpan F, Geselowitz DB. Model Studies of the Magnetocardiogram. Biophysical Journal 1973; 13: 911–925.

Hämäläinen M, Hari Riitta, Ilmoniemi RJ, Knuutila J, Lounasmaa OV. Magnetoencephalography—theory, instrumentation, and applications to noninvasive studies of the working human brain. Rev. Mod. Phys. 1993; 65: 413–497.

Hamaneh MB, Limotai C, Lüders HO. Sphenoidal electrodes significantly change the results of source localization of interictal spikes for a large percentage of patients with temporal lobe epilepsy. J Clin Neurophysiol 2011; 28: 373–379.

Hari R., Joutsiniemi S-L, Sarvas J. Spatial resolution of neuromagnetic records: theoretical calculations in a spherical model. Electroencephalography and Clinical Neurophysiology/Evoked Potentials Section 1988; 71: 64–72.

Hart YM, Shorvon SD. The nature of epilepsy in the general population. I. Characteristics of patients receiving medication for epilepsy. Epilepsy Research 1995a; 21: 43–49.

Hart YM, Shorvon SD. The nature of epilepsy in the general population. II. Medical care. Epilepsy Research 1995b; 21: 51–58.

Helmholtz H. Ueber einige Gesetze der Vertheilung elektrischer Ströme in körperlichen Leitern mit Anwendung auf die thierisch-elektrischen Versuche. Annalen der Physik 1853; 165: 211–233.

Horsley V. Brain Surgery. BMJ 1886; 2: 670–677.

Iwasaki M, Pestana E, Burgess RC, Lüders HO, Shamoto H, Nakasato N. Detection of Epileptiform Activity by Human Interpreters: Blinded Comparison between Electroencephalography and Magnetoencephalography. Epilepsia 2005; 46: 59–68.

Jehi LE, O'Dwyer R, Najm I, Alexopoulos A, Bingaman W. A longitudinal study of surgical outcome and its determinants following posterior cortex epilepsy surgery. Epilepsia 2009; 50: 2040–2052.

Ji Z, Sugi T, Goto S, Wang X, Ikeda A, Nagamine T, et al. An Automatic Spike Detection System Based on Elimination of False Positives Using the Large-Area Context in the Scalp EEG. Biomedical Engineering, IEEE Transactions on 2011; 58: 2478 –2488.

Knowlton RC, Elgavish RA, Bartolucci A, Ojha B, Limdi N, Blount J, et al. Functional imaging: II. Prediction of epilepsy surgery outcome. Annals of Neurology 2008; 64: 35–41.

Köhling Rüdiger, Höhling J-M, Straub Heidrun, Kuhlmann D, Kuhnt Ulrich, Tuxhorn Ingrid, et al. Optical Monitoring of Neuronal Activity During Spontaneous Sharp Waves in Chronically Epileptic Human Neocortical Tissue. J Neurophysiol 2000; 84: 2161–2165.

Kuzniecky R, Devinsky O. Surgery Insight: surgical management of epilepsy. Nature Clinical Practice Neurology 2007; 3: 673–681.

Kwan P, Brodie MJ. Early Identification of Refractory Epilepsy. New England Journal of Medicine 2000; 342: 314–319.

Kwan P, Brodie MJ. Effectiveness of First Antiepileptic Drug. Epilepsia 2001; 42: 1255–1260.

Lau M, Yam D, Burneo J.G. A systematic review on MEG and its use in the presurgical evaluation of localization-related epilepsy. Epilepsy Research 2008; 79: 97–104.

Lehmenkühler A, Nicholson C, Speckmann Erwin-Josef. Threshold extracellular concentration distribution of penicillin for generation of epileptic focus measured by diffusion analysis. Brain Research 1991; 561: 292–298.

Luciano AL, Shorvon SD. Results of treatment changes in patients with apparently drug-resistant chronic epilepsy. Annals of Neurology 2007; 62: 375–381.

Lucka F, Pursiainen S, Burger M, Wolters Carsten H. Hierarchical Bayesian inference for the EEG inverse problem using realistic FE head models: Depth localization and source separation for focal primary currents. NeuroImage 2012; 61: 1364–1382.

Lüders H, Bingaman W, Imad M. Najm. Textbook of Epilepsy Surgery. 1st ed. Informa Healthcare; 2008.

Lüders HO, Najm I, Nair D, Widdess-Walsh P, Bingman W. The epileptogenic zone: general principles. Epileptic Disord 2006; 8 Suppl 2: S1–9.

Merlet I, Paetau R, García-Larrea L, Uutela K, Granström ML, Mauguière F. Apparent asynchrony between interictal electric and magnetic spikes. Neuroreport 1997; 8: 1071–1076.

Noachtar S, Binnie C, Ebersole J, Maugulière F, Sakamoto A, Westmoreland B. Glossar der meistgebrauchten Begriffe in der klinischen Elektroenzephalographie und Vorschläge für die EEG-Befunderstellung*. Zeitschrift für Epileptologie 2005; 18: 71–77.

Ochi Ayako, Otsubo Hiroshi, Chitoku Shiro, Hunjan A, Sharma R, Rutka James T., et al. Dipole Localization for Identification of Neuronal Generators in Independent Neighboring Interictal EEG Spike Foci. Epilepsia 2001; 42: 483–490.

Ochi Ayako, Otsubo Hiroshi, Sharma R, Hunjan A, Rutka James T., Chuang SH, et al. Comparison of Electroencephalographic Dipoles of Interictal Spikes from Prolonged Scalp Video-Electroencephalography and Magnetoencephalographic Dipoles from Short-Term Recording in Children With Extratemporal Lobe Epilepsy. J Child Neurol 2001; 16: 661–667.

Okada Y, Lähteenmäki A, Xu C. Comparison of MEG and EEG on the basis of somatic evoked responses elicited by stimulation of the snout in the juvenile swine. Clinical Neurophysiology 1999; 110: 214–229.

Okada YC, Tanenbaum R, Williamson S. J., Kaufman L. Somatotopic organization of the human somatosensory cortex revealed by neuromagnetic measurements. Experimental Brain Research 1984; 56: 197–205.

Ossadtchi A, Baillet S, Mosher JC, Thyerlei D, Sutherling W, Leahy RM. Automated interictal spike detection and source localization in magnetoencephalography using independent components analysis and spatio-temporal clustering. Clinical Neurophysiology 2004; 115: 508–522.

Otsubo H., Chitoku S., Ochi A., Jay V., Rutka J. T., Smith ML, et al. Malignant rolandic-sylvian epilepsy in children Diagnosis, treatment, and outcomes. Neurology 2001; 57: 590–596.

Otsubo Hiroshi, Ochi Ayako, Elliott I, Chuang SH, Rutka James T., Jay Venita, et al. MEG Predicts Epileptic Zone in Lesional Extrahippocampal Epilepsy: 12 Pediatric Surgery Cases. Epilepsia 2001; 42: 1523–1530.

Pang CCC, Upton ARM, Shine G, Kamath MV. A comparison of algorithms for detection of spikes in the electroencephalogram. Biomedical Engineering, IEEE Transactions on 2003; 50: 521 –526.

Pataraia Ekaterina, Lindinger Gerald, Deecke Lueder, Mayer D, Baumgartner Christoph. Combined MEG/EEG analysis of the interictal spike complex in mesial temporal lobe epilepsy. Neuroimage 2005; 24: 607–614.

Ramantani G, Boor R, Paetau Ritva, Ille N, Feneberg R, Rupp A, et al. MEG versus EEG: influence of background activity on interictal spike detection. J Clin Neurophysiol 2006; 23: 498–508.

Romani GL, Williamson S. J., Kaufman L., Brenner D. Characterization of the human auditory cortex by the neuromagnetic method. Experimental Brain Research 1982; 47: 381–393.

Sato S, Balish M, Muratore R. Principles of magnetoencephalography. J Clin Neurophysiol 1991; 8: 144–156.

Scambler G. Sociology, social structure and health-related stigma. Psychology, Health & Medicine 2006; 11: 288–295.

Schomer DL, Silva FL da. Niedermeyer's Electroencephalography: Basic Principles, Clinical Applications, and Related Fields. 6th Revised ed. Lippincott Williams&Wilki; 2011.

Sheltraw DJ, Coutsias EA. Invertibility of current density from near-field electromagnetic data. Journal of Applied Physics 2003; 94: 5307 –5315.

Speckmann, Erwin-Josef. Experimentelle Epilepsieforschung. Darmstadt: Wissenschaftliche Buchgesellschaft; 1986.

Stefan H, Hummel C, Scheler G, Genow A, Druschky K, Tilz C, et al. Magnetic brain source imaging of focal epileptic activity: a synopsis of 455 cases. Brain 2003; 126: 2396–2405.

Stefan H, Scheler G, Hummel C, Walter J, Romstöck J, Buchfelder M, et al. Magnetoencephalography (MEG) predicts focal epileptogenicity in cavernomas. J. Neurol. Neurosurg. Psychiatr. 2004; 75: 1309–1313.

Stok CJ, Meijs JWH, Peters MJ. Inverse solutions based on MEG and EEG applied to volume conductor analysis. Physics in Medicine and Biology 1987; 32: 99–104.

Tao JX, Baldwin M, Hawes-Ebersole S, Ebersole John S. Cortical Substrates of Scalp EEG Epileptiform Discharges. Journal of Clinical Neurophysiology 2007; 24: 96–100.

Tao JX, Baldwin M, Ray A, Hawes-Ebersole S, Ebersole John S. The impact of cerebral source area and synchrony on recording scalp electroencephalography ictal patterns. Epilepsia 2007; 48: 2167–2176.

Thickbroom GW, Davies HD, Carroll WM, Mastaglia FL. Averaging, spatio-temporal mapping and dipole modelling of focal epileptic spikes. Electroencephalogr Clin Neurophysiol 1986; 64: 274–277.

Vilensky JA. Sir Victor Alexander Haden Horsley (1857–1916): Neurosurgeon and Neuroscientist. Clinical Anatomy 2002; 15: 171–172.

Wagner M, Fuchs M, Drenckhahn R, Wischmann HA, Köhler T, Theissen A. Automatic generation of BEM and FEM meshes. Neuroimage 1997; 5: 389.

Webber WRS, Litt B, Lesser RP, Fisher R.S., Bankman I. Automatic EEG spike detection: what should the computer imitate? Electroencephalography and Clinical Neurophysiology 1993; 87: 364–373.

Wiebe S, Blume WT, Girvin JP, Eliasziw M. A Randomized, Controlled Trial of Surgery for Temporal-Lobe Epilepsy. New England Journal of Medicine 2001; 345: 311–318.

Williamson Samuel J., Lü Z-L, Karron D, Kaufman Lloyd. Advantages and limitations of magnetic source imaging. Brain Topography 1991; 4: 169–180.

Wolters C. H., Köstler H, Möller C, Härdtlein J, Grasedyck L, Hackbusch W. Numerical Mathematics of the Subtraction Method for the Modeling of a Current Dipole in EEG Source Reconstruction Using Finite Element Head Models. SIAM Journal on Scientific Computing 2008; 30: 24–45.

Wolters C.H., Anwander A, Tricoche X, Weinstein D, Koch MA, MacLeod RS. Influence of tissue conductivity anisotropy on EEG/MEG field and return current computation in a realistic head model: A simulation and visualization study using high-resolution finite element modeling. NeuroImage 2006; 30: 813–826.

Wyllie E, Cascino G, Gidal B. Wyllie's Treatment of Epilepsy: Principles and Practice. 0005 ed. Lippencott Williams & Wil; 2010.

Yoshinaga H, Nakahori T, Hattori J, Akiyama T, Oka E, Tomita S, et al. Dipole analysis in a case with tumor-related epilepsy. Brain Dev. 1999; 21: 483–487.

Yoshinaga Harumi, Nakahori Tomoyuki, Ohtsuka Y, Oka Eiji, Kitamura Y, Kiriyama H, et al. Benefit of Simultaneous Recording of EEG and MEG in Dipole Localization. Epilepsia 2002; 43: 924–928.

Zschocke s, Hansen HC. Klinische Elektroenzephalographie. 3. Auflage. Berlin: Springer; 2011.